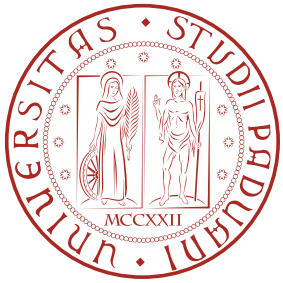

University of Padova

Department of Information Engineering

Ph.D. School of Information Engineering

Information and Communications Science and Technologies

25th Cycle

Transmission Techniques and Resource Allocation in Coordinated Multi-Point Systems

Paolo Baracca

Advisor:
Prof. Nevio Benvenuto

Ph.D. School Director:
Prof. Matteo Bertocco

Academic Year 2012-2013

To my parents

Contents

Abstract

This thesis is focused on the design of transmission schemes and resource allocation algorithms for both downlink and uplink of coordinated multi-point (CoMP) systems.

In current cellular systems, which employ a full frequency reuse of the spectral resource, interference has been recognized as one of the most limiting factor: in particular, user equipments (UEs) close to the cell edge typically suffer strong inter-cell interference (ICI). This interference, which is due to the transmission of neighbouring base stations (BSs) in the downlink and UEs in neighbouring cells in the uplink, limits the fairness across the UEs and, in general, the overall system performance. It has been shown that BS coordination is able to dramatically improve the system performance with respect to non-cooperative schemes by limiting the impact of ICI. Coordination is obtained by sharing among the BSs channel state information (CSI), data to be sent to the UEs in the downlink and signals received by the BSs in the uplink. However, BS coordination also poses several new challenges. First of all, the backhaul may not be able to support the sharing among the BSs of all the data to be sent to the UEs or signals received by BSs. Moreover, obtaining reliable CSI at the BSs for all the UEs in the network may be an issue because of a) limited bandwidth available for the feedback channel in frequency division duplex (FDD) systems and b) noise on channel estimation in time division duplex (TDD) systems. Thereby, it is crucial to develop practical algorithms that deal efficiently with both of these issues in order to achieve, in a realistic scenario, the performance gain enabled by cooperation.

This thesis is basically divided into two parts. In the first part we focus on downlink CoMP systems and we provide four main contributions. First, we propose a novel transmission scheme based on linear precoding and quantization of quadrature amplitude modulation (QAM) constellations. With the aim of reducing the backhaul occupation, a set of cooperative BSs transmit toward the UE a quantized version of the QAM symbol by using a joint precoder, while the serving BS transmits a *quantization error* symbol. In order to avoid modifications of the receiver, we impose that the combination of the two symbols through the channels yields at the UE the original QAM symbol. Numerical results show that this approach ensures a network spectral efficiency close to a theoretical limit obtained by using the more complex Slepian-Wolf encoding. Secondly, we develop a greedy dynamic algorithm to jointly organize BSs in clusters and to schedule UEs in each cluster. A considerable gain is achieved by the proposed approach with respect to both

non-cooperative schemes and static clustering. Thirdly, we focus on the feedback design in FDD systems and we consider a practical strategy where each UE quantizes the CSI by using codebooks designed for a single-cell scenario. We propose two algorithms which allow the UE to a) select a subset of preferred BSs and b) optimize the number of feedback bits allocated to the quantization of each CSI. In particular, more feedback bits are sent to BSs with stronger signals. Finally, we adapt our scheme based on QAM quantization to a different scenario where a set of relays assists the transmission of a BS toward a UE. In such a case, the proposed joint precoding is employed by the relays to serve the UE, whereas the links connecting the relays to the BS represent the backhaul infrastructure.

In the second part of the thesis, we consider the uplink of CoMP systems by assuming that UEs transmit toward BSs by using single carrier frequency division multiple access (SC-FDMA), which is the modulation employed in the uplink of Long Term Evolution (LTE). In this scenario, we propose a new scheduler of the signals exchanged among BSs on the backhaul that allows each BS to share only a subset of the subcarriers of each SC-FDMA block.

Sommario

Questa tesi è incentrata sullo studio di schemi di trasmissione e algoritmi per l'allocazione di risorse sia per il downlink che per l'uplink di sistemi CoMP.

Nei sistemi cellulari odierni, in cui vi è un riutilizzo delle stesse frequenze in ogni cella, l'interferenza inter-cella rappresenta uno dei fattori più limitanti andando a ridurre sensibilmente l'efficienza spettrale degli utenti a bordo cella. Questa interferenza, che è dovuta nel downlink alla trasmissione da parte di stazioni radio base in celle vicine e nell'uplink alla trasmissione di utenti in celle vicine, limita la fairness tra gli utenti e, più in generale, le prestazioni del sistema. Tuttavia, la coordinazione tra stazioni radio base è in grado di limitare l'impatto dell'interferenza inter-cella e migliorare notevolmente le prestazioni rispetto ai sistemi senza cooperazione. La coordinazione prevede la condivisione tra stazioni radio base di informazioni sui canali, dei dati da trasmettere agli utenti nel downlink e dei segnali ricevuti dalle stazioni radio base nell'uplink. L'implementazione pratica della coordinazione pone però molte nuove problematiche. Prima di tutto, l'infrastruttura di backhaul può non essere in grado di supportare la condivisione di dati e segnali tra le stazioni radio base. Inoltre, può essere difficile ottenere una conoscenza affidabile dei canali tra un utente e le stazioni radio base nella rete a) per una banda limitata dedicata al canale di feedback in sistemi a divisione di frequenza e b) per il rumore sulla stima di canale in sistemi a divisione di tempo. Di conseguenza, è importante sviluppare degli algoritmi pratici che tengano in considerazione queste problematiche e mantengano in un sistema reale il guadagno garantito dalla coordinazione.

Questa tesi è divisa in due parti. La prima parte è incentrata sul downlink e vengono forniti quattro contributi principali. In primo luogo, si propone un nuovo schema di trasmissione che si basa sul precoding lineare e la quantizzazione di costellazioni QAM. Con l'obiettivo di ridurre il traffico sulla rete di backhaul, un insieme di stazioni radio base coordinate trasmette verso un utente un simbolo che è una versione quantizzata del simbolo QAM originale, mentre la stazione radio base servente trasmette una versione scalata dell'errore di quantizzazione. Imponendo che la combinazione dei due campioni al ricevitore dia il simbolo QAM originale, lo schema proposto non richiede alcuna modifica al lato utente. I risultati numerici mostrano che l'efficienza spettrale ottenuta con questa tecnica si avvicina a quella ottenuta utilizzando la più complicata codifica di Slepian-Wolf. In secondo luogo, si propone un algoritmo greedy dinamico di scheduling e clustering per

organizzare le stazioni radio base in cluster e per scegliere gli utenti serviti da ciascun cluster. Un guadagno considerevole è ottenuto grazie al metodo proposto rispetto a schemi senza cooperazione e schemi con clustering statico. In terzo luogo, viene studiato il problema del feedback per sistemi a divisione di frequenza e si considera uno schema pratico dove l'utente quantizza i canali utilizzando dei codebook disegnati per sistemi senza coordinazione. Con questo schema si propongono due algoritmi che permettono all'utente di a) selezionare l'insieme preferito di stazioni radio base e b) ottimizzare il numero di bit utilizzati per quantizzare ciascun canale. Nel dettaglio, questi algoritmi allocano più bit per la quantizzazione dei canali più forti. Infine, si adatta lo schema che si basa sulla quantizzazione di costellazioni QAM ad uno scenario dove un insieme di relay assiste la trasmissione di una stazione radio base verso un utente. In questo caso lo schema di precoding è utilizzato dai relay per servire l'utente, mentre i link che connettono i relay alla stazione radio base rappresentano il backhaul.

Nella seconda parte della tesi si considera l'uplink di sistemi CoMP e si assume che gli utenti trasmettano verso le stazioni radio base utilizzando la modulazione SC-FDMA, che è lo schema utilizzato in LTE. Per questo scenario, si propone un nuovo scheduler dei segnali scambiati sul backhaul tra stazioni radio base che consente ad ogni stazione di condividere solo un sottoinsieme delle sottoportanti di ciascun blocco SC-FDMA.

Acknowledgments

First, I want to thank Prof. Nevio Benvenuto, who supervised me in the last three years. Under his supervision I had the opportunity to study new and challenging problems. I also thank Dr. Stefano Tomasin for his precious advices. I am really grateful to Dr. Federico Boccardi and Dr. Volker Braun, whose willingness allowed me to have an important educational experience at the Bell Labs in Stuttgart, where I learnt to always take into account the many issues related to a practical system. A special thank to the people at the Bell Labs with whom I worked: they have always been very helpful to me. Thanks to all my colleagues and friends, with whom I exchanged ideas and opinions, and shared satisfactions, troubles and pleasures: Matteo Bassi, Matteo Canale, Carlo Dal Mutto, Alberto Dall'Arche, Silvia Lattanzio, Francesco Michielin, Andrea Baldisserotto, Francesco Crestani, Jacopo Framarin, Francesco Pace, Antonio Sartori, and Luca Sgulmaro. Finally, I want to thank my family who helped and supported me to become the person I am today.

Innanzitutto, desidero ringraziare il Prof. Nevio Benvenuto che mi ha guidato in questi tre anni. Sotto la sua supervisione ho avuto modo di studiare sempre problemi nuovi e stimolanti. Voglio ringraziare poi il Dr. Stefano Tomasin per i suoi preziosi consigli. Sono veramente riconoscente al Dr. Federico Boccardi e al Dr. Volker Braun, la cui disponibilità mi ha permesso di trascorrere un'esperienza davvero formativa ai Bell Labs di Stoccarda, dove ho imparato a tenere sempre in considerazione i molti problemi che caratterizzano un sistema pratico. Un grazie anche a tutte le altre persone con cui ho avuto modo di collaborare ai Bell Labs e che si sono sempre dimostrate molto disponibili nei miei confronti. Un grazie a tutti i miei colleghi e amici con cui ho avuto la possibilità di scambiare idee ed opinioni e condividere soddisfazioni, difficoltà e momenti di divertimento: Matteo Bassi, Matteo Canale, Carlo Dal Mutto, Alberto Dall'Arche, Silvia Lattanzio, Francesco Michielin, Andrea Baldisserotto, Francesco Crestani, Jacopo Framarin, Francesco Pace, Antonio Sartori e Luca Sgulmaro. Voglio concludere ringraziando la mia famiglia, il cui aiuto e sostegno mi hanno reso la persona che sono oggi.

List of Symbols

$\boldsymbol{X}^T$:	transpose of matrix $\boldsymbol{X}$
$\boldsymbol{X}^*$:	complex conjugate of matrix $\boldsymbol{X}$
$\boldsymbol{X}^H$:	complex conjugate transpose of matrix $\boldsymbol{X}$
$\boldsymbol{X}^{-1}$:	inverse of matrix $\boldsymbol{X}$
$\|\boldsymbol{x}\|$:	Euclidean norm of vector $\boldsymbol{x}$
$[\boldsymbol{X}]_{m,n}$:	(m,n)-th entry of matrix $\boldsymbol{X}$
$[\boldsymbol{X}]_{m,\cdot}$:	m-th row of matrix $\boldsymbol{X}$
$[\boldsymbol{X}]_{\cdot,n}$:	n-th column of matrix $\boldsymbol{X}$
$\boldsymbol{I}_N$:	identity matrix of size N
$\boldsymbol{0}_{M\times N}$:	matrix of size $M \times N$ with all zero entries
$\|\mathcal{X}\|$:	cardinality of set $\mathcal{X}$
$\mathcal{CN}(\boldsymbol{\mu}, \boldsymbol{R})$:	complex Gaussian random vector with mean $\boldsymbol{\mu}$ and covariance matrix $\boldsymbol{R}$
$\mathbb{E}[x]$:	expectation of random variable x
$\Re(x)$:	real part of complex scalar x
$\Im(x)$:	imaginary part of complex scalar x
$\angle(x)$:	phase of complex scalar x

List of Acronyms

ABM	adaptive broadcast multiaccess
ADF	adaptive decode and forward
AF	amplify and forward
AT	absolute threshold
AWGN	additive white Gaussian noise
BM	broadcast multiaccess
BS	base station
CB	coordinated beamforming
CDF	cumulative distribution function
CDI	channel direction information
CoMP	coordinated multi-point
CQI	channel quality information
CS	coordinated scheduling
CSC	cell signal combining
CSI	channel state information
CSS	cell signal selection
CU	central unit
DF	decode and forward
DFT	discrete Fourier transform
DPC	dirty paper coding
DyC	dynamic clustering

EBA equal bit allocation

EPA equal power allocation

FC full coordination

FDD frequency division duplex

IC interference cancellation

ICI inter-cell interference

IDFT inverse discrete Fourier transform

IEEE Institute of Electrical and Electronics Engineers

ISC intra-site cooperation

ISI inter-symbol interference

JP joint processing

LTE Long Term Evolution

MCP multi cell processing

MIMO multiple input multiple output

MMSE minimum mean square error

MRT maximum ratio transmission

MU multi user

OFDM orthogonal frequency division multiplexing

OOC on-off cooperation

OPA optimal power allocation

PAM pulse amplitude modulation

PFS proportional fair scheduling

QAM quadrature amplitude modulation

QCT quantized constellation transmission

QoS quality of service

RB resource block

RT	relative threshold
RVQ	random vector quantization
SC-FDMA	single carrier frequency division multiple access
SCIR	signal to caused interference ratio
SCP	single cell processing
SINR	signal to interference plus noise ratio
SNR	signal to noise ratio
StC	static clustering
SU	single user
TB	theoretical bound
TDD	time division duplex
UE	user equipment
WiMax	Worldwide Interoperability for Microwave Access
ZF	zero forcing
3GPP	3rd Generation Partnership Project

List of Figures

List of Tables

Chapter 1

Introduction

In the past years multiple input multiple output (MIMO) transmission techniques for wireless communication systems have been widely studied because of their benefits with respect to single antenna strategies. In a cellular system, by equipping with multiple antennas the base stations (BSs) and the user equipments (UEs), a great improvement in terms of coverage and spectral efficiency can be obtained both in the downlink and in the uplink. In the downlink, an important distinction is between single user (SU)-MIMO where the multiple spatial channels are allocated to the same UE, and multi user (MU)-MIMO where the spatial channels are allocated to a set of UEs in the same time slot and frequency bandwidth. The importance of MIMO has been recognized also by the industry and the most recent wireless communication standards for high data rates such as Long Term Evolution (LTE) by the 3rd Generation Partnership Project (3GPP) [1, 2, 3] and Worldwide Interoperability for Microwave Access (WiMax) by the Institute of Electrical and Electronics Engineers (IEEE) [4] include MIMO.

One of the main issues that still limits the performance of current cellular systems, which use a full frequency reuse, is the inter-cell interference (ICI) due to the transmission on the same bandwidth and in the same time slot of a) neighbouring BSs in the downlink and b) UEs in neighbouring cells in the uplink: in particular UEs close to the cell edge suffer strong ICI which sensibly limits both the throughput for these UEs and the network spectral efficiency. Recently, network coordination [5] has been shown to limit ICI and greatly improve the system performance with respect to non-cooperative systems. This cooperative technique is also known in literature as multi cell processing (MCP), network MIMO [6] or coordinated multi-point (CoMP) [7], and has been considered for LTE [8, 9]. Downlink network MIMO can be initially seen as a MIMO system where the transmitting antennas are not co-located: BSs, after sharing UE data and channel state information (CSI), employ joint precoding in serving the scheduled UEs. Unluckily, this sharing feature poses many new challenges. First of all the backhaul infrastructure may not be able to support all the data/signal sharing among the BSs in the network and clusters of BSs should be organized. Secondly, while in conventional cellular systems only the channel

between the UE and its serving BS needs to be estimated at the transmitter side, in downlink network MIMO several channels between the UE and the cooperative BSs need to be estimated in order to implement joint precoding. In time division duplex (TDD) systems CSI at the BSs can be obtained through channel estimation in the uplink, whereas in frequency division duplex (FDD) systems CSI at the BSs depends on the feedback sent by the UEs. Consequently, noise on channel estimation in TDD and limited bandwidth available for the feedback channel in FDD may sensibly degrade the CSI at BSs. Then, also the the power can not be shared among the BSs and per-BS power constraints must be considered: however, this issue has been partially studied in MIMO systems with per-antenna power constraints [10].

This thesis is organized as follows.

- In Chapter 2 we consider a downlink multi cell scenario where a set of BSs is serving a set of scheduled UEs. We introduce the important distinction between CoMP with joint processing (JP), where BSs share both data and CSI regarding the UEs, and CoMP with coordinated beamforming (CB)/coordinated scheduling (CS), where only CSI-sharing among the BSs is allowed, and we compare the different CoMP schemes by assuming that the BSs employ linear precoding in serving the UEs. We consider several criteria for precoding design including maximum ratio transmission (MRT), zero forcing (ZF) and signal to caused interference ratio (SCIR). Then, we introduce the concept of clustering as a technique to reduce the backhaul occupation by comparing static clustering (StC), where the clusters are fixed, and dynamic clustering (DyC), where the clusters may change over time.

- In Chapter 3 we consider a downlink multi cell scenario where a central unit (CU) is connected by a finite-throughput backhaul to the BSs which employ linear precoding and quadrature amplitude modulation (QAM) constellation to serve the UEs. In order to satisfy backhaul constraints, we propose a novel transmission scheme in which for each UE all the cooperative BSs transmit a quantized version of the intended QAM symbol, while the serving BS also transmits a quantization error symbol: the two transmitted symbols combine through the channels yielding at the UE the intended QAM symbol. We formalize the problem of maximizing the network spectral efficiency by optimizing a) the QAM constellation size, b) the quantization rate and c) the power allocated to each UE. Since the resulting optimization is a mixed integer programming problem, we investigate a suboptimal solution based on equal power allocation (EPA) among the scheduled UEs. Numerical results show that the proposed approach yields a network spectral efficiency close to the theoretical limit obtained by Slepian-Wolf encoding.

- In Chapter 4 we develop a greedy dynamic joint clustering scheduling algorithm for the downlink of CoMP systems by assuming that the set of candidate clusters is

limited and predetermined, based on UE measurements. The set of non-overlapping selected clusters and the UEs scheduled in each cluster change dynamically in each time slot. The optimization criterion is given by the maximization of the system weighted sum rate. Fairness among the UEs is guaranteed by the proportional fair scheduling (PFS) algorithm [11]. We consider two different criteria to select the set of available clusters based on absolute and relative thresholds on the signal to noise ratios (SNRs) measured by the UEs, and different policies to select the UEs that can be scheduled in each cluster. Numerical results show the gain of the developed approach with respect to both single cell processing (SCP) systems, i.e., when no coordination among the BSs is allowed, and CoMP systems with static clusters composed by BSs belonging to the same site.

- In Chapter 5 we focus on a FDD-CoMP scenario where the CSI at the CU depends on a feedback sent by the UE. We consider the per-cell codebook strategy developed in [12, 13] where each UE employs per-cell codebooks to quantize the set of channels connecting itself to the BSs and optimizes the feedback bits assigned to each BS. By assuming a constraint on the maximum number of feedback bits available at the UE, we develop and compare two novel algorithms to a) select the subset of preferred BSs by whom the UE wants to be served and b) optimize the number of feedback bits used to quantize each channel. The benefits of feedback bit optimization are observed in a SU-CoMP scenario by comparing the proposed algorithms against two suboptimal methods where a) bits are equally split among the BSs and b) all the bits are allocated only to the serving BS.

- In Chapter 6 we consider a relay network where three half-duplex relays are assisting the transmission of a BS toward a UE. In such a scenario the links connecting the relays to the BS represent a wireless backhaul infrastructure. We consider that time consists of a sequence of phases and propose a transmission scheme in which spatial multiplexing is achieved by alternating the transmission of a single relay in odd phases and the remaining couple of relays in even phases by employing the QAM quantization strategy described in Chapter 3. We formalize the problem of maximizing the spectral efficiency optimizing a) QAM size, b) power allocation, c) time allocation and d) relay scheduling. Then, we develop a practical algorithm to perform power and time optimization. The performance of the proposed scheme is compared against existing techniques in typical wireless scenarios showing the merits of the proposed approach.

- In Chapter 7 we consider the uplink of a multi-cell system where BSs cooperate to receive data from UEs which transmit by using single carrier frequency division multiple access (SC-FDMA), and the exchange of information among BSs is limited due to the rate constraint on the backhaul network. We propose a new scheduler of the signals shared among BSs on the backhaul with the objective of maximizing the

SC-FDMA system sum rate: a fundamental feature of the scheduler is that BSs may share received signals only within a subset of the subcarriers of each SC-FDMA block. A greedy algorithm is proposed as a viable solution to the problem. Then, to increase the system sum rate, we also consider interference cancellation (IC), where BSs detect some messages without cooperation, and transmit on the backhaul a suitable linear combination of received and detected signals. The scheduling problem is suitably modified to take into account IC, thus selecting the UEs for which detection occurs before sharing the signal on the backhaul. Numerical results for typical cellular configurations are presented.

- In Chapter 8 we conclude the thesis with a summary of the main findings.

Chapter 2

Beamforming design and clustering in downlink CoMP

Downlink spectral efficiency of cellular networks is strongly limited by ICI and BS coordination has attracted significant attention recently as a mean to limit the impact of ICI and increase the downlink throughput [5]. The idea is to implement a joint (distributed) MIMO system, where antennas located at different BSs transmit to the UEs.

It has been shown in [14, 15] that for the MIMO broadcast channel, which models the downlink of a conventional cellular system, the capacity is achieved by dirty paper coding (DPC), a non linear precoding technique firstly studied in [16]. However, due to the high implementation complexity of DPC, linear precoding (also known as beamforming) has received a lot of attention as a practical technique to achieve a performance close to DPC [17, 18].

Differently from the SU/MU-MIMO scenario, in CoMP the sharing of data among the BSs distributed in the network is limited by the capability of the backhaul and clustering has been considered as a practical technique to deal with this constraint: all the BSs are organized in subsets, i.e., clusters, each one implementing a joint precoding to serve the scheduled UEs.

In this chapter we firstly revise the important difference between CoMP-CB and CoMP-JP. In CoMP-CB only CSI can be shared among the BSs. Therefore, each BS can serve only the UEs in its coverage area by using beamformers designed with the aim of limiting the interference toward the UEs served by the other BSs. On the other hand, in CoMP-JP beyond CSI also data can be shared among the BSs which implement joint precoding.

Then, we consider and compare several beamforming techniques. Maximum ratio transmission (MRT) aims at maximizing the SNR of a served UE and is typically used in SCP when only one UE is served by the BS. Zero forcing (ZF) provides zero interference to the co-scheduled UEs [17], whereas the recently proposed signal to caused interference ratio (SCIR) beamforming maximizes the ratio between the useful signal toward the intended UE to the interference toward the other UEs [19, 20, 21].

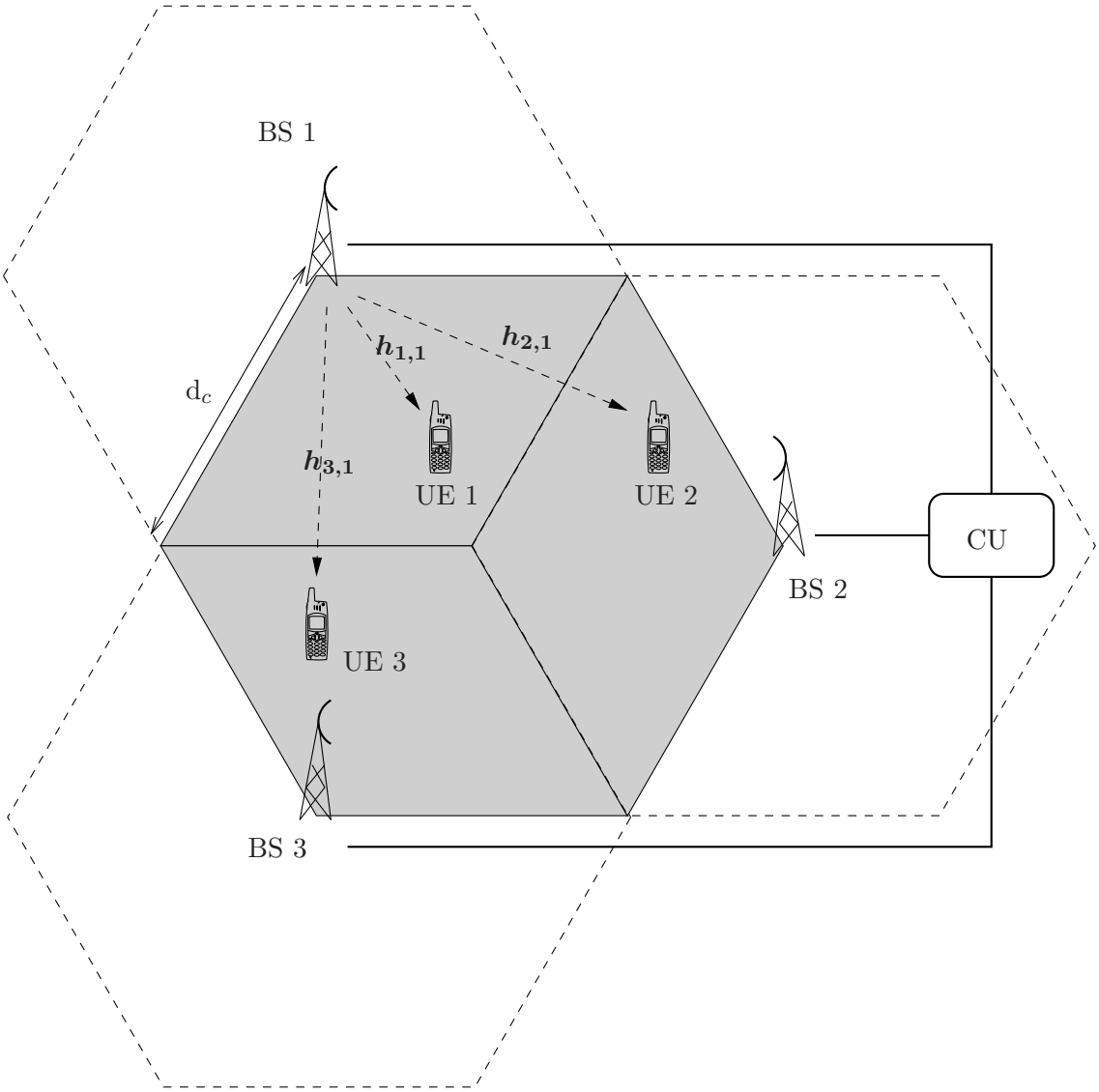

Figure 2.1: Downlink cellular network with $K = 3$ UEs served by 3 adjacent sectors of 3 different sites.

Finally, in order to reduce the backhaul occupation, we also consider CoMP-JP with clustering. In particular, we compare static clustering (StC), where the clusters are fixed and predetermined, and dynamic clustering (DyC) where the clusters may change in each time slot with the aim of maximizing a certain objective function [22].

2.1 System model

We consider a downlink cellular network with a set of J BSs, each with M antennas, serving $K = J$ single-antenna UEs, with $M \geq K$. We consider a star network topology where each BS is connected through a backhaul link to a central unit (CU). We assume a flat-fading channel between each couple of transmitting and receiving antennas and we

indicate with $\boldsymbol{h}_{k,j} \sim \mathcal{CN}\left(\mathbf{0}_{M\times 1}, \sigma_{k,j}^2 \boldsymbol{I}_M\right)$ the $M \times 1$ channel vector between UE k and BS j. Note that this assumption is widely used in literature [6], even if the wireless channel between UEs and BSs typically is frequency-selective. In fact, we assume that orthogonal frequency division multiplexing (OFDM), which converts a frequency-selective channel into a set of parallel flat-fading channels, is the employed modulation scheme as in downlink LTE [2] and WiMax [4]. Therefore, $\boldsymbol{h}_{k,j}$ actually models the channel between UE k and BS j on a set of adjacent subcarriers whose total bandwidth is narrower than the coherence bandwidth of the channel. We also assume that each UE k is randomly dropped in the coverage area of the k-th BS as shown in Fig. 2.1 and a full frequency reuse is considered.

2.1.1 BS coordination

BSs employ beamforming to transmit data to the UEs and can be coordinated in order to limit interference. To this end, data symbols and CSI may be shared to perform joint beamforming. We denote with $\mathcal{K}_j = \left\{k_1, k_2, \ldots, k_{K_j}\right\}$, $j = 1, 2, \ldots, J$, the set collecting the UE indices whose data are known at BS j, and with $\mathcal{J}_k = \{j_1, j_2, \ldots, j_{J_k}\}$, $k = 1, 2, \ldots, K$, the set collecting the BS indices serving UE k. As each BS knows at least the data of the UE in its cell, we have $k \in \mathcal{J}_k$ and $j \in \mathcal{K}_j$. In this chapter we compare several cooperative techniques which require different amount of data and CSI sharing.

- Single cell processing (SCP): each UE is served only by its assigned BS, i.e., $\mathcal{J}_k = \mathcal{K}_k = \{k\}$, and CSI sharing is not allowed, i.e., each BS only knows the channel toward its UE.

- CoMP with coordinated beamforming (CB): each UE is served only by its assigned BS as in SCP, but CSI sharing is partially allowed and each BS knows the channels connecting itself to all the UEs.

- CoMP with joint processing (JP) and *full coordination* (FC): all the BSs cooperate in serving the UEs, i.e, $\mathcal{J}_k = \mathcal{K}_k = \{1, 2, \ldots, K\}$, and full CSI sharing is allowed.

- CoMP with joint processing (JP) and *clustering*: each BS belongs to a certain cluster and knows only the data of the UEs served by that cluster, i.e., $\mathcal{J}_k \subset \{1, 2, \ldots, K\}$ and $\mathcal{K}_j \subset \{1, 2, \ldots, K\}$. In this chapter we consider a simple clustering approach where a set $\mathcal{C}_1$ of D BSs are coordinated in beamforming to their UEs, while the remaining set $\mathcal{C}_2$ of $K - D$ BSs are coordinated in transmitting toward the remaining UEs. Full CSI sharing is still allowed.

Note that CoMP-CB can be seen as the borderline case of CoMP-JP with clustering when each cluster is simply composed by only one BS.

We assume that the CSI at the BSs is perfect, i.e., it is not affected by noise on channel estimation or quantization error due to limited bandwidth available for the feedback in

FDD. In a low mobility scenario, the backhaul throughput required for data sharing is sensibly higher than that for updating CSI. Therefore, in the following we compare the different configurations, which have different requirements in terms of backhaul throughput, by only considering the data sharing.

With SCP and CoMP-CB, each BS knows only data for its served UE, requiring a backhaul throughput for data sharing which is provided by current 3GPP networks. In these schemes, and by considering the star network topology of Fig. 2.1, the total number of exchanged packets in each time slot is K, i.e., one packet transmitted by the CU to each BS.

On the other hand, CoMP-JP requires the maximum data exchange as each BS needs to know the data intended to all the UEs in the network. Hence, the total number of exchanged packets is K^2.

Finally, clustering allows a reduction of the backhaul throughput. In fact, the number of packets transmitted by the CU to BS j is K_j, and the total number of exchanged packets turns out to be

$$\sum_{j=1}^{K} K_j \,. \tag{2.1}$$

2.1.2 SINR computation

Let $x_k \sim \mathcal{CN}(0,1)$ be the complex Gaussian zero mean data symbol with unitary power to be delivered to UE k in a certain time slot. In the following, time is omitted for the sake of clarity. Let also $\boldsymbol{g}_{k,j}$ be the $M \times 1$ beamforming vector used by BS j to send data to UE k. The received signal at UE k can then be written as

$$y_k = \sum_{n=1}^{K} \sum_{j \in \mathcal{J}_n} \boldsymbol{h}_{k,j}^T \boldsymbol{g}_{n,j} x_n + n_k \,, \tag{2.2}$$

where $n_k \sim \mathcal{CN}(0, \sigma_n^2)$ is the additive white Gaussian noise (AWGN) with zero mean and variance σ_n^2 at UE k. The signal to interference plus noise ratio (SINR) for UE k can be written as

$$\mathrm{SINR}_k = \frac{\left| \sum_{j \in \mathcal{J}_k} \boldsymbol{h}_{k,j}^T \boldsymbol{g}_{k,j} \right|^2}{\sum_{n=1, n \neq k}^{K} \left| \sum_{j \in \mathcal{J}_n} \boldsymbol{h}_{k,j}^T \boldsymbol{g}_{n,j} \right|^2 + \sigma_n^2} \,. \tag{2.3}$$

By denoting with $\boldsymbol{z}_{k,n}$ the $MJ_n \times 1$ vector collecting the channels between UE k and all BSs in $\mathcal{J}_n$ serving UE n, i.e.,

$$\boldsymbol{z}_{k,n} = [\boldsymbol{h}_{k,j_1}^T, \boldsymbol{h}_{k,j_2}^T, \ldots, \boldsymbol{h}_{k,j_{J_n}}^T]^T \,, \tag{2.4}$$

and with $\boldsymbol{g}_k$ the $MJ_k \times 1$ vector collecting the beamformers used by BSs in $\mathcal{J}_k$ to serve UE k, i.e.,

$$\boldsymbol{g}_k = [\boldsymbol{g}_{k,j_1}^T, \boldsymbol{g}_{k,j_2}^T, \dots \boldsymbol{g}_{k,j_{J_k}}^T]^T \,, \tag{2.5}$$

the expression in (2.3) can be rewritten as

$$\mathrm{SINR}_k = \frac{\left|\boldsymbol{z}_{k,k}^T \boldsymbol{g}_k\right|^2}{\sum\limits_{n=1,n\neq k}^{K} \left|\boldsymbol{z}_{k,n}^T \boldsymbol{g}_n\right|^2 + \sigma_n^2} \,. \tag{2.6}$$

Note that the power allocated by the CU to UE k turns out to be $P_k = \|\boldsymbol{g}_k\|^2$. Due to the fact that BSs are not co-located, in the following we assume a set of K per-BS power constraints, i.e.,

$$\sum_{k\in\mathcal{K}_j} \|\boldsymbol{g}_{k,j}\|^2 \leq \bar{P} \,, \quad j = 1, 2, \dots, K \,, \tag{2.7}$$

where $\bar{P}$ is the maximum power available at each BS. The spectral efficiency achieved by UE k is $R_k = \log_2(1 + \mathrm{SINR}_k)$ and the *sum rate* or *network spectral efficiency* can be written as

$$R^{(\mathrm{DATA})} = \sum_{k=1}^{K} R_k \,. \tag{2.8}$$

2.2 Beamforming techniques

In this section three metrics are compared for the beamforming design. We start with MRT, which is used in SCP by a BS to serve its UE, and then we discuss ZF and SCIR beamforming, which try to limit the interference created toward the other scheduled UEs by exploiting the additional CSI available at the BSs.

2.2.1 Maximum ratio transmission beamforming

A beamforming method for SCP, where BS k does not know the channels toward the UEs in the other cells, aims at maximizing the SNR at the UE k by solving (see (2.3))

$$\boldsymbol{g}_{k,k}^{(\mathrm{MRT})} = \underset{\boldsymbol{g}:\|\boldsymbol{g}\|^2=P_k}{\mathrm{argmax}} \left|\boldsymbol{h}_{k,k}^T \boldsymbol{g}\right|^2 \,. \tag{2.9}$$

The solution to (2.9) is simply

$$\boldsymbol{g}_{k,k}^{(\mathrm{MRT})} = \sqrt{P_k} \frac{\boldsymbol{h}_{k,k}^*}{\|\boldsymbol{h}_{k,k}\|} \,. \tag{2.10}$$

As MRT is used only with SCP and we are considering only one UE in each cell, we assume that each BS transmits toward its UE at full power, i.e., $P_k = \bar{P}$, $k = 1, 2, \dots, K$.

2.2.2 Zero forcing beamforming

ZF beamforming toward UE k aims at eliminating the interference created toward all the other UEs $n \neq k$ in the network by imposing

$$\boldsymbol{z}_{n,k}^T \boldsymbol{g}_k^{(\mathrm{ZF})} = 0, \quad \forall n \neq k\,. \tag{2.11}$$

Let $\boldsymbol{Z}_k$ be the $K \times MJ_k$ matrix having on its n-th row the channels seen at UE n from BSs transmitting toward UE k, i.e., $[\boldsymbol{Z}_k]_{n,\cdot} = \boldsymbol{z}_{n,k}^T$. If $MJ_k \geq K$, i.e., the number of transmitting antennas in the cluster serving UE k is greater than the number of UEs in the network, the ZF beamformer satisfying constraints (2.11) turns out to be

$$\boldsymbol{g}_k^{(\mathrm{ZF})} = \sqrt{P_k} \frac{\left[\boldsymbol{Z}_k^H (\boldsymbol{Z}_k \boldsymbol{Z}_k^H)^{-1}\right]_{\cdot,k}}{\left\| \left[\boldsymbol{Z}_k^H (\boldsymbol{Z}_k \boldsymbol{Z}_k^H)^{-1}\right]_{\cdot,k} \right\|}. \tag{2.12}$$

Note that ZF can be used both in CoMP-CB and in CoMP-JP. Moreover, we observe that the vector $\boldsymbol{g}_k^{(\mathrm{ZF},d)} = \boldsymbol{g}_k^{(\mathrm{ZF})} / \left\| \boldsymbol{g}_k^{(\mathrm{ZF})} \right\|$, i.e., the direction of the ZF beamformer, still satisfies constraints (2.11). Hence, with ZF the power can be optimized after the computation of the beamformer direction.

Optimal power allocation

After defining $G_k = \left| \boldsymbol{z}_{k,k}^T \boldsymbol{g}_k \right|^2 / \left\| \boldsymbol{g}_k \right\|^2$ and $V_{k,j} = \left\| \boldsymbol{g}_{k,j} \right\|^2 / \left\| \boldsymbol{g}_k \right\|^2$, the optimal power allocation (OPA) with ZF is obtained by maximizing the system sum rate, i.e., by solving

$$\max_{P_1, P_2, \ldots, P_K} \sum_{k=1}^{K} \log_2 \left(1 + \frac{G_k}{\sigma_n^2} P_k \right), \tag{2.13a}$$

subject to

$$\sum_{k \in \mathcal{K}_j} V_{k,j} P_k \leq \bar{P}\,, \qquad j = 1, 2, \ldots, K, \tag{2.13b}$$

$$P_k \geq 0, \qquad k = 1, 2, \ldots, K. \tag{2.13c}$$

Problem (2.13) is a convex optimization problem [23] similar to the classical water-filling problem, but it differs because of the $K > 1$ constraints on the P_k variables: however, it can be efficiently solved numerically by using standard convex optimization software packages, e.g., [24, 25].

Equal power allocation

EPA is a simple suboptimal strategy providing that the same power is allocated to the UEs served in the same cluster. For CoMP-JP with clustering this is obtained by imposing

$P_k = P^{(\mathrm{EP},1)}$, $k \in \mathcal{C}_1$, and $P_k = P^{(\mathrm{EP},2)}$, $k \in \mathcal{C}_2$. Enforcing constraints (2.13b) we obtain

$$P^{(\mathrm{EP},c)} = \frac{\bar{P}}{\max\limits_{j \in \mathcal{C}_c} \sum\limits_{k \in \mathcal{C}_c} V_{k,j}}, \qquad c = 1, 2\,. \tag{2.14}$$

The extension to CoMP-CB and CoMP-JP-FC is straightforward. In fact, with CoMP-CB we simply obtain $\bar{P}_k = \bar{P}$, $\forall k$, which is also the optimal solution to (2.13). With CoMP-JP-FC, by imposing $P_k = P^{(\mathrm{EP})}$, $\forall k$, we obtain

$$P^{(\mathrm{EP})} = \frac{\bar{P}}{\max\limits_{j \in \{1,2,\ldots,K\}} \sum\limits_{k=1}^{K} V_{k,j}}\,. \tag{2.15}$$

2.2.3 Signal to caused interference beamforming

The objective of MRT and ZF are conflicting: MRT aims only at maxmimizing the SNR of the served UE without considering the created ICI, whereas ZF simply nulls the ICI without taking into account the useful signal at the served UE. Recently [19, 20, 21] a new criterion based on the maximization of SCIR has been analyzed both for CoMP-CB and CoMP-JP. The beamformer used to serve UE k is the solution to the following optimization problem

$$\boldsymbol{g}_k^{(\mathrm{SCIR})} = \underset{\boldsymbol{g}:\|\boldsymbol{g}\|^2 = P_k}{\operatorname{argmax}} \frac{\left|\boldsymbol{z}_{k,k}^T \boldsymbol{g}\right|^2}{\sum\limits_{n=1, n\neq k}^{K} \left|\boldsymbol{z}_{n,k}^T \boldsymbol{g}\right|^2 + \sigma_n^2}\,. \tag{2.16}$$

The solution to (2.16) is

$$\boldsymbol{g}_k^{(\mathrm{SCIR})} = \sqrt{P_k} \frac{(\boldsymbol{I}_{MJ_k} + \boldsymbol{B}_k)^{-1} \boldsymbol{z}_{k,k}^*}{\left\|(\boldsymbol{I}_{MJ_k} + \boldsymbol{B}_k)^{-1} \boldsymbol{z}_{k,k}^*\right\|}, \tag{2.17}$$

where

$$\boldsymbol{B}_k = \frac{P_k}{\sigma_n^2} \sum_{n=1, n\neq k}^{K} \boldsymbol{z}_{n,k}^* \boldsymbol{z}_{n,k}^T\,. \tag{2.18}$$

Differently from MRT and ZF, the direction $\boldsymbol{g}_k^{(\mathrm{SCIR},d)} = \boldsymbol{g}_k^{(\mathrm{SCIR})} / \left\|\boldsymbol{g}_k^{(\mathrm{SCIR})}\right\|$ still depends on the allocated power $\bar{P}_k$ (2.18) and, for this reason, power allocation should be performed before the precoder computation. For CoMP-JP and considering per-BS power constraints this fact can be a problem. Therefore, we propose the following suboptimal method based on EPA described here for CoMP − JP with clustering:

- we first compute the precoder $\boldsymbol{g}_k^{(\mathrm{SCIR},0)}$ by assuming EPA and a sum power constraint in the network;

Algorithm 1 EPA for SCIR beamforming

1: compute $\boldsymbol{g}_k^{(\mathrm{SCIR},0)}$ from (2.17) by imposing $P_k = \bar{P}$, $k = 1, 2, \ldots, K$
2: **for** $c \in \{1, 2\}$ **do**
3: $\quad V_{k,j}^{(0)} \leftarrow \left\| \boldsymbol{g}_{k,j}^{(\mathrm{SCIR},0)} \right\|^2$, $k, j \in \mathcal{C}_c$
4: $\quad \alpha_c \leftarrow \dfrac{\bar{P}}{\max\limits_{j \in \mathcal{C}_c} \sum\limits_{k \in \mathcal{C}_c} V_{k,j}^{(0)}}$,
5: $\quad \boldsymbol{g}_k^{(\mathrm{SCIR})} \leftarrow \sqrt{\alpha_c}\, \boldsymbol{g}_k^{(\mathrm{SCIR},0)}$, $k \in \mathcal{C}_c$
6: **end for**

- the final precoder is simply $\boldsymbol{g}_k^{(\mathrm{SCIR})} = \sqrt{\alpha_c}\, \boldsymbol{g}_k^{(\mathrm{SCIR},0)}$, $k \in \mathcal{C}_c$, where the scaling factor α_c is determined by imposing the per-BS power constraints (2.7) in cluster c.

The procedure is summarized in Alg. 1. Note that the extension to CoMP-CB and CoMP-JP-FC is straightforward.

2.3 Static and dynamic clustering

In this chapter we compare two different clustering approaches for CoMP-JP: static and dynamic. In StC the two clusters $\mathcal{C}_1$ and $\mathcal{C}_2$ are the same for all the channel realizations; in terms of performance this setting is equivalent to randomly select the BSs for each channel realization.

On the other hand, in DyC the two clusters may change for each channel realization and are selected with the aim of optimizing a certain objective function. Here, we assume that given a certain power allocation and beamformer, the two clusters are selected by maximizing the network spectral efficiency, i.e.,

$$\left\{ \mathcal{C}_1^{(\mathrm{DyC})}, \mathcal{C}_2^{(\mathrm{DyC})} \right\} = \underset{\mathcal{C}_1, \mathcal{C}_2}{\operatorname{argmax}} \; R^{(\mathrm{DATA})}\left(\mathcal{C}_1, \mathcal{C}_2\right) , \tag{2.19a}$$

subject to

$$\mathcal{C}_1 \subseteq \{1, 2, \ldots, K\} , \qquad \mathcal{C}_2 = \{1, 2, \ldots, K\} \setminus \mathcal{C}_1 , \tag{2.19b}$$

$$|\mathcal{C}_1| = D , \qquad |\mathcal{C}_2| = K - D . \tag{2.19c}$$

Problem (2.19) is an integer programming problem. In Chapter 4 we will study more in detail the clustering optimization. Here we simply solve (2.19) by using an exhaustive search.

2.4 Numerical results

We consider the downlink cellular network of Fig. 2.1 with $K = 3$ BSs, having $M = 3$ transmitting antennas each, serving 3 UEs which are randomly dropped in the coverage area of their assigned BS. The cell size is $d_c = 2$ km. The channel model [19] includes path loss, shadowing and i.i.d. Rayleigh fading according to

$$[\boldsymbol{h}_{k,j}]_m = \psi_{k,j,m}\sqrt{\rho_{k,j}e^{\zeta_{k,j}}}\,, \quad k,j = 1,2,\ldots,K\,,\ m = 0,1,\ldots,M-1 \tag{2.20}$$

where $\psi_{k,j,m} \sim \mathcal{CN}(0,1)$ is i.i.d. Rayleigh fading with unit variance, $e^{\zeta_{k,j}}$ is the shadowing with a lognormal distribution with standard deviation of 8.9 dB, and $\rho_{k,j}$ is the path-loss factor that can be expressed as [26]

$$\rho_{k,j} = \left(\frac{c}{4\pi d_0 f_c}\right)^2 \left(\frac{d_0}{d_{k,j}}\right)^{\eta}\,, \tag{2.21}$$

where $\eta = 3.5$ is the path-loss coefficient, $d_{k,j}$ is the distance between BS j and UE k, $f_c = 1.8$ GHz is the carrier frequency, c is the speed of light, and $d_0 = 10$ m is the minimum distance between BSs and UEs.

For the sake of clarity, in the figures of this section we drop the term CoMP from CoMP-CB and CoMP-JP.

For both StC and DyC we impose $D = 2$: consequently we have one cluster composed of 2 BSs, while the remaining BS employs CB in serving its UE.

In Fig.s 2.2 and 2.3 we plot the average and the 5th percentile of the sum rate $R^{(\mathrm{DATA})}$ with respect to the SNR at the cell edge ($\mathrm{SNR}^{(\mathrm{CE})}$), which is the SNR measured by a UE located in an hexagon vertex of Fig. 2.1 without considering shadowing and Rayleigh fading. The different SNRs are obtained by suitably changing the ratio $\bar{P}/\sigma_n^2$. From both figures we observe that all the CoMP schemes strongly outperform SCP with a higher gain in the interference-limited scenario, i.e., for higher values of $\mathrm{SNR}^{(\mathrm{CE})}$. CB-SCIR outperforms both SCP, which simply maximizes the SNR of the UEs, and CB-ZF, which nulls the ICI. However, in the interference-limited scenario CB-ZF achieves a sum rate very close to CB-SCIR. As expected, JP-FC outperforms CB, whereas JP-DyC outperforms JP-StC and achieves performance close to JP-FC but with a reduced backhaul throughput requirement. In fact, for the considered scenario with $K = 3$ BSs, with JP-FC the CU sends all the UE packets to all the BSs, whereas for JP with clustering the CU sends 2 packets to each BS in the bigger cluster and only one packet to the remaining BS. On the other hand, with CB only 3 packets are sent by the CU (one packet to each BS). Hence, CB and JP with clustering allow a reduction of the backhaul throughput with respect to JP-FC of about 66% and 44%, respectively. Still they strongly outperform SCP. In particular, a very high gain is achieved by CoMP with respect to SCP for the UEs close to the cell edge: CB-ZF and JP-FC-ZF-EPA show a gain in terms of 5th percentile of

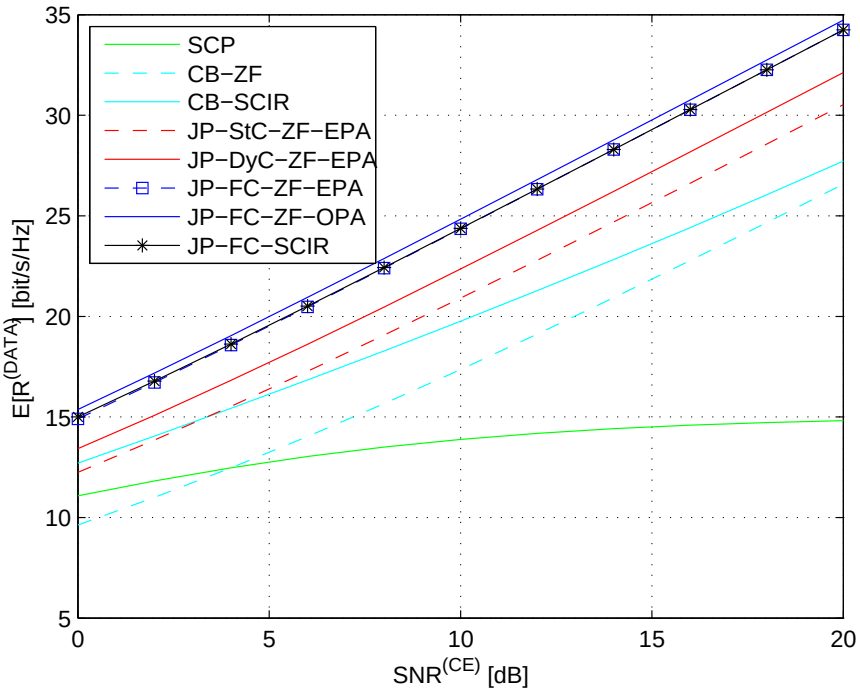

Figure 2.2: Average sum rate with respect to the SNR at the cell edge.

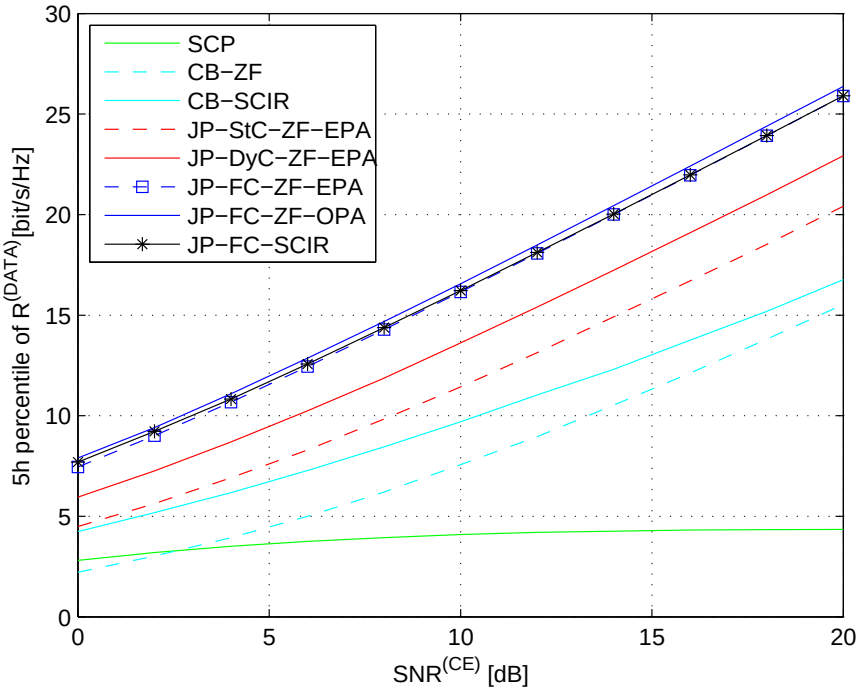

Figure 2.3: 5th percentile of the sum rate with respect to the SNR at the cell edge.

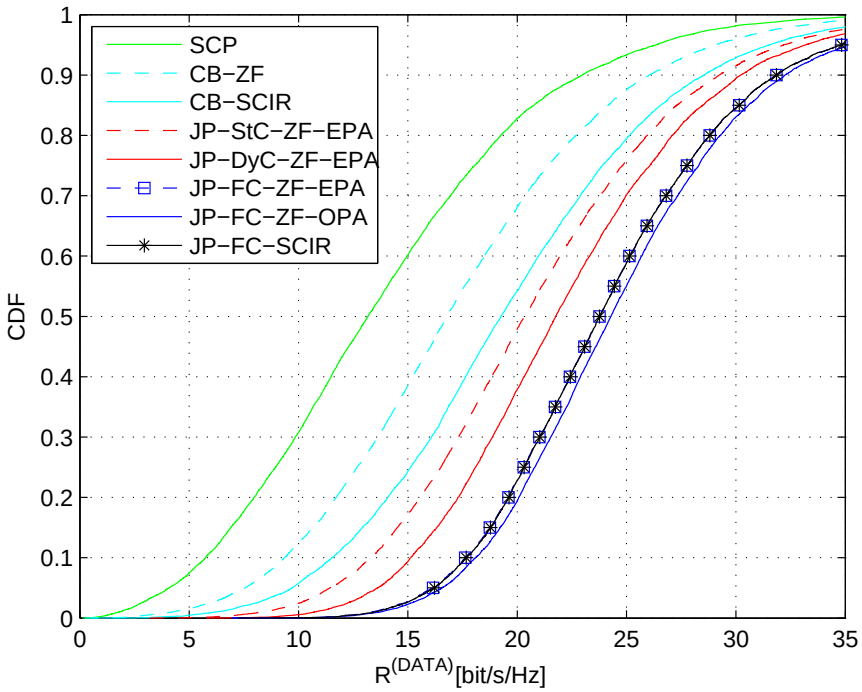

Figure 2.4: CDF of the sum rate when $\mathrm{SNR}^{(\mathrm{CE})} = 10$ dB.

	$\tilde{P}_j/\bar{P}$ (%)
JP-StC-ZF-EPA	89.5
JP-DyC-ZF-EPA	89.2
JP-FC-ZF-EPA	74.5
JP-FC-ZF-OPA	85.8
JP-FC-SCIR	74.4

Table 2.1: Average power $\tilde{P}_j$ used by a BS.

$R^{(\mathrm{DATA})}$ with respect to SCP of about 85% and 294% for $\mathrm{SNR}^{(\mathrm{CE})} = 10$ dB.

In Fig. 2.4 and in Tab. 2.1 at each BS we impose a maximum transmit power $\bar{P} = 40$ dBm and a thermal noise power $\sigma_n^2 = -108$ dBm, which corresponds to $\mathrm{SNR}^{(\mathrm{CE})} = 10$ dB: Fig. 2.4 shows the cumulative distribution function (CDF) of $R^{(\mathrm{DATA})}$, while Tab. 2.1 reports the average power $\tilde{P}_j$ effectively used by BS j. Note that in this framework both SCP and CB exploit all the available power. We observe that JP-FC-ZF-EPA and JP-FC-SCIR achieve almost the same sum rate, whereas JP-FC-ZF-OPA slightly outperforms JP-FC-ZF-EPA and this small gap is due to a better usage of the transmit power.

2.5 Conclusions

In this chapter we have compared several CoMP strategies against SCP for the downlink of cellular systems. We observe that CoMP strongly outperforms SCP with higher

gain in interference-limited scenarios and for UEs close to the cell edge. Better performance is achieved by CoMP-JP where data beyond CSI is shared among the coordinated BSs. Moreover, DyC is able to achieve a sum rate close to that of CoMP-JP, but with an important saving in terms of backhaul throughput.

Chapter 3

Constellation quantization in constrained backhaul downlink CoMP

As already introduced in Chapter 2, one of the most limiting factor for CoMP-JP is the huge data sharing among the cooperative BSs required to implement joint precoding: the backhaul infrastructure may not be able to support such a big overhead. Clustering allows an important saving in terms of backhaul throughput by requiring that each subset of cooperative BSs share only the data of the UEs scheduled in that cluster [22, 27, 28]. However, for a given constraint on the maximum backhaul throughput, the sharing of the full data intended to a UE among the BSs in the cluster is not optimal, and partial sharing of UE data may be a better solution.

Several works have recently investigated the theoretical system performance entangled by a constraint on the backhaul throughput. In [29] the capacity is derived for the downlink of a network MIMO system when the auxiliary BSs transmit a quantized version of the signal transmitted by the serving BS. In [30] a Wyner channel model has been considered and the capacity region has been derived for a transmission employing DPC. A similar analysis has been carried out in [31] for a simple case of two BSs cooperating in the transmission to two UEs. The same scenario has been considered in [32, 33] where two independent messages are transmitted to each UE: a common message known by both the BSs and a private message known only by the serving BS. By resorting to the Slepian and Wolf theorem [34], the capacity region of this system is derived. Although these works provide bounds on the performance of downlink network MIMO, they can not directly be applied to existing cellular systems such as LTE of 3GPP [2], since they require modifications of both transmitter and receiver. Moreover, even in future cellular systems their use would require sophisticated solutions such as DPC and successive interference cancellation schemes in order to allow the decoding of private and common messages.

In this chapter we propose a new transmission scheme for downlink network MIMO

constrained by a finite-throughput backhaul. We assume that for each UE the serving BS has a full knowledge of its related message, whereas the other cooperative BSs have only a partial knowledge. Furthermore, in contrast with [30] and [31], BSs use linear precoding instead of DPC due to its lower complexity and, in contrast with [29] and [30], we perform a transmission that does not introduce quantization noise at the receiver. In particular, data bits are encoded and mapped into symbols of a QAM constellation. The main novelty of this technique lies on the fact that each symbol is split as the sum of two terms: a *quantized symbol* belonging to a smaller size constellation and the corresponding *quantization error symbol*. In order to avoid modifications of the receiver, we impose that the combination of the two signals through the channels yields at the UE the original symbol. The bits representative of the quantized symbol are sent through the backhaul to all the BSs and this symbol is transmitted by a suitable beamforming. Besides the quantized symbol, the serving BS transmits also an additional signal with a scaled version of the quantization error symbol. By a suitable design of both quantization and beamforming, the symbol at the UE belongs to the unquantized constellation. Therefore, with respect to existing communication standards employing QAM, our proposed scheme requires a slight modification of BS transmitter and no modification of UE receiver. We formalize the problem of maximizing the network spectral efficiency on air for all the UEs within an area illuminated by cooperative BSs optimizing a) the QAM constellation size, b) the quantization rate dictated by the finite-throughput backhaul and c) the power allocated by each BS. Since the resulting optimization is a mixed integer programming problem, we investigate a suboptimal solution where the same power is allocated to each UE and obtain a simple algorithm for the rate optimization. The performance of the proposed method is compared against a theoretical bound obtained using Slepian-Wolf encoding, and some suboptimal methods in which BSs share an unquantized version of symbols, showing the merits of the proposed technique.

3.1 System model

Although the proposed technique will apply to a general scenario where many cooperative BSs serve multiple UEs, both equipped with many antennas, for the sake of a simpler notation we focus on the case of the downlink cellular network introduced in Section 2.1 with K cooperative BSs, each with M antennas, serving K single-antenna UEs.

We consider the star network topology of Fig. 2.1 where each BS is connected through a backhaul link to a CU. We assume that each link is error free and is constrained by a maximum available throughput $\bar{R}^{(\mathrm{BH})}$. This scenario models a situation widely considered in the literature [6, 27, 28, 30] where BSs are connected to a CU with a reliable medium as an optical fiber. We assume that the CU has full CSI.

After computing the beamformers, the power allocations (as detailed in Section 3.4) and the signals for the cooperating BSs, the CU sends all this information together with

data messages to BSs through the backhaul links. Under the assumption of reduced Doppler, the backhaul throughput required for data messages is sensibly higher with respect to that for updating CSI, which is therefore neglected in the rest of the chapter. In order to meet the constraints on the backhaul, we propose that the CU sends to auxiliary BSs only a partial information about the data to transmit, while the serving BS has full data knowledge. Let $R_{k,j}^{(\mathrm{BH})}$ be the backhaul throughput used by the CU to transmit the data message of UE k to BS j. The backhaul constraints can be written as

$$\sum_{k=1}^{K} R_{k,j}^{(\mathrm{BH})} \leq \bar{R}^{(\mathrm{BH})}, \quad j = 1, 2, \ldots, K. \tag{3.1}$$

We consider flat-fading channels among BSs and UEs and indicate with $\boldsymbol{h}_{k,j}$ the $M \times 1$ channel vector between UE k and BS j and with $\boldsymbol{h}_k = [\boldsymbol{h}_{k,1}^T, \boldsymbol{h}_{k,2}^T, \ldots, \boldsymbol{h}_{k,K}^T]^T$ the $MK \times 1$ vector collecting the channels seen at UE k for signals from all BSs. In order to obtain a simple scheme, we consider BSs employing linear precoding and each UE treats the other UE signals as interference, i.e., each UE is not able to decode the messages intended to the other UEs in the network.

3.2 Quantized QAM transmission scheme

Let x_k be the symbol belonging to a given QAM constellation with zero mean and unitary statistical power selected by the CU for UE k. As illustrated in Fig. 3.1 we split symbol x_k into the sum of two terms, the quantized symbol $x_k^{(q)}$ belonging to a smaller size constellation and the corresponding quantization error symbol $x_k^{(e)}$ given by

$$x_k^{(e)} = x_k - x_k^{(q)}. \tag{3.2}$$

Through the backhaul links, a binary representation of $x_k^{(q)}$ (more details on the quantization process are provided in Section 3.3) is sent to auxiliary BSs, whereas the serving BS receives a binary representation of x_k.

In other words, due to backhaul constraints (3.1), for each UE k the auxiliary BSs are only able to transmit symbol $x_k^{(q)}$, whereas the serving BS, who has full knowledge of symbol x_k, is also able to transmit symbol $x_k^{(e)}$ beyond $x_k^{(q)}$. In any case, the two symbols are transmitted separately. In fact, as in [33], we assume that $x_k^{(e)}$ is transmitted only by the serving BS using the $M \times 1$ beamformer $\boldsymbol{w}_k$, whereas $x_k^{(q)}$ is transmitted cooperatively by all the BSs in the network using the $MK \times 1$ beamformer $\boldsymbol{g}_k = [\boldsymbol{g}_{k,1}^T, \boldsymbol{g}_{k,2}^T, \ldots \boldsymbol{g}_{k,K}^T]^T$, with $\boldsymbol{g}_{k,j}$ being the beamformer applied by BS j on the signal intended to UE k.

All BSs cooperate in the transmission toward each UE k, because we assume that the CU has already selected the cooperative BSs, for example based on path-loss between each couple BS-UE, in the transmission toward UE k. A more general scenario with an algorithm scheduling cooperative BSs could be considered but is beyond the scope of

this analysis. We assume unit-norm beamformers, i.e., $\|\boldsymbol{w}_k\| = 1$ and $\|\boldsymbol{g}_k\| = 1$, and we define $\|\boldsymbol{g}_{k,j}\|^2 = V_{k,j}$. We denote with $P_k^{(q)}$ and $P_k^{(e)}$ suitable scaling factors (that will be optimized in Section 3.4 to maximize network spectral efficiency) of $x_k^{(q)}$ and $x_k^{(e)}$, respectively. The signal transmitted by BS j is

$$\boldsymbol{z}_j = \boldsymbol{w}_j \sqrt{P_j^{(e)}} x_j^{(e)} + \boldsymbol{g}_{j,j} \sqrt{P_j^{(q)}} x_j^{(q)} + \sum_{k=1, k\neq j}^{K} \boldsymbol{g}_{k,j} \sqrt{P_k^{(q)}} x_k^{(q)} \,, \tag{3.3}$$

and the signals transmitted by the set of K cooperative BSs can be written as

$$\begin{aligned} \begin{bmatrix} \boldsymbol{z}_1 \\ \boldsymbol{z}_2 \\ \vdots \\ \boldsymbol{z}_K \end{bmatrix} = & \begin{bmatrix} \boldsymbol{w}_1 & \boldsymbol{0}_{M\times 1} & \cdots & \boldsymbol{0}_{M\times 1} \\ \boldsymbol{0}_{M\times 1} & \boldsymbol{w}_2 & \cdots & \boldsymbol{0}_{M\times 1} \\ \vdots & \vdots & \ddots & \vdots \\ \boldsymbol{0}_{M\times 1} & \boldsymbol{0}_{M\times 1} & \cdots & \boldsymbol{w}_K \end{bmatrix} \begin{bmatrix} \sqrt{P_1^{(e)}} x_1^{(e)} \\ \sqrt{P_2^{(e)}} x_2^{(e)} \\ \vdots \\ \sqrt{P_K^{(e)}} x_K^{(e)} \end{bmatrix} + \\ & \begin{bmatrix} \boldsymbol{g}_{1,1} & \boldsymbol{g}_{2,1} & \cdots & \boldsymbol{g}_{K,1} \\ \boldsymbol{g}_{1,2} & \boldsymbol{g}_{2,2} & \cdots & \boldsymbol{g}_{K,2} \\ \vdots & \vdots & \ddots & \vdots \\ \boldsymbol{g}_{1,K} & \boldsymbol{g}_{2,K} & \cdots & \boldsymbol{g}_{K,K} \end{bmatrix} \begin{bmatrix} \sqrt{P_1^{(q)}} x_1^{(q)} \\ \sqrt{P_2^{(q)}} x_2^{(q)} \\ \vdots \\ \sqrt{P_K^{(q)}} x_K^{(q)} \end{bmatrix} . \end{aligned} \tag{3.4}$$

By imposing that the total transmit power constraint at each BS is $\bar{P}$, we have

$$\begin{aligned} P_j^{(e)} \mathbb{E}\left[\left|x_j^{(e)}\right|^2\right] + V_{j,j} P_j^{(q)} \mathbb{E}\left[\left|x_j^{(q)}\right|^2\right] + 2\sqrt{P_j^{(e)} P_j^{(q)}} \Re\left\{\boldsymbol{w}_j^H \boldsymbol{g}_{j,j} \mathbb{E}\left[x_j^{(e)*} x_j^{(q)}\right]\right\} + \\ \sum_{k=1, k\neq j}^{K} V_{k,j} P_k^{(q)} \mathbb{E}\left[\left|x_k^{(q)}\right|^2\right] \leq \bar{P} \,, \quad j = 1, 2, \ldots, K \,. \end{aligned} \tag{3.5}$$

Assuming that all UEs and BSs are perfectly synchronized in time and frequency, the received signal at UE k can be written as

$$\begin{aligned} y_k = & \boldsymbol{h}_{k,k}^T \boldsymbol{w}_k \sqrt{P_k^{(e)}} x_k^{(e)} + \boldsymbol{h}_k^T \boldsymbol{g}_k \sqrt{P_k^{(q)}} x_k^{(q)} + \\ & \sum_{j=1, j\neq k}^{K} \left(\boldsymbol{h}_{k,j}^T \boldsymbol{w}_j \sqrt{P_j^{(e)}} x_j^{(e)} + \boldsymbol{h}_k^T \boldsymbol{g}_j \sqrt{P_j^{(q)}} x_j^{(q)} \right) + n_k \,, \end{aligned} \tag{3.6}$$

where n_k is the AWGN with zero mean and variance σ_n^2.

Differently from [33] where $x_k^{(q)}$ and $x_k^{(e)}$ are two independent Gaussian signals, we propose a system design such that the simultaneous transmission of $x_k^{(q)}$ and $x_k^{(e)}$ from the serving and auxiliary BSs combines through the channels at the receiver as a scaled version of the QAM symbol x_k. In this way only one stream of data is transmitted by the

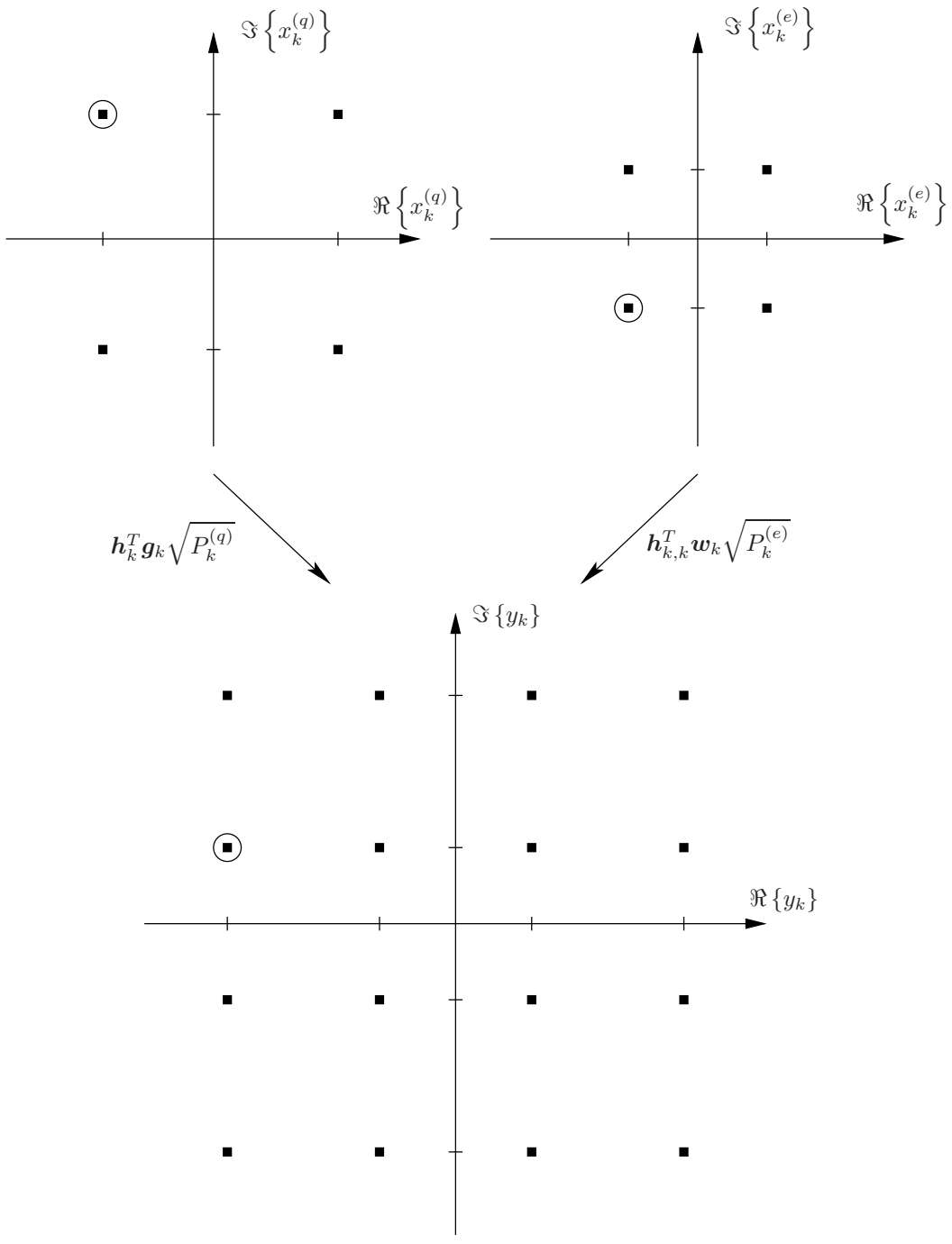

Figure 3.1: Structure of the proposed transmission scheme by assuming that x_k is a 16-QAM point and $x_k^{(q)}$ is a QPSK point. The algorithm to obtain $x_k^{(q)}$ and $x_k^{(e)}$ is described in Section 3.3. The constellation y_k at UE k is drawn by neglecting noise and interference due to the other UE signals.

cooperative BSs toward each UE (rank-1 transmission). Hence, we impose

$$\boldsymbol{h}_{k,k}^T \boldsymbol{w}_k \sqrt{P_k^{(e)}} x_k^{(e)} + \boldsymbol{h}_k^T \boldsymbol{g}_k \sqrt{P_k^{(q)}} x_k^{(q)} = A_k x_k \,, \tag{3.7}$$

where A_k is the equivalent channel seen at UE k. Using (3.2), condition (3.7) forces the cascade of channels and beamformers to be the same for $x_k^{(q)}$ and $x_k^{(e)}$, i.e., it must be

$$\boldsymbol{h}_{k,k}^T \boldsymbol{w}_k \sqrt{P_k^{(e)}} = \boldsymbol{h}_k^T \boldsymbol{g}_k \sqrt{P_k^{(q)}} \,, \tag{3.8}$$

and therefore

$$A_k = \boldsymbol{h}_k^T \boldsymbol{g}_k \sqrt{P_k^{(q)}} \,. \tag{3.9}$$

By using (3.2) and (3.8) in (3.6), the received signal at UE k becomes

$$y_k = \boldsymbol{h}_k^T \boldsymbol{g}_k \sqrt{P_k^{(q)}} x_k + \sum_{j=1, j\neq k}^{K} \left(\boldsymbol{h}_{k,j}^T \boldsymbol{w}_j \sqrt{P_j^{(e)}} x_j^{(e)} + \boldsymbol{h}_k^T \boldsymbol{g}_j \sqrt{P_j^{(q)}} x_j^{(q)} \right) + n_k \,. \tag{3.10}$$

By defining $G_k^{(e)} = \left| \boldsymbol{h}_{k,k}^T \boldsymbol{w}_k \right|^2$ and $G_k^{(q)} = \left| \boldsymbol{h}_k^T \boldsymbol{g}_k \right|^2$, from (3.8) we also obtain

$$G_k^{(e)} P_k^{(e)} = G_k^{(q)} P_k^{(q)} \,. \tag{3.11}$$

Note that in cooperative BS systems knowledge of UE channels in adjacent sectors is commonly assumed although this requires slight modifications at the BS side. However, knowledge of UE channels at each BS is a widely adopted assumption in CoMP scenarios (see [21, 22, 33]).

3.3 Quantized constellation design

Let the original QAM constellation size be rectangular of size 2^{b_k}, where the number of bits per symbol b_k is even, and let $b_k^{(q)} \in \{0, 1, \ldots, b_k\}$ be the number of bits used to represent a quantized QAM constellation point. The *quantization rate* is defined as

$$r_k^{(q)} = \frac{b_k^{(q)}}{b_k} \,. \tag{3.12}$$

The quantized constellation is designed according to the following criteria:

- the 2^{b_k} points of the original QAM constellation are grouped into $2^{b_k^{(q)}}$ disjointed subsets (*quantization regions*) with $2^{b_k - b_k^{(q)}}$ points each;
- each quantization region is represented by one point in the complex plane and all the selected points constitute the quantized constellation;

- for a given $b_k^{(q)}$, the quantization regions and the quantized points are selected in order to minimize the average square distance between each quantized point and the points of the original QAM constellation within the quantization region.

Note that each point of the quantized constellation is the average of the points of the corresponding quantization region. This is also a distinctive feature with respect to the theoretical papers [29] and [30] where the Gaussian codebook for the quantized signal was the capacity achieving solution starting from a Gaussian unquantized signal. An example of this quantization rule for a 16-QAM ($b_k = 4$) constellation and $b_k^{(q)} = 1, 2, 3$, is reported in Fig. 3.2.

By assuming equally likely symbols we have

$$\mathbb{E}\left[x_k^{(e)}\right] = 0\,, \tag{3.13a}$$

$$\mathbb{E}\left[x_k^{(q)*} x_k^{(e)}\right] = 0\,. \tag{3.13b}$$

Let $\gamma_k = \mathbb{E}\left[\left|x_k^{(e)}\right|^2\right]$ and considering that for a rectangular constellation of size 2^{b_k} and unitary statistical power the square of the minimum distance between two symbols can be expressed as $d_k^{(\min)2} = 6/(2^{b_k} - 1)$ [35], after some simple geometrical considerations we obtain

$$\gamma_k = \begin{cases} \dfrac{2^{b_k - b_k^{(q)}} - 1}{2^{b_k} - 1}\,, & \text{if } b_k^{(q)} \text{ is even}\,, \\ \dfrac{\frac{5}{4}2^{b_k - b_k^{(q)}} - 1}{2^{b_k} - 1}\,, & \text{if } b_k^{(q)} \text{ is odd}\,. \end{cases} \tag{3.14}$$

Moreover, as $\mathbb{E}[|x_k|^2] = 1$, from (3.2) and (3.13b) we also have

$$\mathbb{E}\left[\left|x_k^{(q)}\right|^2\right] = 1 - \gamma_k\,. \tag{3.15}$$

Note that for even $b_k^{(q)}$ the resulting quantized constellation is again a rectangular QAM. On the other hand, when $b_k^{(q)}$ is odd the quantization regions designed according to the aforementioned criteria are not unique. However, all choices lead to the same value of γ_k. Fig. 3.2 shows the quantized constellation of size $2^{b_k^{(q)}}$ with $b_k^{(q)}$ odd obtained by considering two pulse amplitude modulation (PAM) signals of size $2^{(b_k^{(q)}-1)/2}$ and $2^{(b_k^{(q)}+1)/2}$ along the real and imaginary components, respectively. Moreover, note that $x_k^{(e)}$ belongs to a QAM constellation of size $2^{b_k - b_k^{(q)}}$.

For given b_k and $b_k^{(q)}$ and for each QAM symbol x_k, the quantized symbol $x_k^{(q)}$ is selected according to the minimum distance criterion, whereas the quantization error is simply obtained from (3.2).

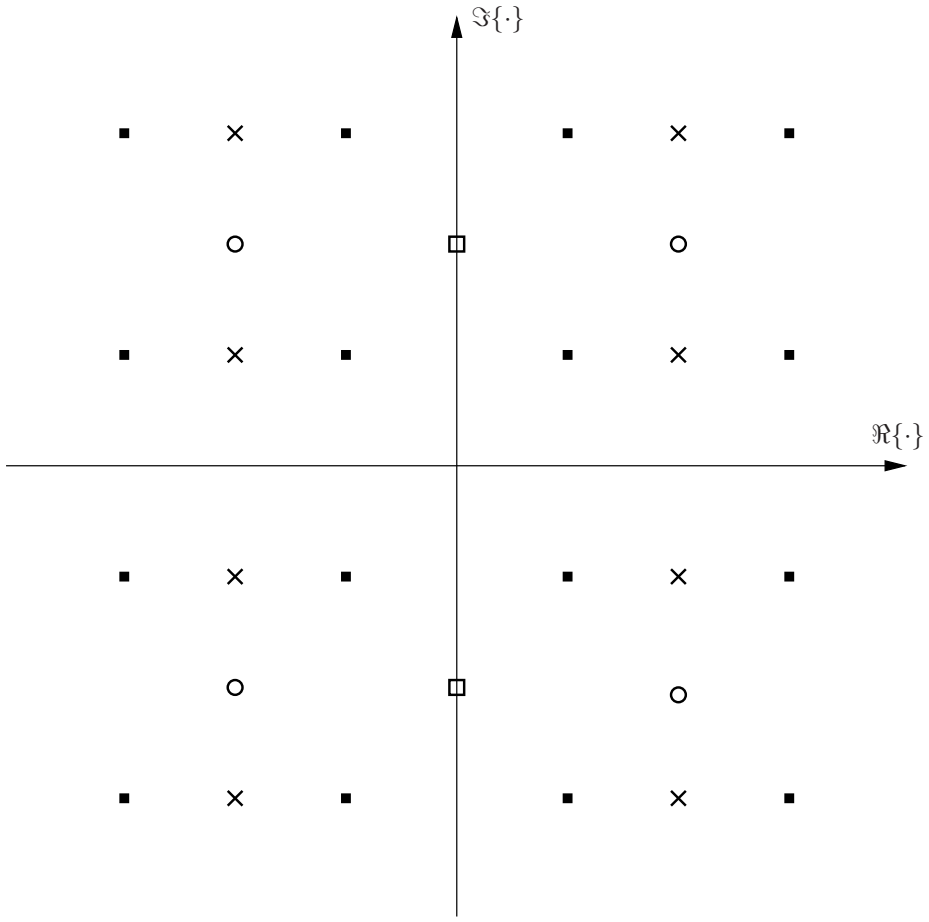

Figure 3.2: 16-QAM constellation (black squares) and its quantized versions with, respectively, $b_k^{(q)} = 1$ (squares), $b_k^{(q)} = 2$ (circles) and $b_k^{(q)} = 3$ (crosses) following the quantization rule of Section 3.3.

Lastly, from (3.11) and (3.13b) the transmit power constraints (3.5) can be expressed in terms of $P_k^{(q)}$, $k = 1, 2, \ldots, K$, as

$$\left(\gamma_j \frac{G_j^{(q)}}{G_j^{(e)}} + V_{j,j}(1-\gamma_j)\right) P_j^{(q)} + \sum_{k=1, k\neq j}^{K} V_{k,j}(1-\gamma_k) P_k^{(q)} \leq \bar{P}\,, \quad j = 1, 2, \ldots, K\,. \tag{3.16}$$

3.3.1 Spectral efficiency on the air

By defining $G_{k,j}^{(I_e)} = \left|\boldsymbol{h}_{k,j}^T \boldsymbol{w}_j\right|^2$ and $G_{k,j}^{(I_q)} = \left|\boldsymbol{h}_k^T \boldsymbol{g}_j\right|^2$ for $j \neq k$ (where I stands for interference), from (3.10) and (3.11) the SINR at UE k can be expressed as

$$\mathrm{SINR}_k = \frac{G_k^{(q)} P_k^{(q)}}{\sigma_n^2 + \sum_{j=1, j\neq k}^{K} \left[G_{k,j}^{(I_e)} \frac{G_j^{(q)}}{G_j^{(e)}} \gamma_j + G_{k,j}^{(I_q)} (1-\gamma_j)\right] P_j^{(q)}}\,. \tag{3.17}$$

The achievable spectral efficiency for an AWGN channel having as input a QAM signal has been derived in [36] and has an elaborate expression. For simplicity, we approximate the spectral efficiency (in bit/s/Hz) on air for UE k as

$$R_k = \min\left\{\log_2\left(1 + \frac{\mathrm{SINR}_k}{\Gamma_{\mathrm{GAP}}}\right),\, b_k\right\}\,, \tag{3.18}$$

where we take into account that:

- the maximum spectral efficiency is b_k;
- Γ_{GAP} is the gap to the capacity due to the use of a given channel code and to the fact that a QAM signal is not Gaussian distributed. For a comparison with other schemes present in the literature, where a) constellation shaping is assumed and b) channel coding is capacity achieving, we assume $\Gamma_{\mathrm{GAP}} = 1$.

3.3.2 Backhaul throughput

The problem of finding the exact value of $R_{k,j}^{(\mathrm{BH})}$ in (3.1) for $j \neq k$ is the problem of estimating the spectral efficiency of the sequence of bits obtained by channel coding, interleaving and quantization of the data bits for UE k. Although the optimal value of $R_{k,j}^{(\mathrm{BH})}$ could be obtained by implementing lossless data compression, a.k.a. entropy coding [37, Ch. 5], on this sequence of bits, its computational complexity may be prohibitive for a practical implementation.

Hence, we approximate the backhaul throughput for the proposed quantization approach as

$$R_{k,j}^{(\mathrm{BH})} \simeq \begin{cases} R_k, & j = k\,, \\ \min\left\{R_k,\, r_k^{(q)}\ b_k\right\}, & j \neq k\,. \end{cases} \tag{3.19}$$

In (3.19) we take into account the fact that the serving BS k receives all data bits, whereas each auxiliary BS $j \neq k$ receives only a quantized version of the encoded and modulated stream. In fact, the CU evaluates the scenario and makes for each BS $j \neq k$ the better choice between:

- transmitting at a spectral efficiency R_k all the data for UE k allowing each BS to perform channel coding and then quantization of the QAM constellation;
- performing channel coding only at the CU and then transmitting the sequence of bits representing the quantized QAM symbols (at a spectral efficiency $b_k^{(q)} = r_k^{(q)} b_k$). For instance, if channel coded bits are mapped into QAM symbols by employing Gray mapping [35], only the most significant $b_k^{(q)}$ bits are sent by the CU for each QAM symbol.

Note that this method provides an upper bound for $j \neq k$ on the exact value of the backhaul throughput.

Moreover, note that even when all data bits are shared with auxiliary BSs ($R_{k,j}^{(\mathrm{BH})} = R_k$, $j \neq k$), the constellation used by auxiliary BSs may still be a quantized version of the original constellation (i.e., we may have $b_k^{(q)} < b_k$) in order to properly allocate transmission power among BSs and satisfy power constraints.

On the exact value of the backhaul throughput

In this section we prove that (3.19) is very close to the exact value for typical system configurations.

Let $\boldsymbol{\alpha}_k$ be the sequence of information bits for UE k and $\boldsymbol{\beta}_k$ the sequence of bits after channel coding, interleaving and quantization. We can write

$$\boldsymbol{\beta}_k = \boldsymbol{\Omega}_k^{(q)} \boldsymbol{\Omega}_k^{(c)} \boldsymbol{\alpha}_k = \boldsymbol{\Omega}_k \boldsymbol{\alpha}_k \,, \tag{3.20}$$

where $\boldsymbol{\Omega}_k^{(c)}$ and $\boldsymbol{\Omega}_k^{(q)}$ represent matrices related to channel coding and quantization, respectively, and both additions and multiplications are defined in the binary numeral system. By defining the code rate

$$r_k^{(c)} = \frac{R_k}{b_k} \,, \tag{3.21}$$

and assuming that BSs employ codewords of size N_c, $\boldsymbol{\Omega}_k$ results in a binary matrix of size $N_c r_k^{(q)} \times N_c r_k^{(c)}$. The exact value of the backhaul throughput for $j \neq k$ is

$$R_{k,j}^{(\mathrm{BH})} = \frac{b_k}{N_c} \mathrm{rank}(\boldsymbol{\Omega}_k) \,. \tag{3.22}$$

When $\boldsymbol{\Omega}_k$ is full rank, i.e.,

$$\mathrm{rank}(\boldsymbol{\Omega}_k) = \min\{N_c r_k^{(q)},\, N_c r_k^{(c)}\} \,, \tag{3.23}$$

we obtain exactly (3.19). On the other hand, if $\mathbf{\Omega}_k$ is not full rank we can perform entropy coding on $\boldsymbol{\beta}_k$ to obtain a lower backhaul throughput.

The structure of $\mathbf{\Omega}_k$ mainly depends on the employed channel codes. However, in the following analysis we model $\mathbf{\Omega}_k$ as a binary random matrix for simplicity. As derived in [38], for $r_k^{(c)} \neq r_k^{(q)}$, the probability that $\mathbf{\Omega}_k$ is full rank converges to 1 as the codeword size increases ($N_c \to +\infty$). Moreover, [38] shows that when $r_k^{(c)} = r_k^{(q)}$, the rank of $\mathbf{\Omega}_k$ is close to its maximum value $r_k^{(c)} N_c$ with probability close to 1.

These considerations show that if $\mathbf{\Omega}_k$ could be modeled as a binary random matrix, the probability that the exact value of the required backhaul throughput is lower than (3.19) would vanish as the codeword length N_c increases.

3.4 Quantization optimization and power allocation

In this section we describe the problem of optimizing the constellation size 2^{b_k}, the quantization rate $r_k^{(q)}$ and the power allocation $P_k^{(q)}$ in order to maximize the network spectral efficiency. Let $\mathcal{M}$ be the set of available constellation sizes. Let also $\Psi(b_k)$ be the set of all possible quantization rates associated to the constellation of size 2^{b_k}, i.e.,

$$\Psi(b_k) = \left\{ r_k^{(q)} = \frac{b_k^{(q)}}{b_k} : b_k^{(q)} \in \{0, 1, \ldots, b_k\} \right\}. \tag{3.24}$$

The problem of maximizing the spectral efficiency on the air by optimizing constellation sizes and powers can be written as

$$\begin{aligned} R^{(\mathrm{DATA})} = & \max_{\{2^{b_k} \in \mathcal{M},\, r_k^{(q)} \in \Psi(b_k),\, P_k^{(q)} \geq 0\}} \sum_{k=1}^{K} R_k \\ & \text{subject to (3.1) and (3.16).} \end{aligned} \tag{3.25}$$

We observe that (3.25) is a mixed integer programming problem belonging to NP-hard class due to the presence of discrete variables $r_k^{(q)}$ and b_k and continuous variables $P_k^{(q)}$. The solution to (3.25) can be found only by using standard global solver tools such as LINDOGLOBAL or BARON in GAMS [25].

Note that the optimization in (3.25) is performed only with respect to parameters b_k, $r_k^{(q)}$ and $P_k^{(q)}$. In fact, we assume that beamformers are pre-computed at the CU in order to coordinate ICI, otherwise the optimization problem (3.25) would become too complex. In particular, in Section 3.6 we consider that $\boldsymbol{g}_k$ are designed using the ZF criterion, which is known to provide performance close to that of DPC in MIMO systems [17]. On the other hand, when $M = 1$ (as will be assumed in Section 3.6), $\boldsymbol{w}_k$ is uniquely determined by (3.8). We observe that the beamforming design method has an influence on the system performance, however as outlined by (3.25) we are still left with power and rate allocation.

3.4.1 Solution with equal power allocation

Due to the difficulty of (3.25), we consider a suboptimal solution by assuming that the total power allocated by the BSs to each UE is the same for all the UEs in the network. Under this assumption, we have a simplification of (3.25), which permits a faster solution to the problem. By numerical results in Section 3.6 we will show that this suboptimal solution has close-to-optimum performance. From (3.4) the power used by all BSs to transmit to UE k can be expressed as

$$P_k^{(\mathrm{tot})} = \gamma_k P_k^{(e)} + (1-\gamma_k)\, P_k^{(q)} = P_k^{(q)} \left[\gamma_k \frac{G_k^{(q)}}{G_k^{(e)}} + (1-\gamma_k) \right], \tag{3.26}$$

using (3.11). By imposing that the set of K BSs employ the same power $P^{(\mathrm{EP})}$ for all the UEs, i.e.,

$$P_k^{(\mathrm{tot})} = P^{(\mathrm{EP})}, \quad k = 1, 2, \ldots, K, \tag{3.27}$$

we obtain $P_k^{(q)} = P^{(\mathrm{EP})} G_k$, where

$$G_k = \frac{G_k^{(e)}}{\gamma_k G_k^{(q)} + (1-\gamma_k) G_k^{(e)}}. \tag{3.28}$$

Within this setting, the SINR (3.17) can now be rewritten as

$$\mathrm{SINR}_k^{(\mathrm{EP})} = \frac{P^{(\mathrm{EP})} G_k^{(q)} G_k}{\sigma_n^2 + P^{(\mathrm{EP})} \displaystyle\sum_{j=1, j\neq k}^{K} \left[G_{k,j}^{(I_e)} \frac{G_k^{(q)}}{G_k^{(e)}} \gamma_k + G_{k,j}^{(I_q)} (1-\gamma_k) \right] G_k}, \tag{3.29}$$

and, for fixed b_k and $r_k^{(q)}$, the objective function in (3.25) becomes a non-decreasing function of $P^{(\mathrm{EP})}$. The K per-BS power constraints (3.16) can be expressed as

$$P^{(\mathrm{EP})} \left[\gamma_j \frac{G_j^{(q)}}{G_j^{(e)}} G_j + \sum_{k=1}^{K} V_{k,j} (1-\gamma_k) G_k \right] \leq \bar{P}, \quad j = 1, 2, \ldots, K, \tag{3.30}$$

which can be replaced altogether by an upper bound on $P^{(\mathrm{EP})}$, namely

$$P^{(\mathrm{EP})} \leq \frac{\bar{P}}{\max\limits_{j \in \{1,2,\ldots,K\}} \left\{ \gamma_j \dfrac{G_j^{(q)}}{G_j^{(e)}} G_j + \displaystyle\sum_{k=1}^{K} V_{k,j} (1-\gamma_k) G_k \right\}}. \tag{3.31}$$

After computing the data and backhaul rates by using (3.29) into (3.18) and (3.19),

respectively, problem (3.25) can be reformulated as follows

$$R^{(\mathrm{DATA})} = \max_{\{2^{b_k}\in\mathcal{M},\, r_k^{(q)}\in\Psi(b_k),\, P^{(\mathrm{EP})}\geq 0\}} \sum_{k=1}^{K} R_k \quad \text{subject to (3.1) and (3.31),} \tag{3.32}$$

where now we have a single power level to optimize.

We emphasize that the left-hand side of (3.1) is now a monotonically non-decreasing function in the variable $P^{(\mathrm{EP})}$, as the objective function. As a consequence of these observations, (3.32) can be solved by this simple algorithm:

1) Perform an exhaustive search among the constellation sizes $2^{b_k} \in \mathcal{M}$ and the quantization rates $r_k^{(q)} \in \Psi(b_k)$ assigned to each UE k, with $k \in \{1, 2, \ldots, K\}$.

- **a)** Compute $\tilde{R}^{(\mathrm{DATA})} = \sum_{k=1}^{K} R_k$ by choosing the value of $P^{(\mathrm{EP})}$ that satisfies power constraint (3.31) with equality.
- **b)** Stop if the obtained solution satisfies backhaul constraints (3.1), otherwise compute the maximum value of $P^{(\mathrm{EP})}$ that satisfies (3.1) by employing the bisection method.

2) The solution is the maximum $\tilde{R}^{(\mathrm{DATA})}$ among all the available constellation sizes and quantization rates.

The complexity of this optimization procedure depends mainly on the value of K and on the cardinality of set $\Psi(b_k)$, which is reasonably low in typical cellular scenarios because of the reduced number of used QAM constellations. In any case, the complexity of problem (3.32) is sensibly lower than that of problem (3.25): indeed, the exhaustive search proposed to solve (3.32) becomes prohibitive in the case of (3.25) as, for each value of the quantization parameters, a non-convex optimization problem should be solved instead of implementing the simple bisection method to optimize variable $P^{(\mathrm{EP})}$.

Lastly, note that the proposed algorithm can be applied to more general cases than equal power allocation. In particular, we can set the fraction of the total power allocated to each UE and still obtain an expression similar to (3.31) for the power constraint.

On-off cooperation

In this section we propose a further suboptimal solution to (3.32) obtained by reducing the domain of the discrete variable $r_k^{(q)}$. In particular, BSs may cooperate for the transmission to some UEs, while they may not cooperate for the transmission to other UEs, and when cooperation occurs no quantization is performed. Therefore, in this case we

have $r_k^{(q)} \in \{0,1\}$ and (3.32) can be reformulated as follows

$$R^{(\mathrm{DATA})} = \max_{\{2^{b_k}\in\mathcal{M},\, r_k^{(q)}\in\{0,1\},\, P^{(\mathrm{EP})}\geq 0\}} \sum_{k=1}^{K} R_k \qquad (3.33)$$
$$\text{subject to (3.1) and (3.31).}$$

Problem (3.33) can be solved by applying the algorithm developed in Section 3.4.1, but with a notable computational saving because the exhaustive search is performed only within a subset of the domain of the quantization parameters.

3.5 Theoretical bound

In this section we evaluate the theoretical bound (TB) obtained by considering the extension of [32, 33] to the case of a general number of BSs.

In fact, under the assumption that each UE k treats the other UE signals as interference, i.e., UE k does not decode the messages intended to the other UEs, the backhaul infrastructure provides a communication system that can be modeled as a multiple access channel with a) a common message shared by all the BSs and sent by using beamformer $\boldsymbol{g}_k$ and b) a private message known and sent only by BS k through beamformer $\boldsymbol{w}_k$ [34]. For each UE k we indicate with $P_k^{(p)}$ and $P_k^{(c)}$ the powers used by the serving BS to transmit the private message and by all the BSs jointly to transmit the common message, respectively, and with $R_k^{(p)}$ and $R_k^{(c)}$ the transmission spectral efficiency of the private and the common message, respectively. By employing the Slepian-Wolf transmission scheme we have that spectral efficiency (3.18) and backhaul throughput (3.19) can now be expressed, respectively, for $k = 1, 2, \ldots, K$, as

$$R_k = R_k^{(p)} + R_k^{(c)}\,, \qquad (3.34)$$

and

$$R_{k,j}^{(\mathrm{BH})} = \begin{cases} R_k^{(p)} + R_k^{(c)}, & j = k, \\ R_k^{(c)}, & j \neq k. \end{cases} \qquad (3.35)$$

Including per-BS power constraints and finite-throughput backhaul links, the network spectral efficiency obtained by Slepian-Wolf encoding is the solution to the following optimization problem

$$R^{(\mathrm{DATA})} = \max_{R_k^{(p)}\geq 0\,, R_k^{(c)}\geq 0\,, P_k^{(p)}\geq 0\,, P_k^{(c)}\geq 0} \sum_{k=1}^{K} \left(R_k^{(p)} + R_k^{(c)}\right) \qquad (3.36a)$$

subject to

$$R_j^{(p)} + \sum_{k=1}^{K} R_k^{(c)} \leq \bar{R}^{(\mathrm{BH})}\,, \qquad j = 1, 2, \ldots, K, \tag{3.36b}$$

$$P_j^{(p)} + \sum_{k=1}^{K} V_{k,j} P_k^{(c)} \leq \bar{P}\,, \qquad j = 1, 2, \ldots, K, \tag{3.36c}$$

$$R_k^{(p)} \leq \log_2 \left(1 + \frac{G_k^{(e)} P_k^{(p)}}{\sigma_n^2 + \sum\limits_{j=1, j\neq k}^{K} \left(G_{k,j}^{(I_e)} P_j^{(p)} + G_{k,j}^{(I_q)} P_j^{(c)} \right)} \right), \qquad k = 1, 2, \ldots, K, \tag{3.36d}$$

$$R_k^{(p)} + R_k^{(c)} \leq \log_2 \left(1 + \frac{G_k^{(e)} P_k^{(p)} + G_k^{(q)} P_k^{(c)}}{\sigma_n^2 + \sum\limits_{j=1, j\neq k}^{K} \left(G_{k,j}^{(I_e)} P_j^{(p)} + G_{k,j}^{(I_q)} P_j^{(c)} \right)} \right), \qquad k = 1, 2, \ldots, K. \tag{3.36e}$$

Problem (3.36) is a non-convex optimization problem and can be solved only by using standard global solver tools in GAMS [25].

3.6 Numerical results

We consider the downlink cellular network of Fig. 2.1 with $K = 3$ BSs having $M = 1$ transmitting antenna each, serving 3 single-antenna UEs, which are randomly dropped in the coverage area of their assigned BS. The cell edge size is $d_c = 2$ km. Note that we consider three-sector hexagonal cells and the $K = 3$ BSs involved in the cooperation are three adjacent sectors of different cells. In fact, by assuming directional antennas we neglect in (3.6) the interference due to the BSs not included in the cluster of K cooperative BSs. However, further ICI could be modeled as part of the noise term. The channel includes path loss, shadowing and i.i.d. Rayleigh fading according to (2.20), and the channel simulation parameters are the same considered in Section 2.4. Then, we impose a maximum transmit power $\bar{P} = 40$ dBm and we consider a noise variance $\sigma_n^2 = -108$ dBm resulting in a SNR of 10 dB at the cell edge.

Beamformers $\boldsymbol{g}_k$ are designed using ZF criterion (2.11). Under this assumption, we have no interference due to quantized constellation at each UE k, i.e., $G_{k,j}^{(I_q)} = 0$, $j \neq k$. Then, as each BS is equipped with only one antenna, beamformers $\boldsymbol{w}_k$ result in complex values that only compensate channel phases, i.e., $\boldsymbol{w}_k = \boldsymbol{h}_{k,k}^* / \|\boldsymbol{h}_{k,k}\|$. We consider the constellations used in 3GPP LTE, i.e., $\mathcal{M} = \{\text{QPSK, 16-QAM, 64-QAM}\}$ [2]. For different values of $b_k^{(q)}$, Tab. 3.1 summarizes the corresponding values of γ_k and $r_k^{(q)}$.

2^{b_k}	b_k	$b_k^{(q)}$	$r_k^{(q)}$	γ_k
QPSK	2	0	0	1
QPSK	2	1	1/2	0.5
QPSK	2	2	1	0
16-QAM	4	0	0	1
16-QAM	4	1	1/4	0.6
16-QAM	4	2	1/2	0.2
16-QAM	4	3	3/4	0.1
16-QAM	4	4	1	0
64-QAM	6	0	0	1
64-QAM	6	1	1/6	0.619
64-QAM	6	2	1/3	0.238
64-QAM	6	3	1/2	0.143
64-QAM	6	4	2/3	0.048
64-QAM	6	5	5/6	0.024
64-QAM	6	6	1	0

Table 3.1: Quantization parameters for the 3GPP LTE constellations.

As a consequence, the maximum spectral efficiency for each UE is $b_{\max} = 6$ bit/s/Hz (uncoded 64-QAM) and with $\bar{R}^{(\mathrm{BH})} \geq 18$ bit/s/Hz the constraints on the backhaul links become useless as all the UE data messages may be available to each BS irrespective of channel conditions. The proposed transmission scheme optimized according to (3.25) and (3.32) is denoted as quantized constellation transmission (QCT) using optimal power allocation (OPA) and equal power allocation (EPA), respectively. Similarly, the transmission scheme optimized according to (3.33) is denoted as on-off cooperation (OOC) using EPA. We compare the performance of the proposed solution against the following schemes:

a) FC: in this case all BSs share data of all UEs, i.e., in (3.25)

$$r_k^{(q)} = 1 \text{ and } \gamma_k = 0\,, \quad k = 1, 2, \ldots, K\,. \tag{3.37}$$

As in this configuration $G_{k,j}^{(I_e)} = 0$, $\forall k \neq j$, OPA can be implemented beyond EPA: in fact, problem (3.25) for a given set of constellation sizes and quantization rates turns out to be a convex optimization problem.

b) SCP: in this case transmission is performed only by the serving BS, i.e., in (3.25)

$$r_k^{(q)} = 0 \text{ and } \gamma_k = 1\,, \quad k = 1, 2, \ldots, K\,. \tag{3.38}$$

We assume that with this configuration each BS serves its assigned UE by transmitting at full power $\bar{P}$.

Furthermore, for a proper comparison with the other techniques employing 64-QAM as the most dense constellation, the network spectral efficiency achieved by TB is computed

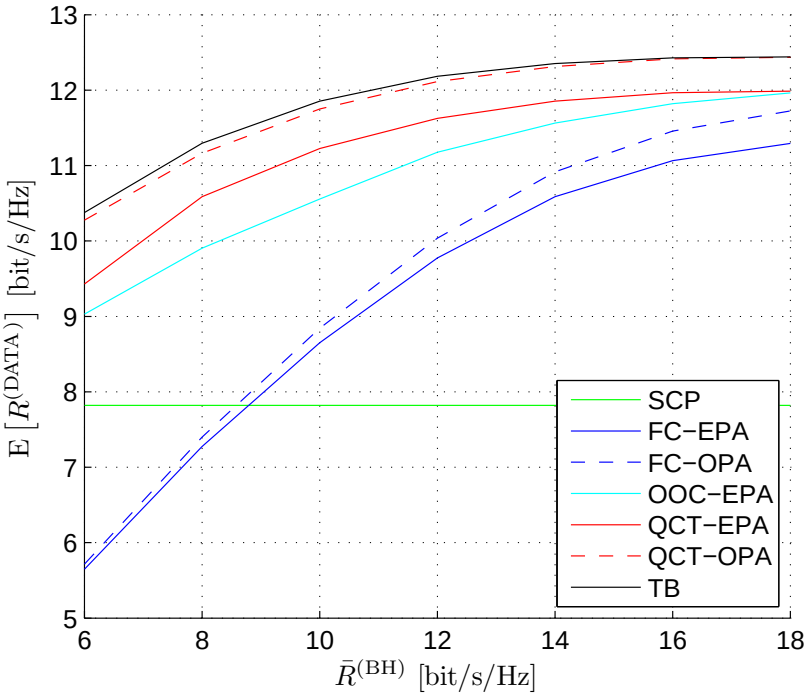

Figure 3.3: Average network spectral efficiency versus the maximum backhaul throughput on each link.

by adding the constraints

$$R_k^{(p)} + R_k^{(c)} \leq b_{\max}\,, \qquad k = 1, 2, \ldots, K, \tag{3.39}$$

to problem (3.36).

Fig. 3.3 shows the average $R^{(\mathrm{DATA})}$ in terms of the maximum backhaul throughput $\bar{R}^{(\mathrm{BH})}$ on each link. The performance of SCP does not depend on the backhaul, as in SCP BSs do not share the UE data and with $\bar{R}^{(\mathrm{BH})} \geq 6$ bit/s/Hz the backhaul constraints become useless. Moreover, TB outperforms all the proposed schemes as expected. Indeed, TB a) achieves optimal power allocation across BSs and b) is not constrained by (3.11). Indeed, with QCT the ratio between the powers used to transmit the quantized constellation symbol and the quantization error can assume values only in a finite set, which depends on the QAM and on the quantization scheme, whereas with TB no constraint is imposed on the power sharing between the private and common messages. We also observe that QCT-EPA performs very close to QCT-OPA, but with a significant computational saving. Moreover, QCT-EPA outperforms all the other suboptimal approaches: in particular, when $\bar{R}^{(\mathrm{BH})}$ is between 6 and 14 bit/s/Hz, QCT-EPA outperforms OOC-EPA showing the merits of quantization when the constraints on the backhaul throughput have a considerable impact. Then, we observe that when backhaul constraints are very restrictive, i.e., $\bar{R}^{(\mathrm{BH})} \leq 9$ bit/s/Hz, FC is outperformed by SCP. Indeed, with FC the CU

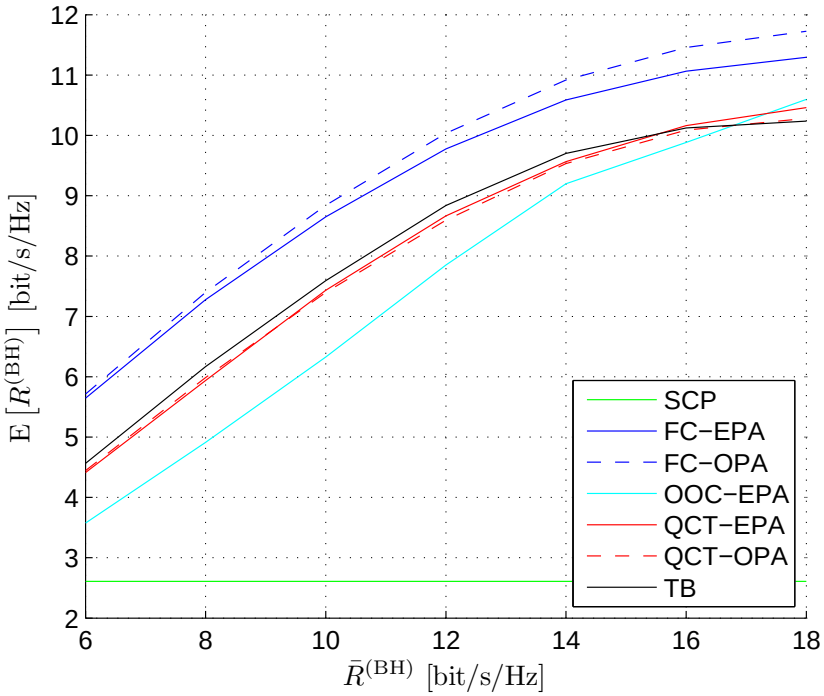

Figure 3.4: Average backhaul throughput versus the maximum backhaul throughput on each link.

sends all UE data to all the BSs and, contrary to the other schemes, the network spectral efficiency is bounded by $\bar{R}^{(\mathrm{BH})}$.

In order to better understand previous results, we report in Fig. 3.4 the average backhaul throughput

$$R^{(\mathrm{BH})} = \frac{1}{K} \sum_{j=1}^{K} \sum_{k=1}^{K} R_{k,j}^{(\mathrm{BH})} \tag{3.40}$$

as a function of the constraint $\bar{R}^{(\mathrm{BH})}$ in the same scenario. As expected, with SCP the average backhaul throughput does not depend on $\bar{R}^{(\mathrm{BH})}$. On the other hand, FC uses all the available backhaul throughput for lower values of $\bar{R}^{(\mathrm{BH})}$ in order to share all UE data and, consequently, is strongly limited by the backhaul constraint. Furthermore, we note that when $\bar{R}^{(\mathrm{BH})}$ is between 6 and 14 bit/s/Hz, a higher network spectral efficiency is achieved both by TB with respect to QCT-EPA and by QCT-EPA with respect to OOC-EPA, thanks to a better usage of the available backhaul.

Note that when we consider EPA and $\bar{R}^{(\mathrm{BH})} = 18$ bit/s/Hz, i.e., full sharing of UE data is allowed among the BSs, FC is outperformed by both QCT and OOC, while OOC is slightly outperformed by QCT. This result is due to the beamformers, which are fixed and not part of the optimization. With FC the BSs serve UEs by using joint ZF beamformers and, for certain channel configurations, this turns out to be a suboptimal solution, because a higher spectral efficiency may be achieved by serving some UEs using the SCP

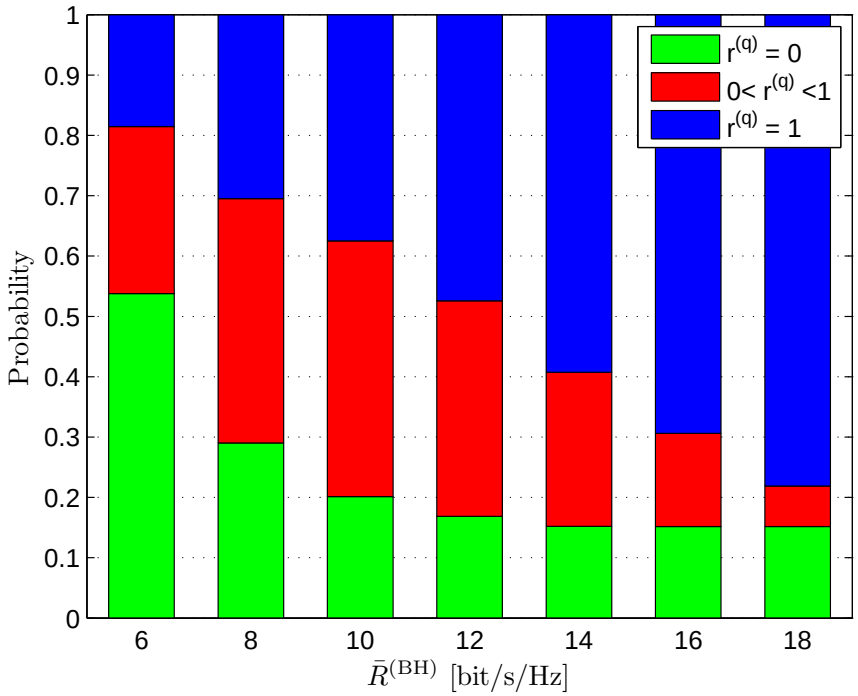

Figure 3.5: Probability distribution of the quantization rate versus the maximum backhaul throughput on each link with QCT-EPA.

mode: note that OOC just performs this kind of selection (3.33). Moreover, QCT slightly outperforms OOC by properly splitting the signal power intended to each UE k between the joint precoder $\boldsymbol{g}_k$ and the precoder $\boldsymbol{w}_k$ used by the anchor BS, adapting to the channel conditions.

The structure of the signal transmitted by the BSs toward UE k with QCT strictly depends on the value of the quantization rate $r_k^{(q)}$. If $r_k^{(q)} = 0$, UE k is served only by BS k and $x_k^{(e)} = x_k$, i.e., no symbol $x_k^{(q)}$ is effectively transmitted. On the other hand, if $r_k^{(q)} = 1$, UE k is served jointly by all the BSs and $x_k^{(q)} = x_k$, i.e., in this case no quantization error symbol is transmitted. Therefore, only when $0 < r_k^{(q)} < 1$ the proposed scheme is effectively exploited with a quantized symbol transmitted jointly and the quantization error sent only by the anchor BS. Fig. 3.5 shows for QCT-EPA the probability distribution of the quantization rate $r_k^{(q)}$ in terms of the maximum backhaul throughput $\bar{R}^{(\mathrm{BH})}$. We observe that the QAM quantization is well exploited for lower values of $\bar{R}^{(\mathrm{BH})}$, e.g., about 45% for $\bar{R}^{(\mathrm{BH})} = 10$ bit/s/Hz. On the other hand, for higher values of $\bar{R}^{(\mathrm{BH})}$ the QAM quantization is not used very often: this also explains why in Fig. 3.3 QCT-EPA outperforms OOC-EPA when the constraint on the backhaul throughput is strict, whereas the gain is almost null when the backhaul constraint is loose.

Fig. 3.6 shows the CDF of $R^{(\mathrm{DATA})}$ for QCT-EPA and TB for different values of $\bar{R}^{(\mathrm{BH})}$. For higher values of $\bar{R}^{(\mathrm{BH})}$ the network spectral efficiency of QCT-EPA is quite close to

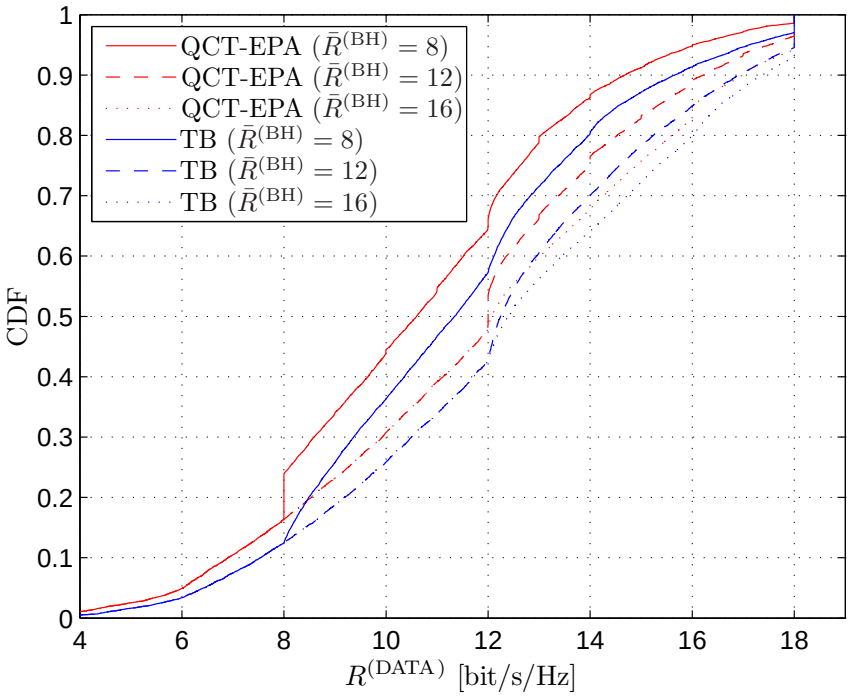

Figure 3.6: CDF of the network spectral efficiency achieved by QCT-EPA and TB for different values of the maximum backhaul throughput on each link.

that of TB, whereas for lower values of $\bar{R}^{(\mathrm{BH})}$ the performance gain of TB becomes more important.

3.7 Conclusions

In this chapter we have considered a downlink CoMP scenario with a constraint on the capacity of the backhaul infrastructure and we have proposed a transmission scheme based on the quantization of QAM constellations at the auxiliary BSs in order to satisfy backhaul requirements. Numerical results show that the proposed approach outperforms methods in which cooperative BSs are allowed to share only full UE data, showing the merits of QCT. Moreover, the proposed solution approaches the performance of the theoretical bound given by the Slepian-Wolf encoding. Finally, we emphasize that QCT requires slight modifications of existing standards employing beamforming and QAM.

Chapter 4

Dynamic joint clustering and scheduling in downlink CoMP

As described in the previous chapters, cooperation among BSs provides a very high gain with respect to SCP by reducing ICI [5] and the best performance is achieved when FC among all the BSs in the network is allowed [6]. However, many implementation issues make CoMP systems still challenging.

A first important problem is the imperfect CSI at the BSs due to limited bandwidth available for the feedback channel in FDD systems and noise on channel estimation in time division duplex TDD systems. Then, delay and bandwidth constraints in the backhaul limit the sharing of data and CSI among the BSs. Hence, to deal with both these issues clustering is typically used: a CU organizes BSs in clusters and schedules, for each cluster and in each time slot, a subset of UEs. However, even if intra-cluster interference can be mitigated by using cooperative transmission techniques within the cluster, UEs at the cluster border suffer strong inter-cluster interference.

While in the previous chapters UE scheduling is not considered, perfect CSI is assumed at the CU and clusters are selected by an exhaustive search (see Section 2.3), in this chapter we consider a more realistic downlink CoMP system with many UEs per cell and many BSs in the network, and study the problem of dynamic joint clustering and scheduling by also assuming limited CSI at the BSs.

Several schemes have been developed in literature to optimize clusters and reduce inter-cluster interference. In [39] static clustering with block diagonalization is considered and precoders are designed in each cluster by nulling the interference toward UEs of neighbouring clusters close to the border. A more flexible solution is obtained with dynamic clustering [22, 27] where the set of clusters changes over time by adapting to the system conditions. A greedy algorithm is developed in [22] where each cluster is formed in two steps: the first BS is selected randomly to guarantee fairness and the other cooperative BSs are optimally selected to maximize joint capacity within the cluster. In [27] a set of candidate clusterings is generated off-line depending on average UE distribution and

channel conditions, and, in each time slot, the best clustering among these candidates is selected. Clustering has also been studied in [40, 41, 42] in order to serve a set of scheduled UEs, i.e., with scheduling performed before clustering. The set of clusters is optimized by maximizing the increase in the achievable UE rate in [40] and by minimizing the interference power in [40, 41], whereas in [42] a BS negotiation algorithm is designed for cluster formation by considering a fixed cluster size. In [43] active clusters are selected by minimizing an overall cost function among a set of candidates which depends on UE average received power. A framework for feedback and backhaul reduction is developed in [44] where each UE feeds back CSI only to a subset of BSs and the clusters are formed by grouping together UEs associated to the same subset of BSs. In [45] a greedy scheduling algorithm with overlapping clusters is proposed where precoders are designed by considering the signal to caused interference maximization criterion.

Differently from other recent works on clustering where a simple round robin scheduler is used, in this chapter we develop an algorithm to jointly optimize clustering and scheduling. By defining a subset of preferred BSs for each UE, we assume that the CU can group BSs by using only these predetermined clusters. After estimating a weighted sum rate for each cluster, the problem of selecting the set of non-overlapping clusters in each time slot is formulated by maximizing the system weighted sum rate. As the optimization problem turns out to be NP-complete, we solve it by using a simple greedy algorithm. Numerical results show a) the gain of the developed approach with respect to schemes employing static clustering and b) a comparison among two criteria used to select the candidate clusters and three different configurations for the UEs that can be scheduled in each cluster.

4.1 System model

We consider a system where a set $\mathcal{J} = \{1, 2, \ldots, J\}$ of BSs, each equipped with M antennas, is serving a set $\mathcal{K} = \{1, 2, \ldots, K\}$ of single-antenna UEs. Differently from Chapters 2 and 3 where $K = J$, we assume that $K \geq JM$: hence, not all the UEs can be served at the same time and UE scheduling is part of the optimization problem. We denote with $\boldsymbol{h}_{k,j}(t) \sim \mathcal{CN}\left(\mathbf{0}_{M\times 1}, \sigma^2_{k,j}\boldsymbol{I}_M\right)$ the channel between UE k and BS j at time $t = 1, 2, \ldots, T$.

We define for each UE k the anchor BS j_k characterized by the highest average SNR, i.e.,

$$j_k = \underset{j\in\mathcal{J}}{\operatorname{argmax}}\ \sigma^2_{k,j}\,. \tag{4.1}$$

We assume that only the channels between UE k and a subset of *preferred* BSs $\mathcal{J}_k \subseteq \mathcal{J}$ are known at the CU, with $j_k \in \mathcal{J}_k$. Note that this assumption may be applied to both TDD (where $\mathcal{J}_k$ is the subset of BSs where channel estimation is reliable) and FDD (where $\mathcal{J}_k$ is the subset of BSs to whom UE k report CSI). We consider that $\mathcal{J}_k$ selection is based

on the large scale fading and we utilize the flexible criteria proposed in [46]:

- absolute threshold (AT): $\mathcal{J}_k$ includes all the BSs whose average SNR is above a certain threshold γ_{TH}, i.e.,

$$\mathcal{J}_k^{(\mathrm{AT})} = \{j_k\} \cup \left\{ j \in \mathcal{J} : \sigma_{k,j}^2 \geq \gamma_{\mathrm{TH}} \right\} , \tag{4.2}$$

- relative threshold (RT): $\mathcal{J}_k$ includes all the BSs whose average SNR is within a certain range ϵ_{TH} with respect to the SNR between UE k and its anchor BS, i.e.,

$$\mathcal{J}_k^{(\mathrm{RT})} = \{j_k\} \cup \left\{ j \in \mathcal{J} : \sigma_{k,j}^2 \geq \epsilon_{\mathrm{TH}}\, \sigma_{k,j_k}^2 \right\} . \tag{4.3}$$

Note that both in (4.2) and (4.3) a better CSI can be recovered by the CU by selecting a lower value of γ_{TH} and ϵ_{TH}, respectively. However, in a practical system these thresholds mainly depend on the coherence time of the channel, which is related to UE mobility, the number M of transmitting antennas and the number K of UEs that need to be served.

Moreover, by denoting with $\hat{\boldsymbol{h}}_{k,j}$ the channel estimated/reconstructed at the BSs, we assume that channels between UE k and BSs in $\mathcal{J}_k$ are known without errors, i.e.,

$$\hat{\boldsymbol{h}}_{k,j}(t) = \begin{cases} \boldsymbol{h}_{k,j}(t), & j \in \mathcal{J}_k\,, \\ \mathbf{0}_{M\times 1}, & \text{otherwise}\,. \end{cases} \tag{4.4}$$

4.2 Joint clustering scheduling algorithm

In the following the term *clustering* denotes a set of non-overlapping clusters, i.e., where each BS may be included in only one cluster.

By considering a maximum cluster size of J_{MAX}, it can be shown that the number of possible clusters is

$$\sum_{j=1}^{J_{\mathrm{MAX}}} \binom{J}{j} . \tag{4.5}$$

This number increases with J and, when $J_{\mathrm{MAX}} = J$, (4.5) becomes $2^J - 1$ making unfeasible the evaluation at the CU of all the possible clusterings (with $J = 21$ there are about 10^6 possible clusters).

However, due to practical implementation issues, only clusters made by neighbouring BSs can be considered. For this reason, we assume that the CU can organize BSs by using only a maximum of C candidate clusters and indicate with $\mathcal{C}_c \subseteq \mathcal{J}$, $c = 1, 2, \ldots, C$, the c-th cluster, and with $\mathcal{C} = \{\mathcal{C}_1, \mathcal{C}_2, \ldots, \mathcal{C}_C\}$ the set collecting all the candidate clusters at the CU. We consider that $\mathcal{C}$ is designed at the CU by including all and only the set of BSs indicated by the UEs (see (4.2) and (4.3)), i.e.,

$$\forall c = 1, 2, \ldots, C,\ \exists k \in \mathcal{K} : \mathcal{C}_c = \mathcal{J}_k\,. \tag{4.6}$$

We denote with $\mathcal{U}_c$ the set of UEs that can be scheduled in cluster c, and in the following we compare three different configurations for set $\mathcal{U}_c$ that can be expressed as:

$$\mathcal{U}_c^{(\mathrm{I})} = \{k \in \mathcal{K} : \mathcal{J}_k = \mathcal{C}_c\} \ , \tag{4.7a}$$

$$\mathcal{U}_c^{(\mathrm{II})} = \{k \in \mathcal{K} : \mathcal{J}_k \subseteq \mathcal{C}_c\} \ , \tag{4.7b}$$

$$\mathcal{U}_c^{(\mathrm{III})} = \{k \in \mathcal{K} : j_k \in \mathcal{C}_c\} \ , \tag{4.7c}$$

where $\mathcal{U}_c^{(i)}$ denotes the set $\mathcal{U}_c$ in configuration $i \in \{\mathrm{I}, \mathrm{II}, \mathrm{III}\}$. Note that $\mathcal{U}_c^{(\mathrm{I})} \subseteq \mathcal{U}_c^{(\mathrm{II})} \subseteq \mathcal{U}_c^{(\mathrm{III})}$. These three configurations provide a different multiuser diversity within each cluster and a different level of inter-cluster interference suffered by the scheduled UEs. In detail, in configuration I, UEs with the same set of preferred BSs are grouped together and, by construction, $\mathcal{U}_c^{(\mathrm{I})} \cap \mathcal{U}_{c'}^{(\mathrm{I})} = \emptyset$, $\forall c \neq c'$. This approach is the one considered in [44, 46] where however no clustering optimization is performed at the CU by considering a simple round robin technique. In configuration II, $\mathcal{U}_c^{(\mathrm{II})}$ comprises all the UEs whose set of preferred BSs is *included* in the cluster $\mathcal{C}_c$. Note that in both configurations I and II and under the assumption of limited CSI (4.4), no inter-cluster interference can be estimated/predicted at the CU: in fact, channels between UEs scheduled in cluster c and BSs that do not belong to this cluster are not known at the CU. Finally, $\mathcal{U}_c^{(\mathrm{III})}$ comprises all the UEs whose anchor BS is included in cluster $\mathcal{C}_c$.

While the above association is based on the large scale fading, we focus now on the problem of finding, for each fading realization, the optimal clustering that maximizes the system weighted sum rate. In detail, the CU at time $t = 1, 2, \ldots, T$, a) determines for each candidate cluster c (independently of all the other clusters $c' \neq c$) a subset of UEs $\mathcal{S}_c(t) \subseteq \mathcal{U}_c$ which are scheduled if the c-th cluster is included in the optimal clustering, and b) estimates a weighted sum-rate $\hat{R}_c(t)$ depending on its channel knowledge (4.4). In fact, the CU solves the following optimization problem

$$\hat{R}_c(t) = \max_{\mathcal{S}_c(t) \subseteq \mathcal{U}_c} \sum_{k \in \mathcal{S}_c(t)} \alpha_k(t) \log_2 \left(1 + \hat{\mathrm{SINR}}_k(t)\right) \ , \quad c = 1, 2, \ldots, C \, , \tag{4.8}$$

where $\alpha_k(t)$ and $\hat{\mathrm{SINR}}_k(t)$ are the quality of service (QoS) and the SINR evaluated at the CU for UE k at time t, respectively. The computation of both $\mathcal{S}_c(t)$ and $\hat{R}_c(t)$ can be performed by considering any kind of scheduler and precoder. However, in Section 4.3 we optimize these parameters in the particular case of ZF beamforming with EPA among the UEs, which are selected by using a greedy user selection algorithm. We define the following two quantities:

$$a_{jc} = \begin{cases} 1, & j \in \mathcal{C}_c, \\ 0, & \text{otherwise}, \end{cases} \tag{4.9}$$

$$x_c(t) = \begin{cases} 1, & c\text{-th cluster scheduled at time } t, \\ 0, & \text{otherwise.} \end{cases} \tag{4.10}$$

The optimal clustering is the solution to the following integer optimization problem (which needs to be solved at each time t)

$$\max_{x_c(t)\in\{0,1\}} \sum_{c=1}^{C} \hat{R}_c(t)\, x_c(t)\,, \tag{4.11a}$$

subject to

$$\sum_{c=1}^{C} a_{jc}\, x_c(t) \leq 1\,,\ j \in \mathcal{J}\,. \tag{4.11b}$$

Differently from [43] where the objective function simply depends on the received power measured by the UEs, here (4.11a) constructs the clustering with the aim of maximizing the system weighted sum rate by implicitly considering scheduling and precoding design in the computation of $\hat{R}_c(t)$ (4.8). Note that (4.11b) forces each BS j to belong to at most one cluster at each time t in the optimal clustering solution (non-overlapping condition). By indicating with $x_c^{(*)}(t)$ the solution to (4.11), the set $\mathcal{S}(t)$ of UEs scheduled at time t can be written as

$$\mathcal{S}(t) = \bigcup_{c\,:\,x_c^{(*)}(t)=1} \mathcal{S}_c(t)\,. \tag{4.12}$$

By defining

$$y_c(t) = 1 - x_c(t)\,,\ c = 1, 2, \ldots, C\,, \tag{4.13a}$$

$$b_j = \sum_{c=1}^{C} a_{jc} - 1\,,\ j \in \mathcal{J}\,, \tag{4.13b}$$

problem (4.11) can be rewritten as

$$\min_{y_c(t)\in\{0,1\}} \sum_{c=1}^{C} \hat{R}_c(t)\, y_c(t)\,, \tag{4.14a}$$

subject to

$$\sum_{c=1}^{C} a_{jc}\, y_c(t) \geq b_j\,, \quad j \in \mathcal{J}\,. \tag{4.14b}$$

Problem (4.14), which is only another formulation of (4.11), is an integer optimization problem and, when $b_j = 1$, $\forall j \in \mathcal{J}$, becomes the *set covering problem*, which is known in literature to be NP-complete [47]. Therefore, an exhaustive search may be an impractical way to find the solution to (4.11).

Algorithm 2 Greedy Cluster Selection

1: $\mathcal{C}^{(\mathrm{A})} \leftarrow \{1, 2, \ldots, C\}$
2: $x_c^{(*)}(t) \leftarrow 0,\ c \in \mathcal{C}^{(\mathrm{A})}$
3: **while** $\mathcal{C}^{(\mathrm{A})} \neq \emptyset$ **do**
4: $\quad \eta \leftarrow \underset{c \in \mathcal{C}^{(\mathrm{A})}}{\operatorname{argmax}} \hat{R}_c(t) / |\mathcal{C}_c|$
5: $\quad x_\eta^{(*)}(t) \leftarrow 1$
6: $\quad \mathcal{C}^{(\mathrm{A})} \leftarrow \mathcal{C}^{(\mathrm{A})} \setminus \bigcup_{c' : \mathcal{C}_{c'} \cap \mathcal{C}_\eta \neq \emptyset} \{c'\}$
7: **end while**

4.2.1 Solution by a greedy cluster selection

We propose to solve (4.11) by using a greedy iterative algorithm which is reported in Algorithm 2. At each iteration, we define the set $\mathcal{C}^{(\mathrm{A})} \subseteq \mathcal{C}$ which includes all the candidate clusters that do not overlap with the clusters scheduled in the previous iterations. Then, at each iteration we select the cluster in $\mathcal{C}^{(\mathrm{A})}$ that maximizes the per-BS weighted sum rate. We start at the first iteration by imposing $\mathcal{C}^{(\mathrm{A})} = \mathcal{C}$ and the algorithm stops when set $\mathcal{C}^{(\mathrm{A})}$ is empty.

Note that working assumption (4.6) allows an efficient implementation of Algorithm 2 by strongly limiting the number C of candidate clusters available at the CU: indeed, for high J and without assumption (4.6) the complexity of Algorithm 2 would be prohibitive. As an example, for a typical scenario with $J = 21$ BSs (7 sites with 3 sectors per site as in Fig. 4.1), $J_{\mathrm{MAX}} = 4$ and 10 UEs per BS, the total number of possible clusters (4.5) is 7546, whereas in our framework the number of candidate clusters is upper bounded by the number of UEs in the network, i.e., $C \leq KJ = 210$, thus allowing an important computational saving. However, due to (4.6), it might happen that the optimal solution to (4.11) does not include all the BSs, i.e., some BSs may be switched off.

4.3 Scheduling and beamforming design in each cluster

In this section we drop the time index t with the aim of simplifying notation. Let us define function $\Psi_c : \{1, 2, \ldots, |\mathcal{C}_c|\} \rightarrow \mathcal{J}$ which maps each BS in the c-th cluster to the set $\mathcal{J}$ collecting all the BSs in the network. Then, we denote with

$$\hat{\boldsymbol{h}}_k^{(c)} = \left[\hat{\boldsymbol{h}}_{k,\Psi_c(1)}^T, \hat{\boldsymbol{h}}_{k,\Psi_c(2)}^T, \ldots, \hat{\boldsymbol{h}}_{k,\Psi_c(|\mathcal{C}_c|)}^T\right]^T, \tag{4.15}$$

the vector collecting all the estimated channels (4.4) between UE k and c-th cluster, with

$$\boldsymbol{g}_k^{(c)} = \left[\boldsymbol{g}_{k,\Psi_c(1)}^T, \boldsymbol{g}_{k,\Psi_c(2)}^T, \ldots, \boldsymbol{g}_{k,\Psi_c(|\mathcal{C}_c|)}^T\right]^T, \tag{4.16}$$

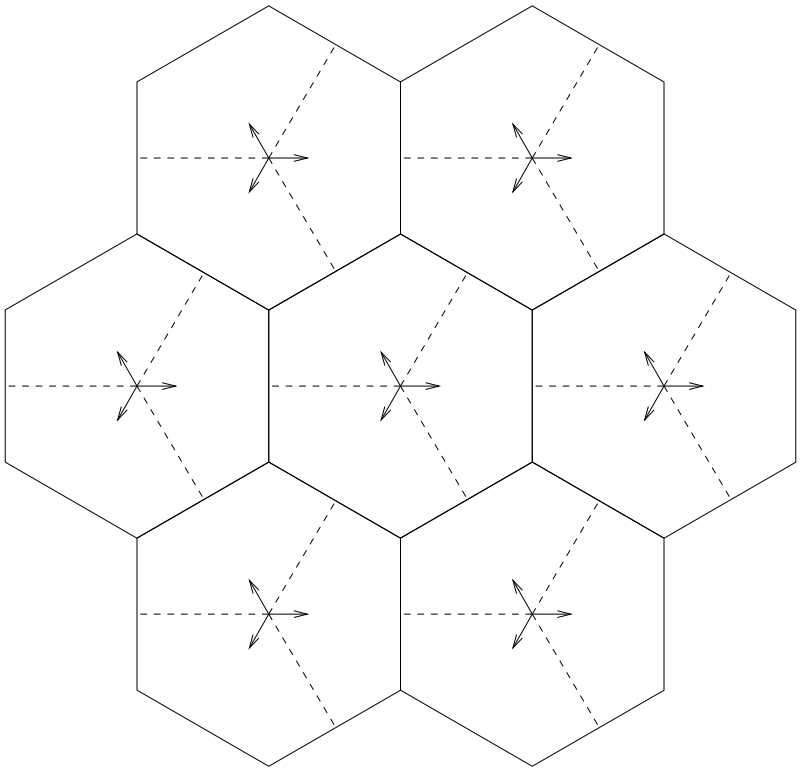

Figure 4.1: Cellular scenario with $J = 21$ BSs grouped in 7 sites each one with 3 co-located BSs.

the unitary-norm precoder used by BSs in c-th cluster to serve UE k and with P_k the power allocated to this UE. The SINR estimated at the CU for UE k can be written as

$$\hat{\text{SINR}}_k = \frac{\left|\hat{\boldsymbol{h}}_k^{(c)T}\boldsymbol{g}_k^{(c)}\right|^2 P_k}{\sigma_n^2 + \xi_k + \sum\limits_{m\in\mathcal{S}_c, m\neq k}\left|\hat{\boldsymbol{h}}_k^{(c)T}\boldsymbol{g}_m^{(c)}\right|^2 P_m}\,, \tag{4.17}$$

where σ_n^2 and ξ_k are the thermal noise power and the inter-cluster interference power estimated at the BSs, respectively. By considering a maximum power $\bar{P}$ available at each BS, the weighted sum rate $\hat{R}_c$ evaluated in the c-th cluster is the solution to the following optimization problem

$$\hat{R}_c = \max_{P_k, \boldsymbol{g}_k^{(c)}, \mathcal{S}_c\subseteq\mathcal{U}_c} \sum_{k\in\mathcal{S}_c} \alpha_k \log_2\left(1 + \hat{\text{SINR}}_k\right)\,, \tag{4.18a}$$

subject to

$$\sum_{k\in\mathcal{S}_c} \|\boldsymbol{g}_{k,j}\|^2 P_k \leq \bar{P}\,, \quad j \in \mathcal{C}_c\,. \tag{4.18b}$$

A special comment has to be provided for the evaluation of ξ_k. In both configurations I and II all the UEs that can be scheduled and served in the c-th cluster suffer low inter-

cluster interference because the set of preferred BSs for each UE belonging to set $\mathcal{U}_c$ is equal to (in configuration I) or a subset of (in configuration II) set $\mathcal{C}_c$. Hence, in these scenarios, if $\xi_k^{(i)}$ is the estimated interference power for UE k when configuration $i \in \{\text{I, II, III}\}$ is considered, we simply impose

$$\xi_k^{(\text{I})} = \xi_k^{(\text{II})} = 0\,. \tag{4.19}$$

On the other hand, in configuration III it might happen that the subset of preferred BSs of a certain UE k is not included in $\mathcal{C}_c$, i.e., $\mathcal{J}_k \setminus \mathcal{C}_c \neq \emptyset$. In this case the CU is aware of the interference ξ_k suffered by UE k, but its exact expression depends on the clustering solution to (4.11), i.e., on the clusters scheduled together with c. Hence, to compute $\hat{R}_c$ independently of the other clusters, we simply approximate

$$\xi_k^{(\text{III})} = \frac{\bar{P}}{M} \sum_{j \in \mathcal{J}_k \setminus \mathcal{C}_c} \left\| \hat{\boldsymbol{h}}_{k,j} \right\|^2 . \tag{4.20}$$

Note that (4.20) is the average interference suffered by UE k from the preferred BSs outside cluster c when each interfering BS serves alone only one UE by using MRT precoding.

We solve (4.18) under the following assumptions.

- Equal power is allocated among the UEs scheduled in the same cluster, i.e., $P_k = P^{(c)}$, $k \in \mathcal{S}_c$, where $P^{(c)}$ is analytically computed from (4.18b) as

$$P^{(c)} = \frac{\bar{P}}{\max\limits_{j \in \mathcal{C}_c} \sum\limits_{k \in \mathcal{S}_c} \| \boldsymbol{g}_{k,j} | \, |^2} . \tag{4.21}$$

- ZF is the criterion used to design precoders with the aim of mitigating intra-cluster interference, i.e., from Section 2.2.2 the precoder used to serve UE $k \in \mathcal{S}_c$ is computed by imposing

$$\hat{\boldsymbol{h}}_m^{(c)T} \boldsymbol{g}_k^{(c)} = 0\,, \quad m \in \mathcal{S}_c \setminus \{k\}\ . \tag{4.22}$$

- The set $\mathcal{S}_c$ of scheduled UEs is determined by using a greedy algorithm where, at each iteration, the best UE in $\mathcal{U}_c$ not yet included in $\mathcal{S}_c$ is added to $\mathcal{S}_c$ only if the weighted sum rate $\hat{R}_c$ increases. Due to the limited number of antennas at the BSs, a maximum of $M\,|\mathcal{C}_c|$ UEs can be scheduled in the c-th cluster. Moreover, at the first iteration of this algorithm the best UE included in $\mathcal{S}_c$ is selected by considering MRT precoding, i.e., from Section 2.2.1 for UE $k \in \mathcal{U}_c$, $\forall j \in \mathcal{C}_c \cap \mathcal{J}_k$, we have

$$\boldsymbol{g}_{k,j}^{(c)} = \sqrt{\bar{P}} \hat{\boldsymbol{h}}_{k,j}^* / \left\| \hat{\boldsymbol{h}}_{k,j} \right\| . \tag{4.23}$$

4.4 Numerical results

We consider an hexagonal cellular scenario with $J = 21$ BSs where 3 BSs, each equipped with $M = 2$ antennas, are co-located in each site (see also Fig. 4.1) and 10 UEs are uniformly dropped in the coverage area of each BS. The power available at each BS is $\bar{P} = 46$ dBm and the thermal noise power at the UE is $\sigma_n^2 = -101$ dBm.

The channel between UE k and the m-th antenna of BS j can be written as

$$[\boldsymbol{h}_{k,j}]_m = \psi_{k,j,m}\sqrt{\Gamma_0\,[d_0/d_{k,j}]^{\eta}\,e^{\zeta_{k,j}}\,A(\theta_{k,j})}\,, \tag{4.24}$$

where $\psi_{k,j,m} \sim \mathcal{CN}(0,1)$ is the fast fading component, $\Gamma_0[d_0/d_{k,j}]^{\eta}$ represents the path-loss where $d_{k,j}$ is the distance between UE k and BS j, $\eta = 3.5$ is the path-loss coefficient and Γ_0 is an average reference SNR when UE k is at distance d_0 from BS j, $e^{\zeta_{k,j}}$ is the lognormal shadowing with 8 dB as standard deviation and $A(\theta_{k,j})$ models the antenna gain as a function of the direction $\theta_{k,j}$ of UE k with respect to the antennas of BS j. As we are considering a system with 3 sectors on each site, the antenna gain can be written as

$$A(\theta_{k,j})\big|_{\mathrm{dB}} = -\min\left\{12\,(\theta_{k,j}/\theta_{3\mathrm{dB}})^2\,, A_s\right\}\,, \tag{4.25}$$

where $\theta_{3\mathrm{dB}} = (70/180)\pi$ and $A_s\big|_{\mathrm{dB}} = 20$ dB [2, Ch. 21]. We consider an inter-site distance of 500 m and a SNR at the cell edge of 10 dB, where the SNR at the cell edge is defined as the SNR measured by a UE at the vertex of the hexagon when only path-loss is included in the channel model. Moreover, we assume a minimum distance $d_{\min} = 35$ m between BSs and UEs, i.e., $d_{k,j} \geq d_{\min}$. Wraparound [48] is used to deal with boundary effects.

The QoS $\alpha_k(t)$ are computed by considering proportional fair scheduling (PFS) [11], i.e., $\alpha_k(t) = 1/R_k^{(\mathrm{av})}(t)$ with $R_k^{(\mathrm{av})}(t+1) = (1-\gamma)R_k^{(\mathrm{av})}(t) + \gamma R_k(t)$, where $\gamma = 0.1$ is the forgetting factor and $R_k(t)$ is the rate achieved by UE k at time t. Note that $R_k(t) = 0$, $k \notin \mathcal{S}(t)$. When UE k is scheduled at time t, the achieved spectral efficiency can be written as

$$R_k(t) = \log_2\left(1 + \frac{\left|\boldsymbol{h}_k^T(t)\boldsymbol{g}_k(t)\right|^2 P_k(t)}{\sigma_n^2 + \sum\limits_{m\in\mathcal{S}(t),m\neq k}\left|\boldsymbol{h}_k^T(t)\boldsymbol{g}_m(t)\right|^2 P_m(t)}\right)\,, \tag{4.26}$$

where $\boldsymbol{h}_k(t) = \left[\boldsymbol{h}_{k,1}^T(t), \boldsymbol{h}_{k,2}^T(t), \ldots, \boldsymbol{h}_{k,J}^T(t)\right]^T$ and $\boldsymbol{g}_k = \left[\boldsymbol{g}_{k,1}^T(t), \boldsymbol{g}_{k,2}^T(t), \ldots, \boldsymbol{g}_{k,J}^T(t)\right]^T$. The QoS for UE k is initialized by using an estimate of the average spectral efficiency, i.e., $R_k^{(\mathrm{av})}(1) = \log_2\left(1 + \sigma_{k,j_k}^2\right)$.

The results are obtained by considering 100 UE drops and $T = 200$ fading realizations for each UE drop. To allow the system to reach a steady state, we compute the average (with respect to fading) UE rate by considering only the last $T/2$ channels for each UE

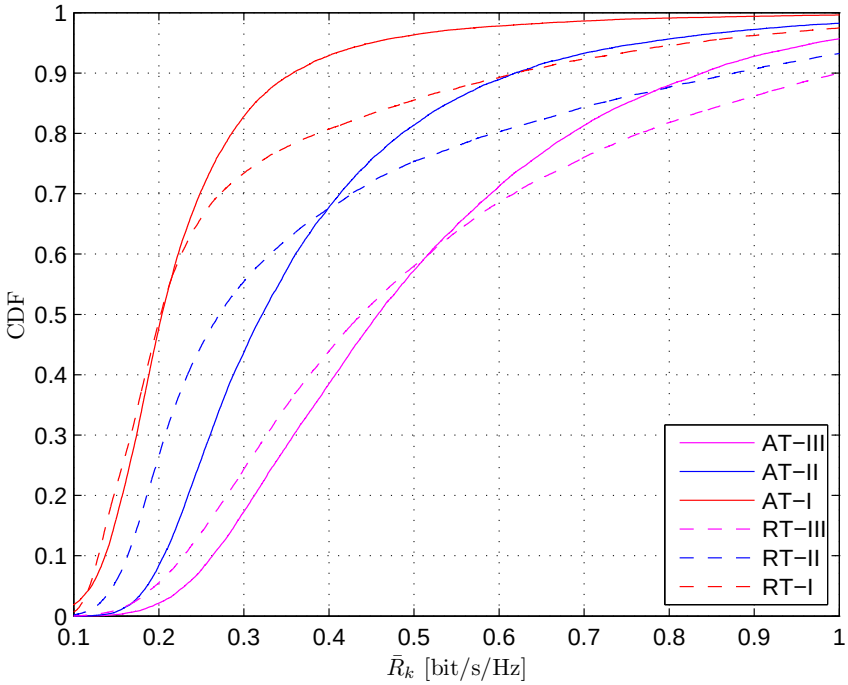

Figure 4.2: CDF of the UE rate $\bar{R}_k$ with AT and RT for $\mathcal{J}_k$ selection and configurations I, II and III for UE scheduling.

drop [49], i.e.,

$$\bar{R}_k = \frac{2}{T} \sum_{t=T/2+1}^{T} R_k(t)\,. \tag{4.27}$$

The developed dynamic clustering scheduling algorithm is compared in terms of the UE rate $\bar{R}_k$ against the following schemes:

- single cell processing (SCP): each UE is connected only to its anchor BS, i.e., $\mathcal{J}_k = \{j_k\}$, and no cooperation is allowed among the BSs;
- intra-site cooperation (ISC): each UE is connected to all the 3 BSs of the closest site and static clustering with clusters composed by the 3 co-located BSs is considered;
- full coordination (FC): all the J BSs in the network cooperate with perfect CSI, i.e., $\mathcal{J}_k = \mathcal{J}$, $\forall k \in \mathcal{K}$.

For a fair comparison in terms of average cluster size against ISC, we numerically set the thresholds in (4.2) and (4.3) such that $\mathbb{E}[|\mathcal{J}_k|] = 3$. In the considered simulation setup we obtain $\gamma_{\text{TH}} = 5.39$ dB and $\epsilon_{\text{TH}} = -12.08$ dB. We also observe that typically AT assigns a bigger set $\mathcal{J}_k$ than RT to UEs close to their anchor BS, whereas RT assigns a bigger set $\mathcal{J}_k$ than AT to UEs close to the cell edge.

In Fig. 4.2 we evaluate AT and RT, and the three configurations for UE scheduling defined at the beginning of Section 4.2 by plotting the CDF of the UE rate $\bar{R}_k$. Note that

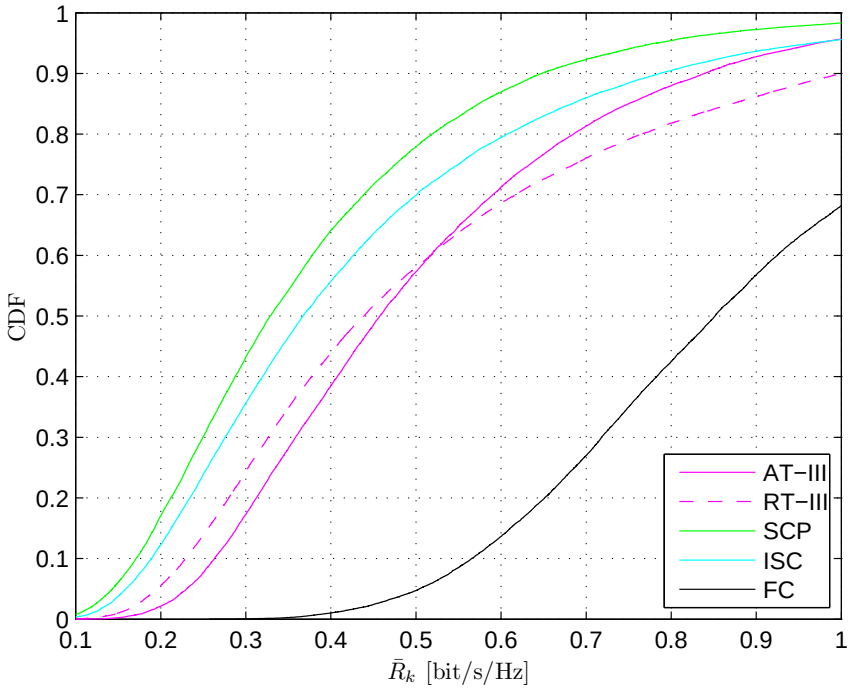

Figure 4.3: CDF of the UE rate $\bar{R}_k$: comparison between the dynamic clustering method and static clustering.

	SCP	ISC	FC	AT-III	RT-III
Average [bit/s/Hz]	0.38	0.44	0.92	0.51	0.54
5th percentile [bit/s/Hz]	0.14	0.16	0.50	0.23	0.20

Table 4.1: Average and 5th percentile of the UE rate $\bar{R}_k$.

the CDF is computed with respect to both the UE index and the UE drop. We observe that configuration III outperforms both configurations I and II. Indeed, in I and II only the UEs far from the cluster border may be served thus limiting the multiuser diversity in each cluster, hence, as we are considering PFS, reducing the average rate achieved by each UE. Moreover, even if AT assigns more BSs to UEs with better SINR conditions, we observe that RT outperforms AT in terms of average UE rate, whereas AT achieves a higher 5th percentile of the UE rate. In fact, with AT criterion PFS schedules the UEs at the cell border more often to guarantee them an acceptable rate and, consequently, less time slots are available to UEs with better SINR conditions. Moreover, we observe that configuration III is more robust than I and II with respect to the choice of the threshold.

In Fig. 4.3 and Tab. 4.1 we observe that AT-III and RT-III outperform ISC, by showing a gain in terms of 5th percentile of the UE rate of about 44% and 25%, respectively. In the considered setup, the performance achieved with FC are still very far. However, note that with FC perfect CSI is available at the CU and UEs are served by only one big cluster that includes all the BSs: hence, interference is completely nulled by employing ZF precoding

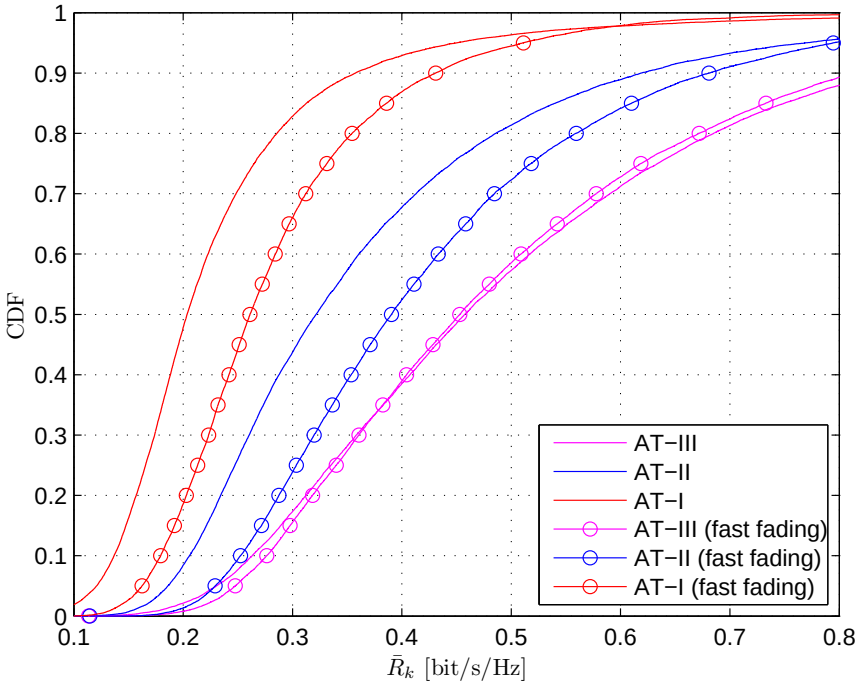

Figure 4.4: CDF of the UE rate $\bar{R}_k$ with AT when $\mathcal{J}_k$ selection depends on the fast fading.

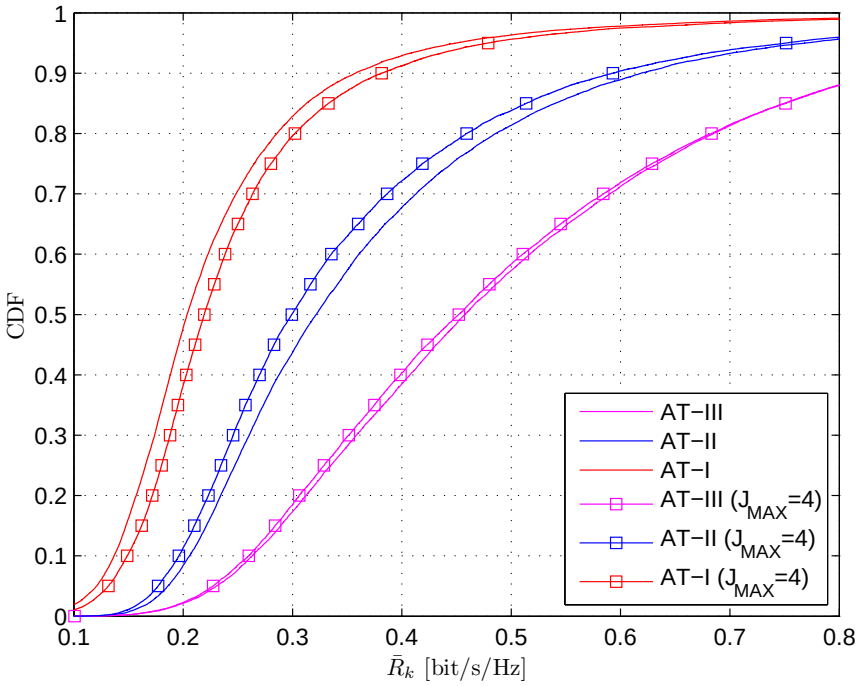

Figure 4.5: CDF of the UE rate $\bar{R}_k$ with AT when $|\mathcal{J}_k| \leq J_{\mathrm{MAX}} = 4$.

among all the BSs in the network.

In Fig. 4.4 we consider a variation of the developed scheme by assuming that the set of candidate clusters changes when fast fading is considered: this is simply obtained by substituting $\|\boldsymbol{h}_{k,j}\|^2/M$ for $\sigma^2_{k,j}$ in (4.1)-(4.3). This variation improves the performance achieved with AT-I and AT-II, but there is almost no gain with AT-III, which still outperforms all the other configurations. Hence, the selection of the candidate clusters based on the large scale fading in (4.6) turns out to be very robust for configuration III, and in a FDD system this results in a reduction of the feedback overhead.

In previous results, we have selected the two thresholds γ_{TH} and ϵ_{TH} by considering an average cluster size of 3. However, from (4.2) and (4.3) there may be candidate clusters scheduled by the CU whose size is much bigger than 3. Hence, to prove that the performance gain achieved by the proposed method with respect to ISC is not due to these big clusters, in Fig. 4.5 we evaluate the performance achieved with AT by assuming a maximum cluster size $J_{\mathrm{MAX}} = \mathbb{E}[|\mathcal{J}_k|] + 1 = 4$: as expected, only a negligible performance loss is observed with AT-III.

Similar results are obtained by substituting RT for AT in Fig.s 4.4 and 4.5.

4.5 Conclusions

In this chapter we have considered the problem of dynamic joint clustering and UE scheduling for downlink CoMP systems with limited CSI. By assuming that the candidate clusters are selected based on UE perspective, we have developed a simple greedy algorithm to select the clustering that maximizes the system weighted sum rate. By comparing different criteria to select the candidate clusters and different configurations for UE scheduling, numerical results show the gain of the proposed approach with respect to static clustering.

Chapter 5

Base station selection and per-cell codebook design in FDD-CoMP

In a FDD system, where downlink and uplink do not use the same frequency band, CSI at the BSs depends on a feedback sent by the UE. Errors due to the imperfect CSI may sensibly degrade or even null the performance gain achieved by the coordination. In non-CoMP systems the codebook-based scheme [50] is the most common feedback strategy: the UE sends back an index related to a codeword in a codebook (agreed with the BS) that best represents the channel.

In [51] a novel bit partitioning algorithm is developed for CoMP-CB, i.e., where BSs are allowed to share only CSI and not data: a different number of bits is allocated to the serving and interfering channels, which are then quantized by using separate codebooks. An extension of this method is developed in [52] by taking into account delays due to both feedback and backhaul transmissions. A joint bit partitioning and beamforming design has been studied in [53, 54]. However, [55] shows that the joint quantization of serving and interfering channels always outperforms methods which employ separate codebooks.

Several works such as [56] have studied the codebook-based strategy applied to a CoMP-JP scenario where each codeword represents the channel connecting the UE to all the cooperative BSs. However, some important implementation issues arise with this strategy: a) very large codebooks need to be stored at the UE, b) change of codebook is required every time the number of cooperative BSs varies and c) codebooks need to be re-designed every time the UE moves to another position in the network. A more flexible solution that partially solves these issues has been developed in [57, 12, 13], where each UE employs per-cell codebooks and optimizes the number of feedback bits assigned to each BS.

In this chapter we focus on CoMP-JP in a FDD scenario and we consider per-cell codebook strategy [57]. Depending on the large scale fading, each UE optimizes the number of feedback bits assigned to each BS and, consequently, the size of the codebook used to quantize each channel. Then, for each fading realization, the UE employs these

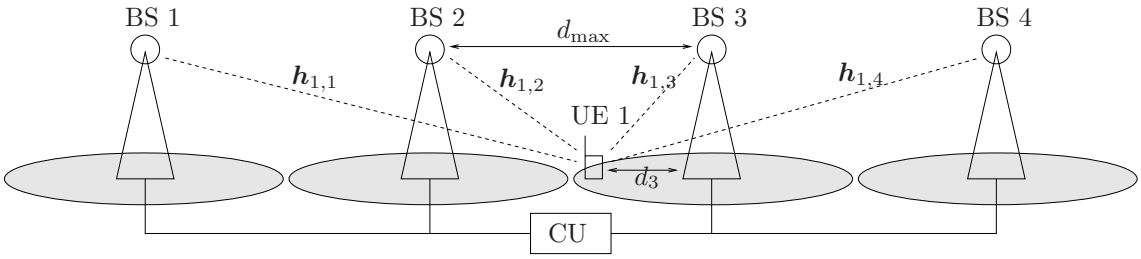

Figure 5.1: CoMP-JP scenario with $J = 4$ BSs serving $K = 1$ UE.

codebooks to jointly select all the codewords, each one representing the channel connecting the UE to a certain BS, and sends back the related indices. Based on this information, a CU that coordinates the BSs can schedule the UEs and compute the beamformers used for downlink transmission.

The main contribution of this chapter is the design of two new algorithms to allocate the feedback bits among the BSs. Differently from [13] where the feedback bits are optimized by maximizing the chordal distance between actual and quantized channels, here we consider as criterion the maximization of the SNR at the UE by assuming MRT and per-BS power constraints. Then, differently from [13], by assuming that only BSs that receive at least one feedback bit are transmitting toward the UE, the developed schemes also allow a selection of the subset of BSs by whom the UE prefers to be served. These two techniques are designed by assuming that for each fading realization the UE independently selects the codewords to represent the channel. However, while the first scheme assumes no phase compensation of the codewords, the second one considers a full compensation of the phase ambiguity. The performance of these two methods are compared in a SU-CoMP scenario and numerical results show a) the flexibility of the proposed techniques that allocate more bits to the strongest channels and b) a performance gain with respect to other techniques where the UE equally splits the feedback bits among the BSs or exploits all the feedback to represent the channel to the closest BS.

5.1 System model

We consider a downlink scenario with J BSs, each equipped with M antennas, transmitting toward K single antenna UEs. We indicate with $\boldsymbol{h}_{k,j} \sim \mathcal{CN}\left(\mathbf{0}_{M\times 1}, \sigma^2_{k,j}\boldsymbol{I}_M\right)$ the channel vector of size $M \times 1$ between UE k and BS j and with $\boldsymbol{h}_k = [\boldsymbol{h}^T_{k,1}, \boldsymbol{h}^T_{k,2}, \ldots, \boldsymbol{h}^T_{k,J}]^T$ the vector collecting the channels between UE k and all the BSs. We consider that BSs are perfectly synchronized in time and frequency and each BS is connected by a free-error and zero-delay backhaul link to a CU that allows full sharing of data and CSI among all BSs (see also Fig. 5.1). As BSs are in general not co-located, we also impose a maximum power $\bar{P}$ available at each BS.

In a FDD system a UE feeds back two types of information to the BSs: a channel direction information (CDI) and a channel quality information (CQI). The CDI is related

to the orientation of the channels, whereas the CQI is related to the supported rate. We assume that each UE has a limited number of feedback bits B to send back the CDI and employs per-cell codebooks [57]. In detail, each UE agrees with the BSs on a set of B codebooks $\mathcal{C}^{(b)} = \{\boldsymbol{c}_1, \boldsymbol{c}_2, \ldots, \boldsymbol{c}_{2^b}\}$, $b = 1, 2, \ldots, B$, where each codeword $\boldsymbol{c}_j$ is a unit-norm vector of size $M \times 1$, i.e., codeword size is equal to the size of vector $\boldsymbol{h}_{k,j}$.

In this chapter we denote with $\boldsymbol{x}^{(d)} = \boldsymbol{x}/\|\boldsymbol{x}\|$ the direction of vector $\boldsymbol{x}$.

The developed feedback technique comprises two main phases.

- *Soft BS association.* Based on an estimate of the large scale fading, UE k allocates $b_{k,j}$ bits to quantize channel $\boldsymbol{h}_{k,j}^{(d)}$ with

$$\sum_{j=1}^{J} b_{k,j} = B\,, \tag{5.1}$$

  and communicates these values to the BSs. Note that this optimization a) requires to be updated only when the large scale fading $\sigma_{k,j}^2$ significantly changes, for instance because the UE is moving to another position, and b) sets codebook $\mathcal{C}^{(b_{k,j})}$ for UE k to represent channel $\boldsymbol{h}_{k,j}^{(d)}$. In Section 5.2 we develop two techniques to perform this optimization.

- *Feedback transmission.* The instantaneous value of the channel varies because of fast fading and we assume that UE k perfectly estimates channel $\boldsymbol{h}_k$ by using pilot signals transmitted by the J BSs. Then, it computes and feeds back CDI and CQI. Based on this information, the CU schedules a subset of the K UEs and perform downlink transmission.

By considering a low-mobility scenario, the uplink bandwidth used by UE k to communicate $b_{k,j}$ to the BSs is negligible with respect to the bandwidth used for CDI and CQI feedback.

If $\hat{\boldsymbol{h}}_{k,j}$ is the reconstructed channel between UE k and BS j, in the following we indicate with $\hat{\boldsymbol{h}}_k = [\hat{\boldsymbol{h}}_{k,1}^T, \hat{\boldsymbol{h}}_{k,2}^T, \ldots, \hat{\boldsymbol{h}}_{k,J}^T]^T$ the channel reconstructed at the CU on the basis of the feedback sent by UE k. Differently from [12, 13], we make the practical assumption that if UE k does not send feedback for channel $\boldsymbol{h}_{k,j}$, i.e., $b_{k,j} = 0$, the CU has no knowledge about this channel and we simply set $\hat{\boldsymbol{h}}_{k,j} = \boldsymbol{0}_{M\times 1}$. Under this assumption we can write the subset of BSs by whom UE k prefers to be served as $\mathcal{J}_k = \{j : b_{k,j} > 0\}$. As the CU needs to know the amplitude of channels between UE k and each BS, we assume that a set of CQIs is sent by UE k to allow the CU to reconstruct the set of amplitudes $\{\|\boldsymbol{h}_{k,j}\| : j \in \mathcal{J}_k\}$. The design of CQI feedback is an interesting topic but is beyond the scope of this work and here we simply consider that CQIs are reported without errors.

Note that no error on CQI feedback becomes unrealistic if considered jointly with the assumptions employed in [13], where each BS also employs a codebook with only one codeword when $b_{k,j} = 0$. In such a case, to reconstruct channel $\hat{\boldsymbol{h}}_k$, a CQI has to be

reported for all the BSs in the network (and this can be troublesome for BSs with a low SNR), whereas in our framework UE k sends back amplitude $\|\boldsymbol{h}_{k,j}\|$ only if $b_{k,j} > 0$.

By defining for ease of notation $\mathcal{C}^{(0)} = \emptyset$, UE k jointly selects the codewords by minimizing the chordal distance between the actual channel $\boldsymbol{h}_k$ and the reconstructed channel at the CU $\hat{\boldsymbol{h}}_k$, i.e.,

$$\left(\hat{\boldsymbol{h}}_{k,1}^{(d)}, \hat{\boldsymbol{h}}_{k,2}^{(d)}, \ldots, \hat{\boldsymbol{h}}_{k,J}^{(d)}\right) = \underset{(\boldsymbol{w}_1, \boldsymbol{w}_2, \ldots, \boldsymbol{w}_J) \in \mathcal{C}^{\left(b_{k,1}\right)} \times \mathcal{C}^{\left(b_{k,2}\right)} \times \ldots \times \mathcal{C}^{\left(b_{k,J}\right)}}{\operatorname{argmax}} \left| \sum_{j=1}^{J} \|\boldsymbol{h}_{k,j}\|^2 \, \boldsymbol{w}_j^H \boldsymbol{h}_{k,j}^{(d)} \right| . \tag{5.2}$$

After selecting the codewords, UE k sends back to the BSs the related indices together with the CQIs. The channel reconstructed at the CU for UE k can be written as

$$\hat{\boldsymbol{h}}_k = \left[\|\boldsymbol{h}_{k,1}\| \, \hat{\boldsymbol{h}}_{k,1}^{(d)T}, \|\boldsymbol{h}_{k,2}\| \, \hat{\boldsymbol{h}}_{k,2}^{(d)T}, \ldots, \|\boldsymbol{h}_{k,J}\| \, \hat{\boldsymbol{h}}_{k,J}^{(d)T} \right]^T . \tag{5.3}$$

5.2 Soft BS association

The codeword selection performed by UE k in (5.2) depends on the number of bits used to quantize each channel $\boldsymbol{h}_{k,j}^{(d)}$. The optimal criterion to allocate these bits is the maximization of the average spectral efficiency, i.e., UE k should solve

$$\begin{aligned} &\underset{b_{k,j} \in \{0,1,\ldots,B\},\, j=1,2,\ldots,J}{\operatorname{argmax}} \quad \mathbb{E}\left[\log_2\left(1 + \mathrm{SINR}_k\right)\right] \\ &\text{subject to } (5.1) \,, \end{aligned} \tag{5.4}$$

where SINR_k is the signal to interference plus noise ratio at UE k and the expectation is with respect to all the random variables. An intuition in solving (5.4) is that more feedback bits should be used to quantize channels of closer BSs, i.e., channels characterized by higher energy. However, the general formulation (5.4) is prohibitive to solve because UE k knows only the statistical powers $\sigma_{k,j}^2$, $j = 1, 2, \ldots, J$, and it does not know neither the position nor the channels of the other UEs in the network. Moreover, the solution to (5.4) depends on the structure of the codebooks and on the downlink transmission strategies employed by the BSs.

In the following we propose two suboptimal solutions to (5.4) based on some assumptions widely exploited in literature [13, 56]. In detail, for both solutions we consider that:

- in (5.4) the spectral efficiency is approximated with the SINR (low SINR regime), i.e.,
$$\log_2\left(1 + \mathrm{SINR}_k\right) \approx \log_2 e \cdot \mathrm{SINR}_k \,; \tag{5.5}$$
- random vector quantization (RVQ) is the criterion used to design codebooks, i.e., each codeword is independently chosen from the isotropic distribution on the unit

sphere [58] ;

- UE k independently chooses the best codeword for each link, i.e.,

$$\hat{\boldsymbol{h}}_{k,j}^{(d)} \approx \underset{\boldsymbol{w}\in\mathcal{C}^{(b_{k,j})}}{\operatorname{argmax}} \left|\boldsymbol{w}^H \boldsymbol{h}_{k,j}^{(d)}\right| , \quad j = 1, 2, \ldots, J ; \tag{5.6}$$

- all the BSs to whom UE k sends a feedback, i.e., all the BSs belonging to set $\mathcal{J}_k$, employ MRT in serving only this UE, i.e., the signal $\boldsymbol{z}_j$ transmitted by BS j turns out to be

$$\boldsymbol{z}_j = \sqrt{\bar{P}} \hat{\boldsymbol{h}}_{k,j}^{(d)*} x_k , \tag{5.7}$$

where $x_k \sim \mathcal{CN}\{0, 1\}$ is the information symbol, modeled as complex Gaussian, intended to UE k.

5.2.1 MRT without phase compensation

Let us define the function

$$\mathbb{1}(x) = \begin{cases} 1, & x > 0 , \\ 0, & x \leq 0 . \end{cases} \tag{5.8}$$

From BS j, as no transmission is assumed toward other UEs but UE k, no interference arises. Note that from (5.6) phase $\angle\left(\boldsymbol{h}_{k,j}^{(d)H} \hat{\boldsymbol{h}}_{k,j}^{(d)}\right)$ is uniformly distributed in the interval $[0, 2\pi]$ and is independent of $\angle\left(\boldsymbol{h}_{k,i}^{(d)H} \hat{\boldsymbol{h}}_{k,i}^{(d)}\right)$, $i \neq j$. Therefore, the average SNR at UE k is proportional to the quantity

$$\mathbb{E}\left[\left|\sum_{j=1}^{J} \boldsymbol{h}_{k,j}^T \hat{\boldsymbol{h}}_{k,j}^{(d)*} \mathbb{1}\left(b_{k,j}\right)\right|^2\right] = \sum_{j=1}^{J} \mathbb{E}\left[\left\|\boldsymbol{h}_{k,j}\right\|^2\right] \mathbb{E}\left[\left|\boldsymbol{h}_{k,j}^{(d)H} \hat{\boldsymbol{h}}_{k,j}^{(d)}\right|^2\right] \mathbb{1}\left(b_{k,j}\right) . \tag{5.9}$$

As $\left\|\boldsymbol{h}_{k,j}\right\|^2$ is Erlang distributed with scale parameter M and rate parameter $1/\sigma_{k,j}^2$, we have that $\mathbb{E}\left[\left\|\boldsymbol{h}_{k,j}\right\|^2\right] = M\sigma_{k,j}^2$. After defining [59, 6.1.1]

$$\Gamma\left(x\right) = \int_0^{+\infty} y^{x-1} e^{-y} dy , \tag{5.10}$$

and [59, 6.2.2]

$$\beta\left(x, y\right) = \frac{\Gamma(x)\Gamma(y)}{\Gamma(x+y)} , \tag{5.11}$$

and exploiting [60, eq. (12)], we can write

$$\mathbb{E}\left[\left|\boldsymbol{h}_{k,j}^{(d)H} \hat{\boldsymbol{h}}_{k,j}^{(d)}\right|^2\right] = 1 - 2^{b_{k,j}} \beta\left(2^{b_{k,j}}, \frac{M}{M-1}\right) . \tag{5.12}$$

Finally, by using (5.12) into (5.9), the optimization (5.4) can be simplified as

$$\underset{b_{k,j}\in\{0,1,\ldots,B\},\, j=1,2,\ldots,J}{\operatorname{argmax}} \sum_{j=1}^{J} M\sigma_{k,j}^2 \left(1 - 2^{b_{k,j}}\beta\left(2^{b_{k,j}}, \frac{M}{M-1}\right)\right) \mathbb{1}\left(b_{k,j}\right) \qquad (5.13)$$
$$\text{subject to } (5.1)\,,$$

which is a combinatorial problem and can be solved by an exhaustive search.

Note that (5.13) differs from [13, eq. (4)] because here we are considering that only the BSs belonging to set $\mathcal{J}_k$, i.e., BSs to whom UE k explicitly sends a feedback, transmit a signal by observing per-BS power constraints. These assumptions suit a practical CoMP system where a certain UE can be served only by a subset of the all BSs in the network, mainly because of bandwidth and latency constraints in the backhaul.

5.2.2 MRT with phase compensation

In this section we propose a different solution to (5.4) by still considering that MRT toward UE k is performed by each BS $j \in \mathcal{J}_k$. However, differently from Section 5.2.1 where the strict enforcing of assumption (5.6) implies that phase difference between signals coming from different BSs are not compensated at UE k, here we assume that $\angle\left(\boldsymbol{h}_{k,j}^{(d)H}\hat{\boldsymbol{h}}_{k,j}^{(d)}\right) = \angle\left(\boldsymbol{h}_{k,i}^{(d)H}\hat{\boldsymbol{h}}_{k,i}^{(d)}\right)$, $\forall j \neq i$. This assumption partially takes into account that in a real system the codewords are jointly selected at the UE by using (5.2). Similarly to (5.9), the average SNR at UE k can be written, except for a scaling factor, as

$$\begin{aligned}&\sum_{j=1}^{J} \mathbb{E}\left[\|\boldsymbol{h}_{k,j}\|^2\right] \mathbb{E}\left[\left|\boldsymbol{h}_{k,j}^{(d)H}\hat{\boldsymbol{h}}_{k,j}^{(d)}\right|^2\right] \mathbb{1}\left(b_{k,j}\right) + \\ &\quad + \sum_{j=1}^{J}\sum_{i=1,j\neq i}^{J} \mathbb{E}\left[\|\boldsymbol{h}_{k,j}\|\right] \mathbb{E}\left[\|\boldsymbol{h}_{k,i}\|\right] \cdot \mathbb{E}\left[\left|\boldsymbol{h}_{k,j}^{(d)H}\hat{\boldsymbol{h}}_{k,j}^{(d)}\right|\right] \mathbb{E}\left[\left|\boldsymbol{h}_{k,i}^{(d)H}\hat{\boldsymbol{h}}_{k,i}^{(d)}\right|\right] \mathbb{1}\left(b_{k,j}b_{k,i}\right)\,.\end{aligned} \qquad (5.14)$$

Let us define $\Psi_{k,j} = \mathbb{E}\left[\|\boldsymbol{h}_{k,j}\|\right]$ and $\Upsilon\left(b_{k,j}\right) = \mathbb{E}\left[\left|\boldsymbol{h}_{k,j}^{(d)H}\hat{\boldsymbol{h}}_{k,j}^{(d)}\right|\right]$. As $\|\boldsymbol{h}_{k,j}\|^2$ is Erlang distributed, we can write the CDF of $\|\boldsymbol{h}_{k,j}\|$ in (5.14) as

$$F_{\|\boldsymbol{h}_{k,j}\|}(x) = F_{\|\boldsymbol{h}_{k,j}\|^2}(x^2) = 1 - \sum_{m=0}^{M-1} \frac{x^{2m}\, e^{-x^2/\sigma_{k,j}^2}}{m!\,\sigma_{k,j}^{2m}}\,, \qquad (5.15)$$

and

$$\begin{aligned}\Psi_{k,j} &= \mathbb{E}\left[\|\boldsymbol{h}_{k,j}\|\right] = \int_0^{+\infty}\left(1-F_{\|\boldsymbol{h}_{k,j}\|}(x)\right)dx \\ &= \sum_{m=0}^{M-1}\frac{1}{m!\sigma_{k,j}^{2m}}\int_0^{+\infty}x^{2m}e^{-x^2/\sigma_{k,j}^2}dx \\ &= \frac{\sigma_{k,j}}{2}\sum_{m=0}^{M-1}\frac{1}{m!}\int_0^{+\infty}y^{m-1/2}e^{-y}dy \\ &= \frac{\sigma_{k,j}}{2}\sum_{m=0}^{M-1}\frac{1}{m!}\Gamma\left(m+\frac{1}{2}\right).\end{aligned} \tag{5.16}$$

Moreover, by using [60, eq. (7)], we can write the CDF of $\left|\boldsymbol{h}_{k,j}^{(d)H}\hat{\boldsymbol{h}}_{k,j}^{(d)}\right|$ in (5.14) as

$$\begin{aligned}F_{\left|\boldsymbol{h}_{k,j}^{(d)H}\hat{\boldsymbol{h}}_{k,j}^{(d)}\right|}(x) &= F_{\left|\boldsymbol{h}_{k,j}^{(d)H}\hat{\boldsymbol{h}}_{k,j}^{(d)}\right|^2}(x^2) \\ &= \sum_{r=0}^{2^{b_{k,j}}}\sum_{k=0}^{r(M-1)}\binom{2^{b_{k,j}}}{r}\binom{r(M-1)}{k}(-1)^{r+k}x^{2k}, \quad x\in[0,1],\end{aligned} \tag{5.17}$$

and

$$\begin{aligned}\Upsilon(b_{k,j}) &= \mathbb{E}\left[\left|\boldsymbol{h}_{k,j}^{(d)H}\hat{\boldsymbol{h}}_{k,j}^{(d)}\right|\right] = \int_0^{+\infty}\left(1-F_{\left|\boldsymbol{h}_{k,j}^{(d)H}\hat{\boldsymbol{h}}_{k,j}^{(d)}\right|^2}(x^2)\right)dx \\ &= 1-\sum_{r=0}^{2^{b_{k,j}}}\sum_{k=0}^{r(M-1)}\binom{2^{b_{k,j}}}{r}\binom{r(M-1)}{k}(-1)^{r+k}\int_0^1 x^{2k}dx \\ &= 1-\sum_{r=0}^{2^{b_{k,j}}}\sum_{k=0}^{r(M-1)}\binom{2^{b_{k,j}}}{r}\binom{r(M-1)}{k}\frac{(-1)^{r+k}}{2k+1} \\ &= 1-\sum_{r=0}^{2^{b_{k,j}}}\binom{2^{b_{k,j}}}{r}(-1)^r r(M-1)\beta\left(r(M-1),\frac{3}{2}\right).\end{aligned} \tag{5.18}$$

Due to a numerical instability observed for high values of $b_{k,j}$ in the computation of the binomial coefficient in (5.18), in Section 5.3 we approximate

$$\Upsilon(b_{k,j}) \approx \sqrt{\mathbb{E}\left[\left|\boldsymbol{h}_{k,j}^{(d)H}\hat{\boldsymbol{h}}_{k,j}^{(d)}\right|^2\right]}, \tag{5.19}$$

which can be easily computed from (5.12).

The optimal bit allocation under this assumption is the solution to the following opti-

mization problem

$$\underset{b_{k,j}\in\{0,1,\ldots,B\},\, j=1,2,\ldots,J}{\operatorname{argmax}} \sum_{j=1}^{J} M\sigma_{k,j}^2 \left(1 - 2^{b_{k,j}}\beta\left(2^{b_{k,j}}, \frac{M}{M-1}\right)\right) \mathbb{1}\left(b_{k,j}\right) + \\ + \sum_{j=1}^{J}\sum_{i=1, j\neq i}^{J} \Psi_{k,j}\Psi_{k,i}\Upsilon\left(b_{k,j}\right)\Upsilon\left(b_{k,i}\right)\mathbb{1}\left(b_{k,j}b_{k,i}\right) \tag{5.20}$$

subject to (5.1) .

Note that (5.20) is a combinatorial problem which can be solved by an exhaustive search as (5.13).

5.2.3 Complexity analysis

The computational complexity of the exhaustive search used in solving both (5.13) and (5.20) mainly depends on the number N_C of vectors $[b_{k,1}, b_{k,2}, \ldots, b_{k,J}]$ that satisfy constraint (5.1). We observe that N_C is the number of B-combinations with repetition of the J BSs [61, Ch. 1], i.e.,

$$N_C = \binom{B+J-1}{B}. \tag{5.21}$$

However, when $J \geq B$, the exhaustive search used to solve (5.13) and (5.20) is simplified by considering that the feedback bits can be sent only to the best B BSs characterized by the highest $\sigma_{k,j}^2$. Therefore, the value of N_C in (5.21) can be reduced to

$$N_C = \binom{B+\min\{B,J\}-1}{B}. \tag{5.22}$$

5.3 Numerical results

The gain of CoMP is important when the number of UEs in the network is high and coordination is able to strongly limit the impact of ICI. However, in such a scenario, beyond the feedback problem, many other issues related to UE scheduling, clustering and precoding design arise. Therefore, in order to compare and evaluate only the performance of the developed feedback algorithms, we consider a very simple scenario similar to the one reported in Fig. 5.1 where a linear array of $J = 4$ BSs is serving only $K = 1$ UE and $d_{\max}$ is the distance between two neighboring BSs. As only one UE is dropped in the network, we assume that BSs, after receiving a feedback from the UE, employ MRT precoding (5.7) and the achievable spectral efficiency can be written as (see also left-hand side of (5.9))

$$R = \log_2\left(1 + \frac{\bar{P}}{\sigma_n^2}\left|\sum_{j=1}^{J} \boldsymbol{h}_{1,j}^T \hat{\boldsymbol{h}}_{1,j}^{(d)*}\mathbb{1}\left(b_{1,j}\right)\right|^2\right), \tag{5.23}$$

where σ_n^2 is the variance of the noise at the UE. Note that in (5.23) we are assuming that BS j serves the UE only if it explicitly receives feedback bits from the UE, i.e., only if $b_{1,j} > 0$.

The channel model includes path-loss with a path-loss exponent $\eta = 3.5$ and Rayleigh fading. By assuming unitary transmitted power $\bar{P} = 1$, unitary noise variance $\sigma_n^2 = 1$ at the UE and indicating with $d_{1,j}$ the distance between the UE and BS j, we define the average SNR at the UE with respect to BS j, as

$$S_j = \sigma_{1,j}^2 = \mathrm{SNR}^{(\mathrm{CE})} \left(\frac{d_{\max}/2}{d_{1,j}} \right)^{\eta} , \tag{5.24}$$

where $\mathrm{SNR}^{(\mathrm{CE})}$ is the average SNR at the cell edge, i.e., when $d_{1,j} = d_{\max}/2$. In the following we consider $\mathrm{SNR}^{(\mathrm{CE})} = 10$ dB.

Let us denote with ALG1 and ALG2 solutions to (5.13) and (5.20), respectively.

In Fig.s 5.2 and 5.3 we assume that the UE is moving from the cell edge between BSs 2 and 3 toward BS 3.

Fig. 5.2 shows the number of feedback bits allocated by the UE to the BSs when $B = 4$ by employing ALG1 and ALG2. As expected, we observe that the number of bits allocated by the UE to the *serving* BS, i.e., the closest to the UE, increases with S_3. Furthermore, for a given value of S_3, ALG1 tends to concentrate more bits to the serving BS than ALG2, which exploits more the cooperation of the *auxiliary* BSs, i.e., the farthest from the UE. For instance, when $S_3 = \mathrm{SNR}^{(\mathrm{CE})}$, i.e., the UE is at the cell edge, ALG2 allocates 1 bit to each BS, whereas ALG1 allocates 2 bits to the two closest BSs.

In Fig. 5.3 we compare the average spectral efficiency $\mathbb{E}[R]$ in terms of S_3 and with $B = 4$ achieved by the proposed techniques against two other methods:

- single cell processing (SCP), i.e., the UE sends all the bits to the serving BS which transmits toward the UE without the cooperation of the auxiliary BSs;
- equal bit allocation (EBA) among the BSs, i.e., $b_{1,j} = B/J$, $j = 1, 2, \ldots, J$.

By assuming RVQ, both ALG1 and ALG2 outperform EBA and SCP: in particular, they show a considerable gain over SCP when the UE is close to the cell edge, and over EBA when the UE is close to the serving BS. We also observe that ALG1 slightly outperforms ALG2 when $S_3 \in [10, 16]$ dB, whereas ALG2 performs better than ALG1 when $S_3 \in [17, 22]$ dB. Note that the *steps* observed in the curves are related to changes in the feedback bit distribution among the BSs: for instance, the step of ALG1 at $S_3 = 17$ dB is due to the fact that the UE starts sending all the feedback bits only to BS 3 (see also Fig. 5.2). Moreover, even if few feedback bits are available at the UE, the performance of the considered techniques is very close to the upper bound achieved when perfect CSI is available at the BSs: this upper bound is obtained from (5.23) by neglecting the step function $\mathbb{1}(b_{1,j})$ and imposing $\hat{\boldsymbol{h}}_{k,j}^{(d)} = \boldsymbol{h}_{k,j}^{(d)}$. In fact, due to the absence of interference, the effects of imperfect CSI are less important in a SU case than in a MU scenario [58].

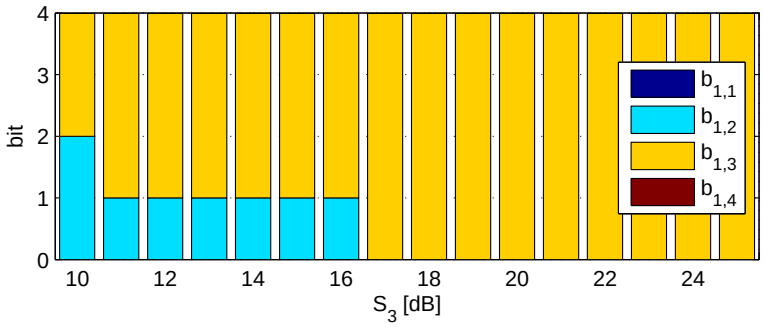

(a) Bits allocated by ALG1.

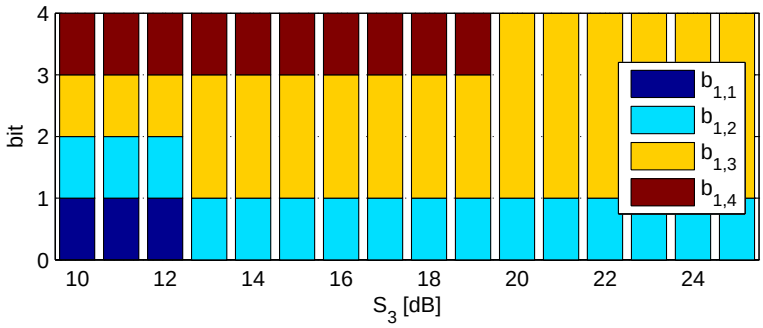

(b) Bits allocated by ALG2.

Figure 5.2: Bits allocated by the UE to the BSs versus the average SNR between the UE and BS 3 when $B = 4$.

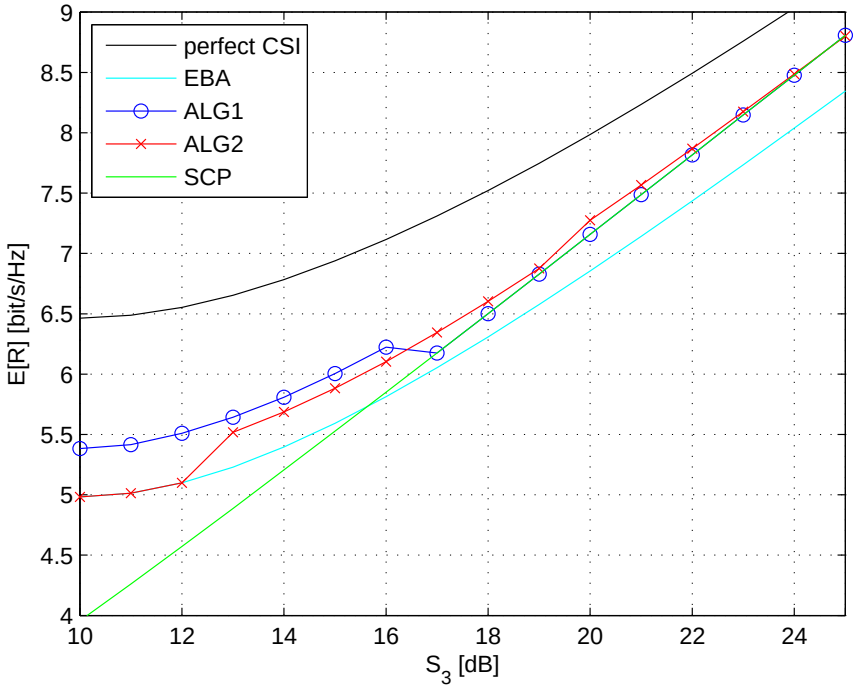

Figure 5.3: Average spectral efficiency versus the average SNR between the UE and BS 3 when $B = 4$.

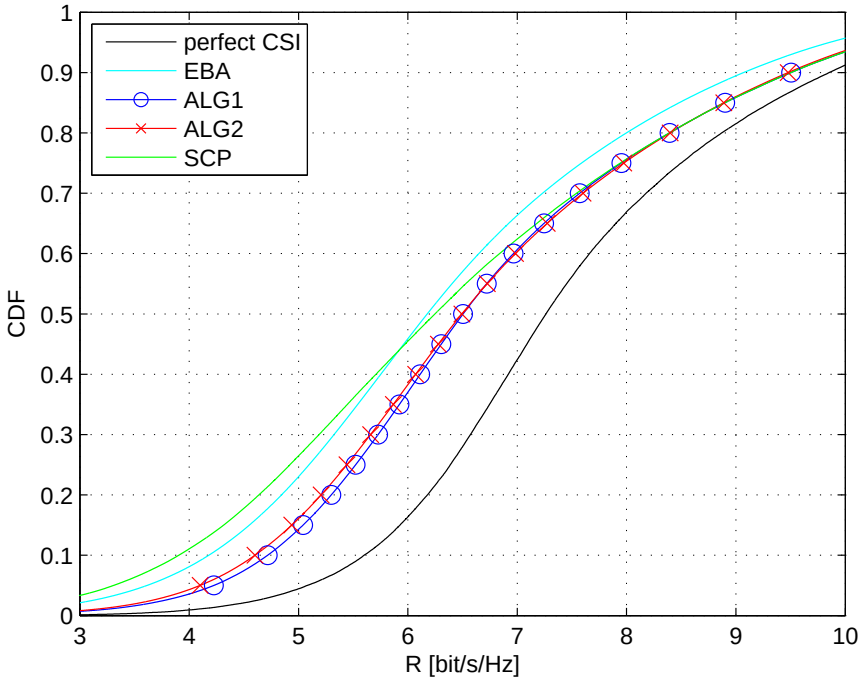

Figure 5.4: CDF of the spectral efficiency when $B = 4$.

	EBA	ALG1	ALG2	SCP
$\mathbb{E}[R]$ $(B = 4)$	6.40	6.81	6.77	6.48
$\mathbb{E}[R]$ $(B = 8)$	6.94	7.16	7.16	6.56
$\mathbb{E}[R]$ $(B = 12)$	7.22	7.32	7.34	6.56
5th perc. of R $(B = 4)$	3.62	4.23	4.10	3.31
5th perc. of R $(B = 8)$	4.52	4.76	4.77	3.39
5th perc. of R $(B = 12)$	4.91	4.98	5.02	3.39

Table 5.1: Average and 5th percentile of the spectral efficiency in [bit/s/Hz] when $B = 4, 8, 12$.

We consider now the case when the UE is uniformly distributed in the coverage area of the four cells and we assume a minimum distance $d_{\min}$ between the UE and each BS, i.e., $d_{1,j} \geq d_{\min}$, $j = 1, 2, \ldots, J$, such that the maximum average SNR is 30 dB. Fig. 5.4 shows the CDF of the spectral efficiency achieved by the different techniques with $B = 4$, whereas Tab. 5.1 reports the average and the 5th percentile of R for different values of B. These results confirm that ALG1 and ALG2 outperform both EBA and SCP. We also observe that for higher values of B the gain achieved by the developed algorithms over EBA is low (around 2% in terms of 5th percentile of R), whereas for $B = 4$ the gain is considerable (up to 17% in terms of 5th percentile of R), showing the importance of a proper bit allocation among the BSs.

5.4 Conclusions

In this chapter we have considered CoMP-JP with per-cell codebooks and we have designed two new algorithms that suit a SU case to a) select the subset of BSs by whom the UE prefers to be served and b) allocate the feedback bits among these BSs. Numerical results show the flexibility of the proposed methods that exploit more bits to represent strongest channels.

Chapter 6

Power and time-sharing optimization in three half-duplex relay networks

Relay networks, where the transmission from a source toward a destination is assisted by other nodes, have shown to be an interesting solution to implement distributed MIMO systems. Initial works on relay networks have considered a single relay node [62] and various transmission techniques, including decode and forward, amplify and forward and compress and forward [63, 64, 65]. As relay nodes are being deployed, e.g. in fourth generation cellular networks and in wide metropolitan area networks [66, 67], there is an increasing interest in using more than one relay. In fact, beamforming can be used by cooperative relays with the aim of transmitting coherently toward the destination. Networks with multiple relays have been widely studied under the full-duplex assumption in [68, 69]. The achievable rates for various techniques have been derived in [70] for the case of half duplex relays in the absence of interference for a network with two relays.

In this chapter we consider a network with three half-duplex relays assisting the transmission of a source toward a destination and with no direct connection between these two nodes. In order to limit the complexity of the network, we assume that relays cannot communicate with each other, but only with the source and the destination. This scenario is similar to the one considered in Chapter 3, where here the wireless links between relays and the source node can be seen as a backhaul network. We consider that the transmission time is a sequence of phases, where in odd phases a subset of relays is transmitting and the rest is receiving, while in the even phases the role of the relays is swapped. For this scenario, we formulate the optimization problem that maximizes the throughput from the source to the destination by assuming transmission power constraints at each node. First, we consider a class of schemes where all the three relays are transmitting and receiving at the same time. Then, in order to achieve spatial multiplexing, we consider a second class of schemes where one relay is transmitting during odd phases, whereas the remaining

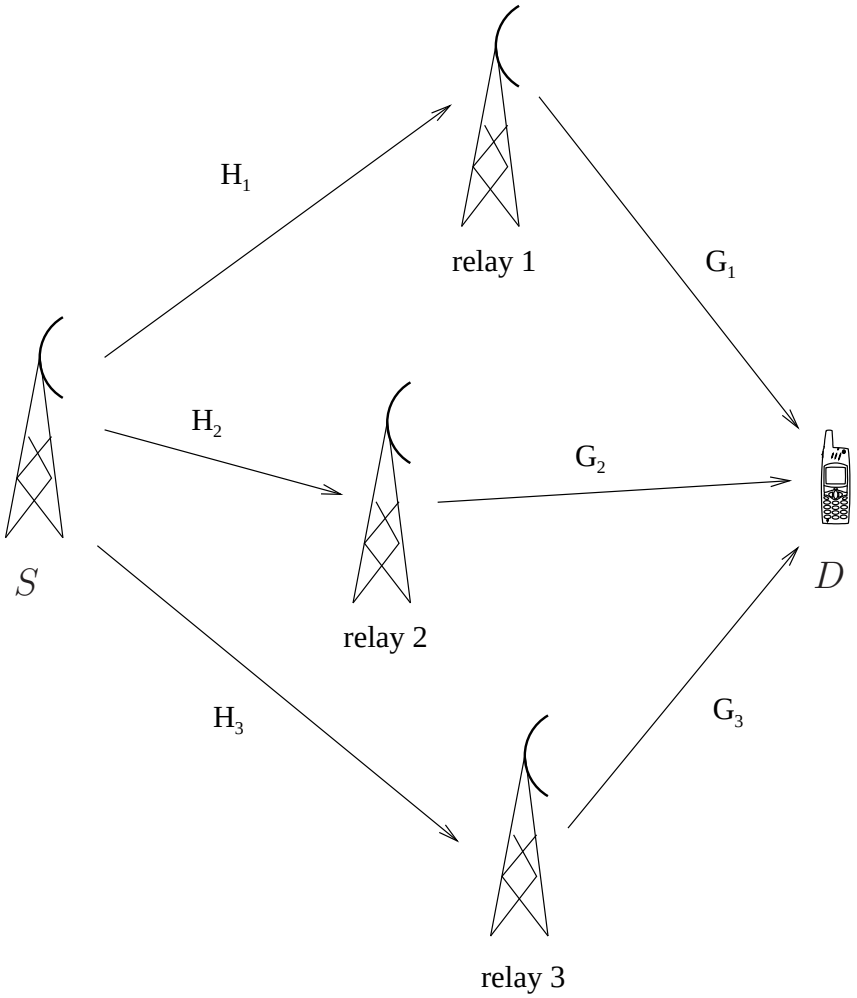

Figure 6.1: The considered relay network with three half-duplex relays between S and D.

couple of relays cooperatively transmit during even phases. In this setup, we adapt the quantized constellation transmission (QCT) scheme developed in Chapter 3 for downlink CoMP. The two cooperative relays transmit in general different signals which turn out to be scaled and rotated symbols belonging to two different QAM constellations, whose sizes depend on the achievable rate between the source and each relay. The two signals combine at the destination to a scaled QAM symbol thus allowing a simplification of the receiver implementation. Moreover, we propose a practical algorithm to perform power allocation and time-sharing optimization with the aim of maximizing the spectral efficiency between the source and the destination. The performance of the proposed solution is compared with respect to existing approaches, showing a significant improvement of the network throughput in typical wireless scenarios.

6.1 System model

We consider the relay network shown in Fig. 6.1 consisting of three relays assisting a source S transmitting toward a destination D. All the nodes are equipped with a single antenna, and we indicate with $h_i \in \mathbb{C}$, $g_i \in \mathbb{C}$, $i = 1, 2, 3$, the flat fading channel between S and relay i and between relay i and D, respectively. S transmits a signal x, and the signal received by relay i can be written as

$$y_i = h_i x + w_i \,, \tag{6.1}$$

where w_i is the AWGN with zero mean. We indicate the signal transmitted by relay i with z_i and consider a unitary power constraint for each node in the network, i.e., $\mathbb{E}\left[|x|^2\right] \leq 1$, $\mathbb{E}\left[|z_i|^2\right] \leq 1$, $i = 1, 2, 3$. By assuming CSI of the relay-destination link at the relay, the transmission performed by relays can be done coherently adjusting the phases of z_i, $i = 1, 2, 3$. For this reason and without loss of generality, in the following we only consider the channel gains

$$H_i = |h_i|^2 \,, \tag{6.2a}$$

$$G_i = |g_i|^2 \,. \tag{6.2b}$$

Without loss of generality we assume that all noises have unitary variance, while the effective SNR at the receiver is obtained by a proper scaling of the channel gains. We assume that a central unit (CU) knows all channels, correspondingly allocates resources to nodes, including power and constellation sizes. Hence, the determined network spectral efficiency can be assumed as a bound for cases where only a partial CSI is available.

Nodes operate in half-duplex mode, i.e., they cannot transmit and receive simultaneously. Each relay alternates a phase in which it receives data from the source and a phase when it transmits to the destination. No communication among relays is allowed. Moreover, we assume no direct transmission from S to D because of shadowing or the long distance between S and D. Let the time used for two consecutive phases be unitary. The odd phases are assigned a time λ, and the even phases are assigned a time $1-\lambda$, where the parameter λ will be optimized. The scheduling of transmission is then fully characterized by the variable

$$\delta_i = \begin{cases} 0, & \text{relay } i \text{ transmits during even phases}\,, \\ 1, & \text{relay } i \text{ transmits during odd phases}\,, \end{cases} \tag{6.3}$$

for $i = 1, 2, 3$.

In this chapter we denote the link spectral efficiency for a given SNR μ as

$$C(\mu) = \log_2(1 + \mu) \,. \tag{6.4}$$

6.2 Schemes without relay scheduling

In this section we review transmission schemes proposed in literature where all relays receive in odd phases and transmit in even phases, i.e., $\delta_i = 0$, $i = 1, 2, 3$. In detail, we consider the amplify and forward (AF), the decode and forward (DF), and the broadcast multiaccess (BM) techniques.

6.2.1 Amplify and forward

With AF each relay simply retransmits a scaled version of the received signal, i.e., $z_i = \gamma_i y_i$, observing the unitary power constraint $\gamma_i^2(H_i + 1) \leq 1$. The signal received at node D can be written as

$$r = \sum_{i=1}^{3} \sqrt{G_i} z_i + w_D = x \sum_{i=1}^{3} \gamma_i \sqrt{G_i H_i} + w_D + \sum_{i=1}^{3} w_i \gamma_i \sqrt{G_i}\,, \tag{6.5}$$

where w_D is complex Gaussian with zero mean and unitary variance. Note that with AF no optimization of the time-allocation λ is performed. Indeed, each relay retransmits the whole received signal from S toward D, therefore equal-time has to be assigned to both phases, i.e., $\lambda = 1/2$. The spectral efficiency is obtained by (6.4), where from (6.5) the signal power is $\left|\sum_{i=1}^{3} \sqrt{G_i H_i}\gamma_i\right|^2$ and the noise power is $1 + \sum_{i=1}^{3} G_i \gamma_i^2$. Scaling factors γ_i are selected in order to maximize the network spectral efficiency, i.e.,

$$R^{(\mathrm{AF})} = \max_{\gamma_i} \frac{1}{2} C \left(\frac{\left| \sum_{i=1}^{3} \sqrt{G_i H_i}\gamma_i \right|^2}{1 + \sum_{i=1}^{3} G_i \gamma_i^2} \right) \tag{6.6a}$$

subject to

$$\gamma_i^2 \,(H_i + 1) \leq 1\,, \quad i = 1, 2, 3, \tag{6.6b}$$

$$\gamma_i \geq 0\,, \quad i = 1, 2, 3. \tag{6.6c}$$

Note that the factor $1/2$ in (6.6a) is due to the equal duration of phases.

Moreover, we observe that (6.6) is a non-linear non-convex optimization problem in the three variables γ_i, $i = 1, 2, 3$.

6.2.2 Decode and forward

With DF a relay decodes the information received from S, which is transmitted coherently with the other relays toward D [65]. A bottleneck of this scheme is the channel between S and each relay, as the spectral efficiency is strongly limited by the worst channel

$\min_i H_i$. For this reason we also consider a selection of the relays involved in the operations. For each subset $\mathcal{S} \subseteq \{1,2,3\}$, in order to maximize the information rate from S to D, we impose the equality of the spectral efficiency in both phases, i.e.,

$$R^{(\mathrm{DF})}(\mathcal{S}) = \lambda C\left(\min_{i\in\mathcal{S}} H_i\right) = (1-\lambda)C\left(\left(\sum_{i\in\mathcal{S}}\sqrt{G_i}\right)^2\right). \tag{6.7}$$

The optimal value of λ is obtained by solving (6.7) for each subset $\mathcal{S}$, i.e.,

$$\lambda = \frac{C\left(\left(\sum_{i\in\mathcal{S}}\sqrt{G_i}\right)^2\right)}{C\left(\min_{i\in\mathcal{S}} H_i\right) + C\left(\left(\sum_{i\in\mathcal{S}}\sqrt{G_i}\right)^2\right)}. \tag{6.8}$$

The network spectral efficiency is then computed optimizing the choice of $\mathcal{S}$, yielding

$$R^{(\mathrm{DF})} = \max_{\mathcal{S}\subseteq\{1,2,3\}} R^{(\mathrm{DF})}(\mathcal{S}) = \max_{\mathcal{S}\subseteq\{1,2,3\}} \frac{C\left(\min_{i\in\mathcal{S}} H_i\right) C\left(\left(\sum_{i\in\mathcal{S}}\sqrt{G_i}\right)^2\right)}{C\left(\min_{i\in\mathcal{S}} H_i\right) + C\left(\left(\sum_{i\in\mathcal{S}}\sqrt{G_i}\right)^2\right)}. \tag{6.9}$$

Note that (6.9) is an integer optimization problem, which can be easily solved by an exhaustive search among all the subsets of relay nodes.

6.2.3 Broadcast multiaccess

Only for this section we assume for simplicity that $H_1 \geq H_2 \geq H_3$. With the BM scheme, in the first phase we have a Gaussian broadcast channel [37], where S transmits three messages M_1, M_2 and M_3, at rates R_1, R_2 and R_3, respectively, where M_1 is decoded only by relay 1, M_2 is decoded by both relay 1 and relay 2, and M_3 is decoded by all three relays. In the second phase we have a Gaussian multiple access channel with correlated information [34], where relays send different but not independent information. We indicate with α_1, α_2 and α_3 the powers used by S to transmit the messages M_1, M_2 and M_3, respectively, γ_{11}, γ_{12} and γ_1 the powers used by relay 1 to transmit M_1, M_2 and M_3, respectively, γ_{21} and γ_2 the powers used by relay 2 to transmit M_2 and M_3, respectively, and γ_3 the power used by relay 3 to transmit M_3. Note that here we are extending the BM scheme with two relays of [70] to the case of three relays. Therefore, the network spectral efficiency is the solution to the following optimization problem:

$$R^{(\mathrm{BM})} = \max_{\alpha_i,\gamma_u,\lambda} R_1 + R_2 + R_3 \tag{6.10a}$$

subject to

$$R_1 \leq \lambda C\left(\alpha_1 H_1\right), \tag{6.10b}$$

$$R_2 \leq \lambda C\left(\frac{\alpha_2 H_2}{1+\alpha_1 H_2}\right), \tag{6.10c}$$

$$R_3 \leq \lambda C\left(\frac{\alpha_3 H_3}{1+\alpha_1 H_3+\alpha_2 H_3}\right), \tag{6.10d}$$

$$R_1 \leq (1-\lambda) C\left(\gamma_{11} G_1\right), \tag{6.10e}$$

$$R_1+R_2 \leq (1-\lambda) C\left(\gamma_{11} G_1+\left(\sqrt{\gamma_{12} G_1}+\sqrt{\gamma_{21} G_2}\right)^2\right), \tag{6.10f}$$

$$\begin{aligned} R_1+R_2+R_3 \leq (1-\lambda) C\Bigg(\gamma_{11} G_1+\left(\sqrt{\gamma_{12} G_1}+\sqrt{\gamma_{21} G_2}\right)^2+ \\ \left(\sqrt{\gamma_1 G_1}+\sqrt{\gamma_2 G_2}+\sqrt{\gamma_3 G_3}\right)^2\Bigg), \end{aligned} \tag{6.10g}$$

$$\alpha_1+\alpha_2+\alpha_3 \leq 1, \tag{6.10h}$$

$$\gamma_{11}+\gamma_{12}+\gamma_1 \leq 1, \tag{6.10i}$$

$$\gamma_{21}+\gamma_2 \leq 1, \tag{6.10j}$$

$$\gamma_3 \leq 1, \tag{6.10k}$$

$$0 \leq \lambda \leq 1, \quad \alpha_i \geq 0, \quad \gamma_u \geq 0. \tag{6.10l}$$

Note that i) constraints (6.10b)-(6.10d) represent the rate-region of the Gaussian broadcast channel between S and the relays, ii) constraints (6.10e)-(6.10g) represent the rate region of the Gaussian multiple access channel with correlated information between the relays and D, and iii) constraints (6.10h)-(6.10k) represent the power constraints at node S and at the relays, respectively. Similarly to (6.6), (6.10) is a non-linear non-convex optimization problem.

6.3 Schemes with relay scheduling

In this section we assume that the three relays are not forced to receive and transmit simultaneously at the same phase. As we consider only two phases, in the following we assume that only one relay transmits during odd phases, whereas the remaining two relays can cooperatively transmit during even phases, i.e.,

$$\sum_{i=1}^{3} \delta_i = 1, \quad \delta_i \in \{0,1\}, \quad i=1,2,3. \tag{6.11}$$

Even if variables δ_i, $i=1,2,3$, will be optimized, for the sake of clarity we introduce three indices to distinguish the relays for a given relay scheduling configuration and we consider

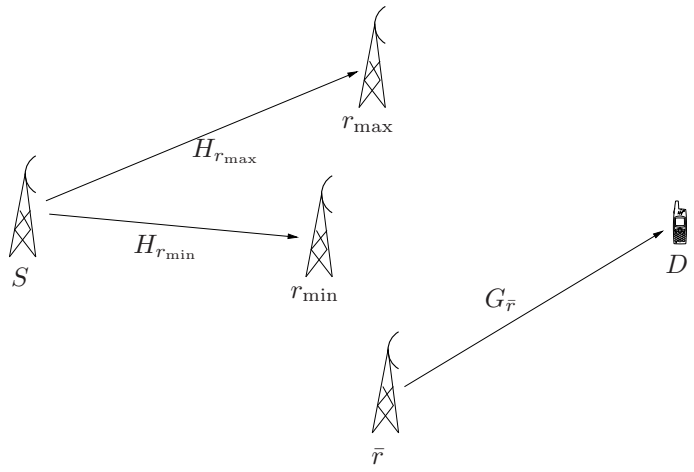

(a) Odd phases.

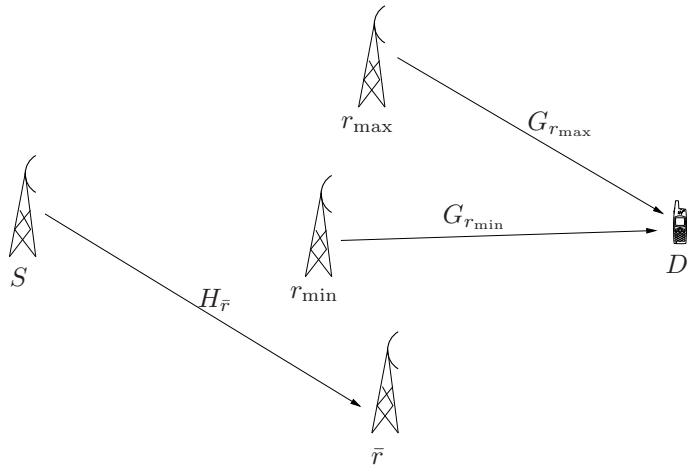

(b) Even phases.

Figure 6.2: The relay scheduling considered in Section 6.3.

(see also Fig. 6.2)

$$\bar{r} = i \longleftrightarrow \delta_i = 1\,, \tag{6.12a}$$

$$r_{\max} = \underset{i:\delta_i=0}{\operatorname{argmax}} H_i\,, \tag{6.12b}$$

$$r_{\min} = \underset{i:\delta_i=0}{\operatorname{argmin}} H_i\,. \tag{6.12c}$$

Let us denote with $R^{(\mathrm{O})}$ and $R^{(\mathrm{E})}$ the spectral efficiencies achieved from S to D with the assistance of $\bar{r}$ and with the assistance of relays $r_{\max}$ and $r_{\min}$, respectively. In the following, we first describe an extension of DF and BM schemes denoted as adaptive decode and forward (ADF) and adaptive broadcast multiaccess (ABM), respectively. Then, in Section 6.3.3 we propose i) an alternative solution based on QCT introduced in Chapter 3 and ii) a practical algorithm to perform power allocation and time-sharing optimization.

6.3.1 Adaptive decode and forward

With ADF relay $\bar{r}$ simply retransmits the message received from S. On the other hand, two solutions can be adopted by the couple of relays $r_{\max}$ and $r_{\min}$ that transmit during even phases.

- *Solution I*: S transmits a message which is firstly decoded by both relays and then cooperatively retransmitted toward D.
- *Solution II*: S transmits a message which is decoded only by relay $r_{\max}$ and next this message is retransmitted toward D.

Note that in solution I spatial diversity can be achieved in the transmission toward D, however the overall performance is strongly limited by relay $r_{\min}$ which has the worst channel. The network spectral efficiency achieved by solution I is

$$R^{(\mathrm{ADF,I})} = \max_{0\leq\lambda\leq 1,\delta_i} R^{(\mathrm{O})} + R^{(\mathrm{E})} \tag{6.13a}$$

subject to

$$R^{(\mathrm{O})} \leq \lambda C\left(G_{\bar{r}}\right) , \tag{6.13b}$$

$$R^{(\mathrm{O})} \leq (1-\lambda) C\left(H_{\bar{r}}\right) , \tag{6.13c}$$

$$R^{(\mathrm{E})} \leq \lambda C\left(H_{r_{\min}}\right) , \tag{6.13d}$$

$$R^{(\mathrm{E})} \leq (1-\lambda) C\left(\left(\sqrt{G_{r_{\max}}} + \sqrt{G_{r_{\min}}}\right)^2\right) , \tag{6.13e}$$

and subject to (6.11), (6.12).

On the other hand, by employing solution II we obtain

$$R^{(\mathrm{ADF,II})} = \max_{0\leq\lambda\leq 1,\delta_i} R^{(\mathrm{O})} + R^{(\mathrm{E})} \tag{6.14a}$$

subject to

$$R^{(\mathrm{E})} \leq \lambda C\left(H_{r_{\max}}\right) , \tag{6.14b}$$

$$R^{(\mathrm{E})} \leq (1-\lambda) C\left(G_{r_{\max}}\right) , \tag{6.14c}$$

and subject to (6.11), (6.12), (6.13b), (6.13c).

The ADF scheme simply selects the best solution, i.e.,

$$R^{(\mathrm{ADF})} = \max\left\{R^{(\mathrm{ADF,I})}, R^{(\mathrm{ADF,II})}\right\} . \tag{6.15}$$

Note that (6.13) and (6.14) are both mixed integer programming problems. However, their solutions can be computed by performing an exhaustive search in the variables δ_i, $i = 1, 2, 3$, and, for each relay scheduling configuration (i.e., for fixed $\bar{r}$, $r_{\max}$ and $r_{\min}$),

by solving the resulting subproblem which is a simple linear optimization problem in the variable λ.

6.3.2 Adaptive broadcast multiaccess

In this section we assume that relays $r_{\max}$ and $r_{\min}$ are able to decode multiple and different messages transmitted by S. In detail, we model the channel between S and relays $r_{\max}$ and $r_{\min}$ as a Gaussian broadcast channel where S transmits with power α a private message at rate $R^{(\mathrm{E,P})}$, which is decoded only by relay $r_{\max}$, and with power $1-\alpha$ a common message at rate $R^{(\mathrm{E,C})}$, which is decoded by both relays. Then, the two relays retransmit the decoded messages toward D by employing Slepian-Wolf encoding [34]. In particular, private and common messages are transmitted by relay $r_{\max}$ with powers $P_{r_{\max}}^{(\mathrm{P})}$ and $1-P_{r_{\max}}^{(\mathrm{P})}$, respectively, whereas relay $r_{\min}$ transmits at full power. Here $R^{(\mathrm{E})} = R^{(\mathrm{E,P})} + R^{(\mathrm{E,C})}$. At node D successive interference cancellation is required to decode both messages. Relay $\bar{r}$ operates as in the ADF scheme. The achievable network spectral efficiency can be written as

$$R^{(\mathrm{ABM})} = \max_{\alpha, P_{r_{\max}}^{(P)}, \lambda, \delta_i} R^{(\mathrm{O})} + R^{(\mathrm{E,P})} + R^{(\mathrm{E,C})} \tag{6.16a}$$

subject to

$$R^{(\mathrm{E,P})} \leq \lambda C\left(\alpha H_{r_{\max}}\right), \tag{6.16b}$$

$$R^{(\mathrm{E,C})} \leq \lambda C\left(\frac{(1-\alpha)H_{r_{\min}}}{1+\alpha H_{r_{\min}}}\right), \tag{6.16c}$$

$$R^{(\mathrm{E,P})} \leq (1-\lambda)C\left(P_{r_{\max}}^{(\mathrm{P})} G_{r_{\max}}\right). \tag{6.16d}$$

$$R^{(\mathrm{E,P})} + R^{(\mathrm{E,C})} \leq (1-\lambda)C\left(P_{r_{\max}}^{(\mathrm{P})} G_{r_{\max}} + \left(\sqrt{(1-P_{r_{\max}}^{(\mathrm{P})})G_{r_{\max}}} + \sqrt{G_{r_{\min}}}\right)^2\right), \tag{6.16e}$$

$$0 \leq \lambda \leq 1\,, \quad 0 \leq \alpha \leq 1\,, \quad 0 \leq P_{r_{\max}}^{(P)} \leq 1\,, \tag{6.16f}$$

and subject to (6.11), (6.12), (6.13b), (6.13c).

For the cooperative relays (both having $\delta_i = 0$) (6.16b) and (6.16c) bound the spectral efficiency in the first phase, while (6.16d) and (6.16e) give the bound for the common and private messages in the second phase.

6.3.3 ABM with QCT

In this section we develop an alternative solution to Slepian-Wolf encoding used by cooperative relays in ABM. We call this scheme ABM-QCT. In particular, we assume that relays $r_{\max}$ and $r_{\min}$ employ QAM constellations to transmit toward D. Due to channel condition, relay $r_{\max}$ has a full knowledge of the message to be sent toward D,

whereas $r_{\min}$ has only a partial knowledge of this information. In detail, $r_{\max}$ knows the full QAM symbol a to be sent, while $r_{\min}$ knows only a quantized version $a^{(q)}$ of a with

$$a^{(q)} = a - a^{(e)}\,, \tag{6.17}$$

where $a^{(e)}$ is the quantization error. We denote with b and $b^{(q)} \in \{0, 2, 4, \ldots, b\}$ the sizes of the full and the quantized constellations, respectively. Assuming $\mathbb{E}\left[|a|^2\right] = 1$ and following the quantized constellation design of Section 3.3 where $\mathbb{E}\left[a^{(e)}\right] = 0$ and $\mathbb{E}\left[a^{(q)*}a^{(e)}\right] = 0$, we have

$$\mathbb{E}\left[\left|a^{(e)}\right|^2\right] = \frac{2^{b-b^{(q)}} - 1}{2^b - 1} = f\left(b, b^{(q)}\right)\,. \tag{6.18}$$

The signals transmitted by relays $r_{\min}$ and $r_{\max}$ can be written, respectively, as

$$z_{r_{\min}} = \sqrt{P^{(\mathrm{C})}_{r_{\min}}}a^{(q)}\,, \quad z_{r_{\max}} = \sqrt{P^{(\mathrm{C})}_{r_{\max}}}a^{(q)} + \sqrt{P^{(\mathrm{P})}_{r_{\max}}}a^{(e)}\,. \tag{6.19}$$

Scaling factors $\left\{P^{(\mathrm{P})}_{r_{\max}}, P^{(\mathrm{C})}_{r_{\max}}, P^{(\mathrm{C})}_{r_{\min}}\right\}$ are optimized by imposing that the combination of the signals $z_{r_{\max}}$ and $z_{r_{\min}}$ through channels at node D results in a scaled version of symbol a. Hence, using (6.17) and (6.19) we obtain

$$\sqrt{G_{r_{\max}}P^{(\mathrm{C})}_{r_{\max}}} + \sqrt{G_{r_{\min}}P^{(\mathrm{C})}_{r_{\min}}} = \sqrt{G_{r_{\max}}P^{(\mathrm{P})}_{r_{\max}}}\,. \tag{6.20}$$

As the noise has unitary variance, using (6.20) it can be shown that the SNR at D turns out to be $G_{r_{\max}}P^{(\mathrm{P})}_{r_{\max}}$. Note that with this transmission scheme the implementation complexity is significantly reduced with respect to the ABM scheme because node D receives only a sequence of symbols belonging to the full QAM constellation and does not require the implementation of successive interference cancellation.

Moreover, as S is required to provide signals $a^{(q)}$ and $a^{(e)}$ to relays $\{r_{\max}, r_{\min}\}$ through a Gaussian broadcast channel, from Section 3.3.2 we approximate the spectral efficiency of $a^{(q)}$ with $\min\left\{(1-\lambda)b^{(q)}, R^{(\mathrm{E})}\right\}$ and that of $a^{(e)}$ with $\min\left\{(1-\lambda)(b-b^{(q)}), R^{(\mathrm{E})}\right\}$. Then, similarly to Section 6.3.2, we denote with α and $1-\alpha$ the power used by S to transmit during odd phases the signal representation of $a^{(e)}$ and $a^{(q)}$, respectively.

In the following we also develop a practical algorithm to optimize system parameters with this transmission scheme. In detail, discrete variables $\left\{\delta_i, b, b^{(q)}\right\}$ are optimized by an exhaustive search and for each i) relay scheduling configuration (i.e., fixed $\bar{r}$, $r_{\max}$ and $r_{\min}$) and ii) constellation sizes (i.e., fixed b and $b^{(q)}$), we perform a) power allocation and b) time-sharing optimization with the aim of maximizing spectral efficiency $R^{(\mathrm{E})}$ achieved with the assistance of relays $r_{\max}$ and $r_{\min}$. In fact, the problem of maximizing spectral efficiency $R^{(\mathrm{E})}$ can be written as

$$R^{(\mathrm{E},*)} = \max_{\alpha,\lambda,P^{(\mathrm{P})}_{r_{\max}},P^{(\mathrm{C})}_{r_{\max}},P^{(\mathrm{C})}_{r_{\min}}} \quad (1-\lambda)\min\left\{b, C\left(G_{r_{\max}}P^{(\mathrm{P})}_{r_{\max}}\right)\right\} \tag{6.21a}$$

subject to

$$(1-f(b,b^{(q)}))P_{r_{\max}}^{(\mathrm{C})}+f(b,b^{(q)})P_{r_{\max}}^{(\mathrm{P})}\leq 1\,, \tag{6.21b}$$

$$(1-f(b,b^{(q)}))P_{r_{\min}}^{(\mathrm{C})}\leq 1\,, \tag{6.21c}$$

$$\sqrt{G_{r_{\max}}P_{r_{\max}}^{(\mathrm{C})}}+\sqrt{G_{r_{\min}}P_{r_{\min}}^{(\mathrm{C})}}=\sqrt{G_{r_{\max}}P_{r_{\max}}^{(\mathrm{P})}}\,, \tag{6.21d}$$

$$(1-\lambda)\min\left\{\left(b-b^{(q)}\right),\min\left\{b,C\left(G_{r_{\max}}P_{r_{\max}}^{(\mathrm{P})}\right)\right\}\right\}\leq\lambda C\left(\alpha H_{r_{\max}}\right)\,, \tag{6.21e}$$

$$(1-\lambda)\min\left\{b^{(q)},\min\left\{b,C\left(G_{r_{\max}}P_{r_{\max}}^{(\mathrm{P})}\right)\right\}\right\}\leq\lambda C\left(\frac{(1-\alpha)H_{r_{\min}}}{1+\alpha H_{r_{\min}}}\right)\,, \tag{6.21f}$$

$$0\leq\alpha\leq 1\,,\quad 0\leq\lambda\leq 1\,, \tag{6.21g}$$

$$P_{r_{\max}}^{(\mathrm{P})}\geq 0\,,\quad P_{r_{\max}}^{(\mathrm{C})}\geq 0\,,\quad P_{r_{\min}}^{(\mathrm{C})}\geq 0\,. \tag{6.21h}$$

Note that i) in (6.21a) we consider a maximum spectral efficiency b depending on the size of the full QAM constellation, ii) (6.21b) and (6.21c) represent the power constraints at relays $r_{\max}$ and $r_{\min}$, respectively, and iii) (6.21e) and (6.21f) bound the rate of the Gaussian broadcast channel between S and relays $r_{\max}$ and $r_{\min}$.

Power allocation

In (6.21) powers $\left\{P_{r_{\max}}^{(\mathrm{P})},\,P_{r_{\max}}^{(\mathrm{C})},\,P_{r_{\min}}^{(\mathrm{C})}\right\}$ can be optimized separately with the aim of maximizing $C\left(G_{r_{\max}}P_{r_{\max}}^{(\mathrm{P})}\right)$ by solving

$$\max_{P_{r_{\max}}^{(\mathrm{P})},\,P_{r_{\max}}^{(\mathrm{C})},\,P_{r_{\min}}^{(\mathrm{C})}}\quad P_{r_{\max}}^{(\mathrm{P})}\,, \tag{6.22}$$

subject to (6.21b), (6.21c), (6.21d) and (6.21h).

We denote with $\left\{P_{r_{\max}}^{(\mathrm{P},*)},\,P_{r_{\max}}^{(\mathrm{C},*)},\,P_{r_{\min}}^{(\mathrm{C},*)}\right\}$ the optimal solution to (6.22). Note that when:

- $b^{(q)}=0$ (i.e., $f(b,b^{(q)})=1$) relay $r_{\max}$ transmits symbol $a^{(e)}=a$ at full power $P_{r_{\max}}^{(\mathrm{P})}=1$ while relay $r_{\min}$ remains silent;
- $b^{(q)}=b$ (i.e., $f(b,b^{(q)})=0$) both relays $r_{\max}$ and $r_{\min}$ transmit $a^{(q)}=a$ at full powers $P_{r_{\max}}^{(\mathrm{C})}=P_{r_{\min}}^{(\mathrm{C})}=1$ and $P_{r_{\max}}^{(\mathrm{P})}$ can be directly computed from (6.21d);
- $0<b^{(q)}<b$ (i.e., $0<f(b,b^{(q)})<1$) i) (6.21c) represents only an upper bound on $P_{r_{\min}}^{(\mathrm{C})}$ and ii) (6.21b) is satisfied with equality by the optimal solution to (6.22).

Hence, after defining

$$\xi(x)=\sqrt{G_{r_{\max}}\,x}-\sqrt{\frac{G_{r_{\max}}(1-f(b,b^{(q)})\,x)}{1-f(b,b^{(q)})}}\,, \tag{6.23}$$

problem (6.22) can be written as

$$\max_{0\leq P_{r_{\max}}^{(\mathrm{P})}\leq 1/f(b,b^{(q)})} \quad P_{r_{\max}}^{(\mathrm{P})} \tag{6.24a}$$

subject to

$$0 \leq \xi\left(P_{r_{\max}}^{(\mathrm{P})}\right) \leq \sqrt{\frac{G_{r_{\min}}}{1-f(b,b^{(q)})}}\,. \tag{6.24b}$$

By observing that $\xi(x)$ is an increasing function of x for $x \in \left[0, 1/f(b,b^{(q)})\right]$ and that $\xi(1)=0$, the optimal power $P_{r_{\max}}^{(\mathrm{P},*)}$ is the solution to

$$\max_{1\leq P_{r_{\max}}^{(\mathrm{P})}\leq 1/f(b,b^{(q)})} \quad P_{r_{\max}}^{(\mathrm{P})} \tag{6.25a}$$

subject to

$$\xi\left(P_{r_{\max}}^{(\mathrm{P})}\right) \leq \sqrt{\frac{G_{r_{\min}}}{1-f(b,b^{(q)})}}\,. \tag{6.25b}$$

Note that maximization (6.25) can be solved by the simple bisection method which selects the maximum value of variable $P_{r_{\max}}^{(\mathrm{P})} \in \left[1, 1/f(b,b^{(q)})\right]$ that satisfies constraint (6.25b). Furthermore, from (6.21b) and (6.21d) we obtain

$$P_{r_{\max}}^{(\mathrm{C},*)} = \frac{1-f(b,b^{(q)})P_{r_{\max}}^{(\mathrm{P},*)}}{1-f(b,b^{(q)})}\,, \quad P_{r_{\min}}^{(\mathrm{C},*)} = \frac{\xi^2\left(P_{r_{\max}}^{(\mathrm{P},*)}\right)}{G_{r_{\min}}}\,. \tag{6.26}$$

Time-sharing optimization

After performing the power allocation described in the previous section, (6.21) can be written as

$$\max_{\alpha,\lambda} \quad (1-\lambda)\min\left\{b, C\left(G_{r_{\max}}P_{r_{\max}}^{(\mathrm{P},*)}\right)\right\}\,, \tag{6.27}$$

subject to (6.21e), (6.21f), and (6.21g). We denote with $\left\{\alpha^{(*)},\, \lambda^{(*)}\right\}$ the optimal solution to (6.27). By defining

$$k_1 = \min\left\{b-b^{(q)}, C\left(G_{r_{\max}}P_{r_{\max}}^{(\mathrm{P},*)}\right)\right\}\,, \quad k_2 = \min\left\{b^{(q)}, C\left(G_{r_{\max}}P_{r_{\max}}^{(\mathrm{P},*)}\right)\right\}\,, \tag{6.28}$$

(6.27) can be rewritten as

$$\min_{0\leq\alpha\leq 1,\, 0\leq\lambda\leq 1} \quad \lambda \tag{6.29a}$$

subject to

$$\lambda \geq \frac{k_1}{k_1 + C\left(\alpha H_{r_{\max}}\right)} = \psi_1(\alpha)\,, \tag{6.29b}$$

$$\lambda \geq \frac{k_2}{k_2 + C\left(\frac{(1-\alpha)H_{r_{\min}}}{1+\alpha H_{r_{\min}}}\right)} = \psi_2(\alpha)\,. \tag{6.29c}$$

We observe that $\psi_1(\alpha)$ and $\psi_2(\alpha)$ are decreasing and increasing functions, respectively, in the interval $\alpha \in [0,1]$. After defining $\psi_3(\alpha) = \psi_1(\alpha) - \psi_2(\alpha)$ and observing that $\psi_3(0) > 0$ and $\psi_3(1) < 0$, the optimal $\alpha^{(*)}$ is obtained by solving

$$\psi_3(\alpha^{(*)}) = 0\,. \tag{6.30}$$

Note that $\alpha^{(*)}$ can be computed in (6.30) by applying the simple bisection method. Furthermore, the optimal $\lambda^{(*)}$ is simply given by

$$\lambda^{(*)} = \psi_3\left(\alpha^{(*)}\right)\,. \tag{6.31}$$

Spectral efficiency computation

After the computation of $\left\{P_{r_{\max}}^{(\mathrm{P},*)}, P_{r_{\max}}^{(\mathrm{C},*)}, P_{r_{\min}}^{(\mathrm{C},*)}, \alpha^{(*)}, \lambda^{(*)}\right\}$, the available spectral efficiencies can be written from (6.13b), (6.13c) and (6.21a) as

$$R^{(\mathrm{E},*)} = (1-\lambda^{(*)}) \min\left\{b, C\left(G_{r_{\max}} P_{r_{\max}}^{(\mathrm{P},*)}\right)\right\}\,, \tag{6.32a}$$

$$R^{(\mathrm{O},*)} = \min\left\{\lambda^{(*)} \min\left\{b_{\max}, C\left(G_{\bar{r}}\right)\right\}, (1-\lambda^{(*)}) C\left(H_{\bar{r}}\right)\right\}\,. \tag{6.32b}$$

By denoting with $\mathcal{B} = \{2, 4, \ldots, b_{\max}\}$ the sizes of available QAM constellations at relays $r_{\max}$ and $r_{\min}$, the network spectral efficiency from S to D is

$$R^{(\mathrm{ABM-QCT})} = \max_{\delta_i\,,\, b\in\mathcal{B}\,,\, b^{(q)}\in\{0,2,4,\ldots,b\}} R^{(\mathrm{E},*)} + R^{(\mathrm{O},*)} \tag{6.33}$$

subject to (6.11) and (6.12). Problem (6.33) can be solved by an exhaustive search in the discrete variables $\left\{\delta_i, b, b^{(q)}\right\}$.

6.4 Cut-set upper bound

In this section we derive an upper bound for the sum rate that can be achieved in the considered scenario. Since S and D are always transmitting and receiving, respectively, there are at most $2^3 = 8$ configurations of $\{\delta_i\}$. Only for this section we denote with $\bar{\lambda}$ the fraction of the total unitary time when no relay is transmitting, λ when all relays are transmitting, λ_i when only relay i is transmitting and $\bar{\lambda}_i$ when only relay i is not transmitting. Moreover, there are eight different *cuts* that separate S from D, and each one is related to a constraint on the information-rate. The cut-set upper bound for the

considered relay network can be expressed as [71]

$$R^{(\text{cut}-\text{set b.})} = \max_{\left\{\bar{\lambda},\lambda_i,\bar{\lambda}_i,\lambda\right\}\geq 0} R \tag{6.34a}$$

subject to

$$R \leq \bar{\lambda} C\left(\sum_i H_i\right) + \sum_i \lambda_i C\left(\sum_{j\neq i} H_j\right) + \sum_i \bar{\lambda}_i C\left(H_i\right) , \tag{6.34b}$$

$$\begin{aligned} R \leq & \bar{\lambda} C\left(\sum_{j\neq i} H_j\right) + \lambda_i \left[C\left(\sum_{j\neq i} H_j\right) + C\left(G_i\right)\right] + \sum_{j\neq i} \lambda_j C\left(H_{k:k\neq i,j}\right) + \\ & \sum_{j\neq i} \bar{\lambda}_j \left[C\left(H_j\right) + C\left(G_i\right)\right] + \lambda C\left(G_i\right) , \quad i = 1,2,3 , \end{aligned} \tag{6.34c}$$

$$\begin{aligned} R \leq & \bar{\lambda} C\left(H_i\right) + \sum_{j\neq i} \lambda_j \left[C\left(H_i\right) + C\left(G_j\right)\right] + \bar{\lambda}_i \left[C\left(H_i\right) + C\left(\left(\sum_{j\neq i} \sqrt{G_j}\right)^2\right)\right] + \\ & \sum_{j\neq i} \bar{\lambda}_j C\left(G_{k:k\neq i,j}\right) + \lambda C\left(\left(\sum_{j\neq i} \sqrt{G_j}\right)^2\right) , \quad i = 1,2,3 , \end{aligned} \tag{6.34d}$$

$$R \leq \sum_i \lambda_i C\left(G_i\right) + \sum_i \bar{\lambda}_i C\left(\left(\sum_{j\neq i} \sqrt{G_j}\right)^2\right) + \lambda C\left(\left(\sum_i \sqrt{G_i}\right)^2\right) , \tag{6.34e}$$

$$\bar{\lambda} + \sum_i \left(\lambda_i + \bar{\lambda}_i\right) + \lambda \leq 1 . \tag{6.34f}$$

Note that (6.34) is a convex optimization problem.

6.5 Numerical results

We consider that all nodes are located in a plane. Channel gains are related to the path loss, hence can be written as

$$H_i = \frac{\kappa}{d_{Si}^{\eta}} , \quad G_i = \frac{\kappa}{d_{iD}^{\eta}} , \quad i = 1,2,3, \tag{6.35}$$

where d_{Si} and d_{iD} are the distances between S and relay i and between relay i and D, respectively, $\eta = 2$ is the path loss coefficient and κ is a normalization factor that determines the SNR for a unitary distance. We assume that source node S is located at $(-d_{\max}, 0)$ and destination node D at $(0, d_{\max})$. Even if we neglect the direct link connecting S to D, we define the parameter $\text{SNR}^{(\text{ref})} = \kappa/(2d_{\max})^{\eta}$ that describes the size of the network. For ABM-QCT we consider $b_{\max} = 8$ and $\mathcal{B} = \{2,4,6,8\}$. We compute

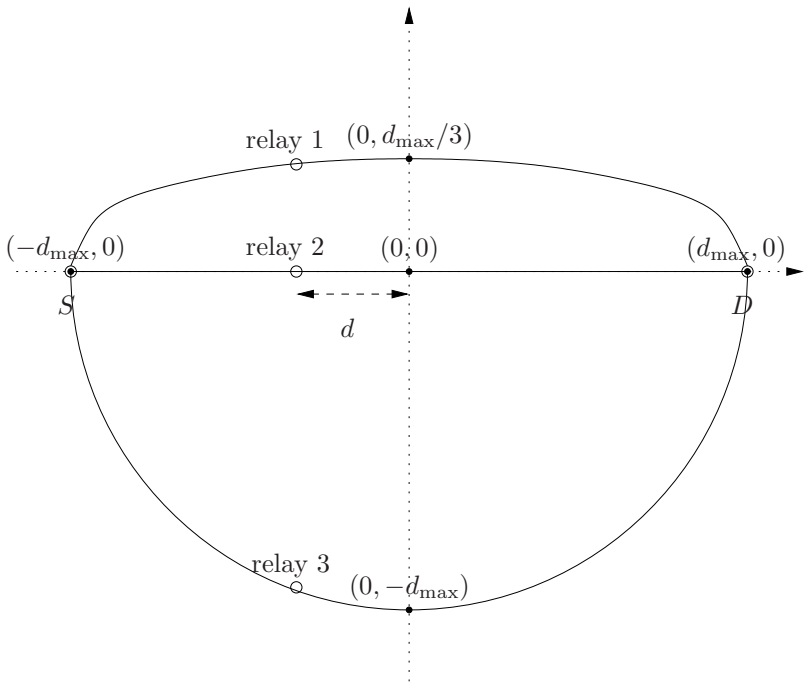

Figure 6.3: Network model with the three relays moving from S to D on a set of ellipses centered in $(0, 0)$.

the solution to problems (6.6), (6.10) and (6.16) by using standard global solver tools in GAMS [25], thanks to the limited size of the considered scenario. Developed schemes are compared in terms of the spectral efficiency.

Firstly, we assume that relays are moving from S to D on a set of ellipses centered in $(0, 0)$ with the semi-major axes long $d_{\max}$ and different values for the semi-minor axes as shown in Fig. 6.3. In detail, relay 1 is located at $(d, d_{\max}/3\sqrt{1-(d/d_{\max})^2})$, relay 2 at $(d, 0)$ and relay 3 at $(d, -d_{\max}\sqrt{1-(d/d_{\max})^2})$, with $-d_{\max} < d < d_{\max}$. For this setup we report in Fig. 6.4 the spectral efficiency achieved by the considered schemes in terms of d when $\mathrm{SNR}^{(\mathrm{ref})} = 2$ dB. We observe that schemes as ABM, ABM-QCT and ADF significantly outperform the other schemes which do not achieve spatial multiplexing, and ABM strictly outperforms ABM-QCT. As expected (see also [70]) BM strictly outperforms DF. Then, DF outperforms AF when the relays are clustered around S, whereas AF strictly outperforms DF when the relays are half way between S and D.

In Fig. 6.5 we consider a different scenario where relays are randomly dropped in a square area centered in $(0, 0)$ and whose sides have length $2(d_{\max} - d_{\min})$ where $d_{\min}$ is the minimum distance between S or D and each relay. We also consider a Rayleigh fading channel where each κ variable in (6.35) is multiplied by an independent exponential random variable with unitary mean, and we set $\kappa/d_{\min}^2 = 30$ dB which determines the maximum value assumed by H_i and G_i, neglecting fading. Note that with this value of $d_{\min}$ the saturation of the spectral efficiency due to the use of a finite set of QAM constellations in ABM-QCT is negligible. In this scenario we report in Fig. 6.6 the average spectral

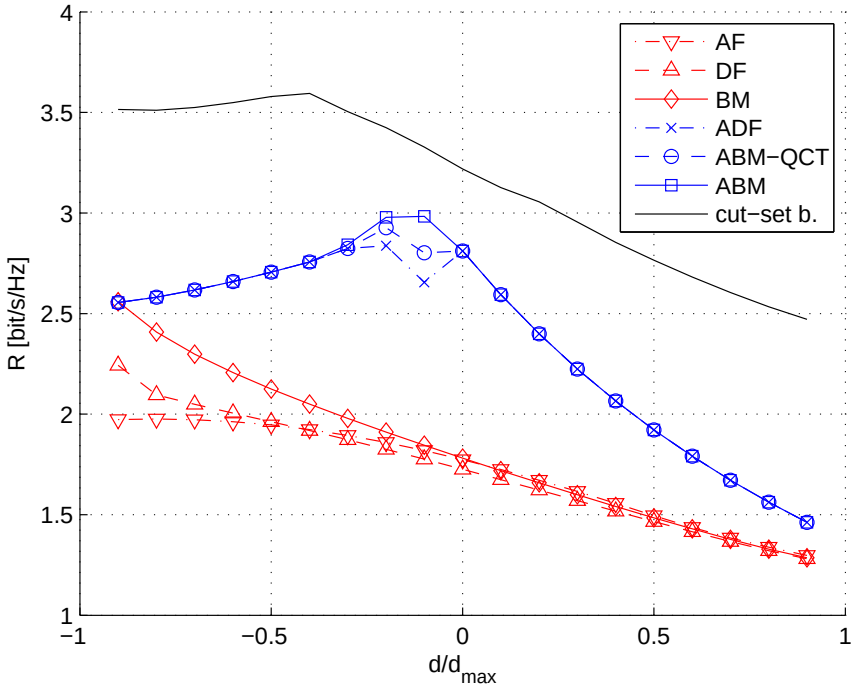

Figure 6.4: Spectral efficiency versus d for the network model described in Fig. 6.3 and $\mathrm{SNR}^{(\mathrm{ref})} = 2$ dB.

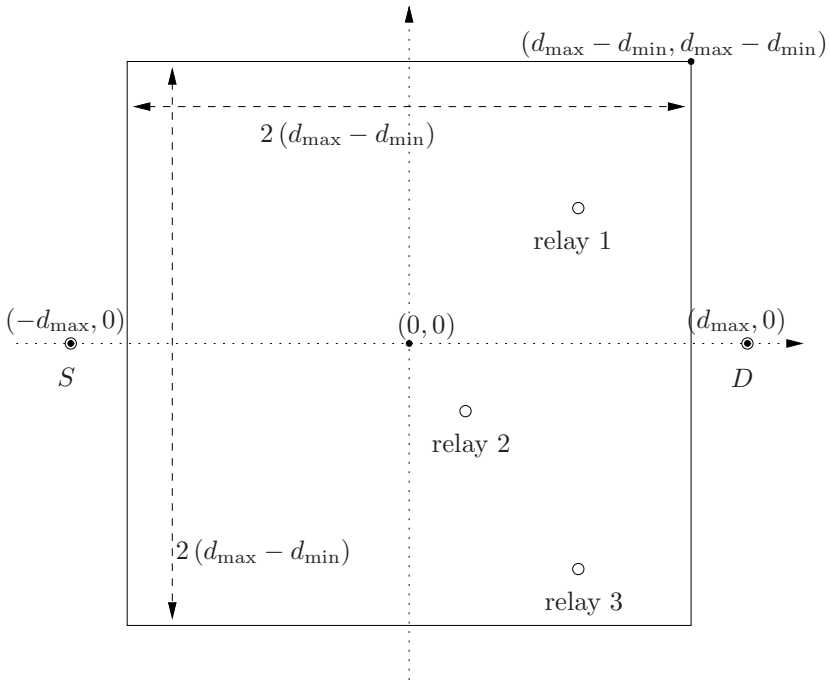

Figure 6.5: Network model with the three relays randomly dropped in a square area between S and D.

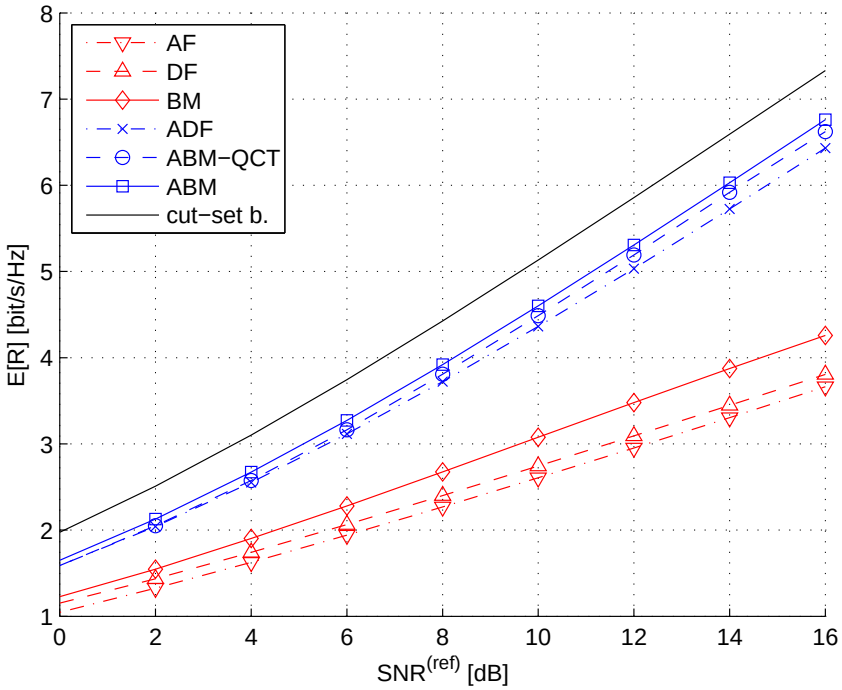

Figure 6.6: Average spectral efficiency versus $\mathrm{SNR}^{(\mathrm{ref})}$ for the network model described in Fig. 6.5.

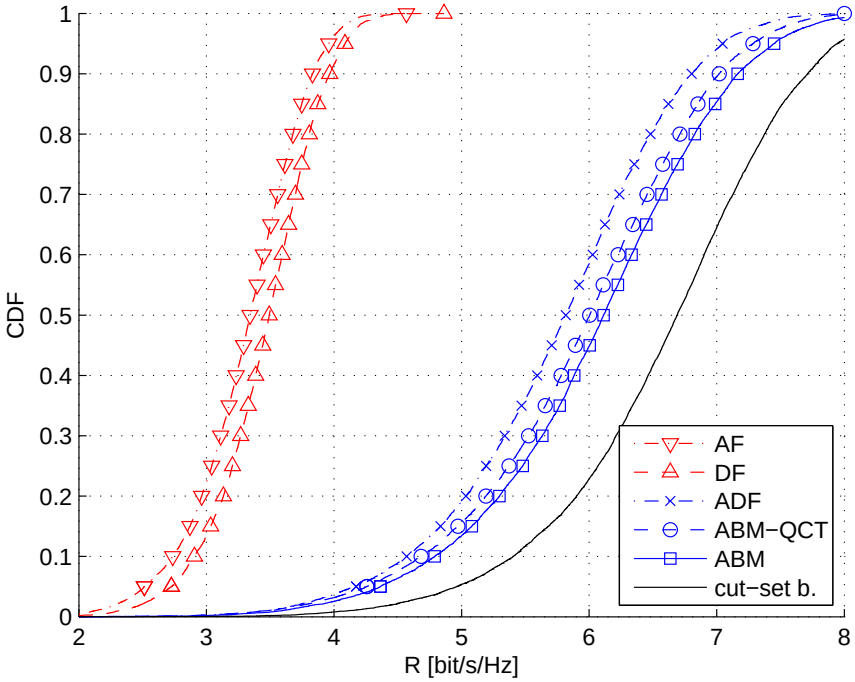

Figure 6.7: CDF of the spectral efficiency for the network model described in Fig. 6.5 and $\mathrm{SNR}^{(\mathrm{ref})} = 14$ dB.

efficiency in terms of $\mathrm{SNR}^{(\mathrm{ref})}$, and in Fig. 6.7 the CDF of the spectral efficiency when $\mathrm{SNR}^{(\mathrm{ref})} = 14$ dB. As expected, ABM outperforms all the other schemes. However, the performance gain of ABM with respect to ADF, due to the fact that $r_{\max}$ and $r_{\min}$ can decode private and common messages, is not very high, about 5% with $\mathrm{SNR}^{(\mathrm{ref})} \in [6, 16]$ dB. Moreover, ABM-QCT outperforms ADF and approaches ABM for higher values of $\mathrm{SNR}^{(\mathrm{ref})}$. Note that the spectral efficiency achieved by AF, DF, and BM is considerably lower than that achieved by ADF. Also the CDF confirms that ABM is the best scheme and slightly outperforms ABM-QCT. In particular, in the lower tail of the CDF (i.e., CDF = 0.1) ABM-QCT shows a performance gain with respect to ADF of about 2.9% and a performance loss with respect to ABM of about 2.7%.

However, note that the implementation complexity of ABM-QCT is lower than that of ABM as node D is not required to implement successive interference cancellation in order to decode private and common messages.

6.6 Conclusions

In this chapter we have considered a network with three half-duplex relays assisting the transmission of a source toward a destination. Spatial multiplexing is achieved by allowing a single relay to transmit in odd phases and the other two relays to transmit in even phases. In such a case we have proposed a new transmission scheme denoted adaptive broadcast multiaccess (ABM)-quantized constellation transmission (QCT) and have developed a practical algorithm to perform power allocation and time-sharing optimization. Simulation results show that ABM-QCT slightly outperforms ADF and achieves a spectral efficiency close to the one obtained by the more complex ABM.

Chapter 7

Resource allocation in SC-FDMA uplink CoMP

Differently from previous chapters focused on the downlink, in this chapter we consider the uplink of cellular systems. In this scenario the backhaul infrastructure limits the amount of information that the BSs can exchange in decoding the messages sent by the UEs.

The first studies from a information theoretic point of view [72, 73, 74] have derived rate regions (or bounds on the regions) for the constrained backhaul uplink CoMP, and more recently the effect of imperfect CSI has been considered [75]. It turns out that scheduling of both UE transmissions and backhaul resources is of paramount importance in these systems, in order to exploit at best the potentials of CoMP. Various approaches have been proposed in the literature. In [76] a mathematical framework is developed for observing both capacity improvement and backhaul occupation, and an heuristic algorithm is proposed based on this framework. In [77] a trade-off between the rate of the wireless link and the backhaul occupation is achieved by scheduling the UE transmissions. In [78] the set of BSs that cooperate for the decoding of signals is selected based on the outage probability assuming that transmissions use a hybrid automatic repeat request protocol. The maximization of the network rate for a given UE deployment is considered as objective in the selection of cooperating BSs in [79]. Similar to the scenario studied in Chapter 6, a related problem is the allocation of resources in the uplink of relay-assisted networks, where the connection from the relay to the BSs can be seen as a backhaul network [80].

All of the above cited studies focus on achievable rates and scheduling (on the wireless link and the backhaul) for uplink CoMP by assuming that transmissions occur on a set of parallel flat-fading channels as in OFDM. However, the LTE of 3GPP, in the uplink, has adopted single carrier frequency division multiple access (SC-FDMA) [81], where a single carrier signal is allocated to a specific band by use of discrete Fourier transforms (DFTs). Moreover, the addition of a cyclic prefix yields a simplified receiver architecture since equalization of dispersive channels can be performed in the frequency domain by means

of efficient DFTs [82]. In practice, linear equalizers are used in order to limit complexity, at the expense of reduced performance with respect to non-linear equalizers [83]. For SC-FDMA systems, scheduling of UE transmission for interference mitigation is considered in [84, 85], but among the BSs no sharing of signals received from UEs is considered.

In this chapter we consider CoMP for the uplink of a SC-FDMA based cellular system, under a backhaul rate constraint. The main objective is a scheduling algorithm for transmission on the backhaul network in order to maximize the system sum rate achieved on the wireless link, while satisfying a constraint on the maximum rate on the backhaul. To limit backhaul rate, we propose that on the backhaul the BSs share the received samples only within a subset of the SC-FDMA subcarriers. In turn, this set is selected dynamically according to the channel conditions of each UE-BS link and considering the backhaul rate constraint. The shared samples are then suitably gathered by each BS in order to reconstruct an improved version of the received signal from the served UEs. In particular, before data detection two equalization approaches are considered, both in the frequency domain: signal selection and combining. In the first approach the serving BS may substitute the signals received directly from the UEs with those shared on the backhaul. In the combining approach instead each BS performs a combining of the signals received directly and those shared on the backhaul. In both cases, the weighting of the useful signal against noise plus interference is carried out by both a zero forcing and mean square error criterion. Since scheduling turns out to be a non-linear integer programming problem, a greedy algorithm is proposed for an efficient implementation. Lastly, to further increase the system performance, we propose that BSs detect messages from some UEs without cooperation, then adjust the amplitude and phase of the detected signals before transmitting them on the backhaul. This adjustment allows a perfect cancellation of the interference caused by the detected signals at the cooperating BSs. The scheduling problem is suitably modified in order to take into account the benefits of interference cancellation (IC), thus shaping the ordering of decoding of the various messages. To assess the merits of the proposed solutions, numerical results in a realistic LTE scenario allow a comparison between the proposed greedy algorithm and an upper bound given by a backhaul with no constraint.

7.1 System model

We consider the uplink of a cellular system comprising a set $\mathcal{K} = \{1, 2, \ldots, K\}$ of UEs transmitting to a set $\mathcal{J} = \{1, 2, \ldots, J\}$ of BSs. Both UEs and BSs are assumed to have one antenna each. In the following we describe the transmission both from the UEs to the BSs on the wireless link and among the BSs over the backhaul.

7.1.1 Conventional SC-FDMA transmission

According to SC-FDMA, the available spectrum of N subcarriers is divided into S resource blocks (RBs) each of M subcarriers, i.e., $N = MS$. In particular, let $\mathcal{S} =$

$\{0, 1, \dots S-1\}$ be the set of available RBs and $\mathcal{N}_s = \{sM, sM+1, \dots, sM+M-1\}$, $s \in \mathcal{S}$, the set of subcarriers associated to RB s. With reference to UE $k \in \mathcal{K}$ we define as $\mathcal{S}^{(k)} \subseteq \mathcal{S}$ the set of allocated RBs and $\mathcal{N}^{(k)} = \left\{n \in \mathcal{N}_s : s \in \mathcal{S}^{(k)}\right\}$ the corresponding set of subcarriers. Moreover, let $\mathcal{K}^{(j)} \subseteq \mathcal{K}$ be the set of UEs anchored to BS j, with

$$\bigcup_{j \in \mathcal{J}} \mathcal{K}^{(j)} = \mathcal{K}\,, \quad \mathcal{K}^{(j)} \cap \mathcal{K}^{(i)} = \emptyset\,,\ i \neq j\,. \tag{7.1}$$

In fact, only UEs belonging to two distinct $\mathcal{K}^{(j)}$ sets may end up using the same RB. In the following we assume that the assignment of RBs $\mathcal{S}^{(k)}$ to UE k, $k \in \mathcal{K}^{(j)}$, has already been performed by BS j. In Section 7.4 this assignment is performed by allocating randomly to each UE $k \in \mathcal{K}^{(j)}$ exactly $S/\left|\mathcal{K}^{(j)}\right|$ adjacent RBs. Lastly, let $\mathcal{K}_s \subseteq \mathcal{K}$ be the set of UEs transmitting on a given RB s. This set specifies inter-cell interference (ICI).

Data transmission performed by UE k is organized into blocks also in the time domain. We start from $M|\mathcal{S}^{(k)}|$ symbols, $d_m^{(k)}$, $m = 0, 1, \dots, M|\mathcal{S}^{(k)}| - 1$, each symbol taken from a QAM constellation with unitary power. This sequence is first transformed by a unitary $M|\mathcal{S}^{(k)}|$-size DFT to obtain the signal $D_\ell^{(k)}$, $\ell = 0, 1, \dots, M|\mathcal{S}^{(k)}|-1$. In turn this sequence is mapped into the RBs with indices $\mathcal{S}^{(k)}$. The augmented signal of size N is called $X_n^{(k)}$, $n = 0, 1, \dots, N-1$. Note that $X_n^{(k)}$ is non-zero only for $n \in \mathcal{N}^{(k)}$.

Signal $X_n^{(k)}$ is transformed by an N-size inverse discrete Fourier transform (IDFT) into the time domain and is extended with a cyclic prefix of size L, i.e., the last L samples of each block are pre-pended to the first sample of the block, and the obtained time domain sample sequence of size $N + L$ is transmitted onto the channel.

The channel between UE k and BS j is represented by a filter, followed by the addition of white Gaussian noise. The channel is time-invariant for the duration of the transmission of a block.

At BS j, the first L samples of the received signal are discarded and an N-size DFT is applied on the remaining samples to obtain the frequency-domain signal

$$Y_n^{(j)} = \sum_{k \in \mathcal{K}} H_n^{(j,k)} X_n^{(k)} + W_n^{(j)}\,,\ n = 0, 1, \dots, N-1, \tag{7.2}$$

where $H_n^{(j,k)}$ is the n-th entry of the N-size DFT of the channel impulse response (including transmit and receive filters) from UE k to BS j, and $W_n^{(j)}$ is the AWGN term with zero mean and unitary variance. If we were interested in detecting the signal coming from the UE k anchored to BS j, we would rewrite (7.2) as

$$Y_n^{(j)} = H_n^{(j,k)} X_n^{(k)} + \sum_{k' \in \mathcal{K} \setminus \{k\}} H_n^{(j,k')} X_n^{(k')} + W_n^{(j)} = H_n^{(j,k)} X_n^{(k)} + I_n^{(j,k)}\,,\ n \in \mathcal{N}^{(k)}\,, \tag{7.3}$$

where $I_n^{(j,k)}$ is the ICI plus noise that can be modeled as zero-mean with power (let

$n = sM + r$)

$$\gamma_{sM+r}^{(j,k)} = \sum_{k' \in \mathcal{K}_s \setminus \{k\}} \left| H_{sM+r}^{(j,k')} \right|^2 + 1 \,,\; s \in \mathcal{S}^{(k)} \,,\; r = 0, 1, \ldots, M-1 \,. \tag{7.4}$$

Note that in (7.3) $Y_n^{(j)}$, $n \in \mathcal{N}^{(k)}$, is a signal of size $M|\mathcal{S}^{(k)}|$. Linear equalization follows, by multiplying $Y_n^{(j)}$ with suitable complex coefficients $E_n^{(j)}$, $n \in \mathcal{N}^{(k)}$. The equalized signal is then transformed into the time domain by an $M|\mathcal{S}^{(k)}|$-size IDFT, and the obtained signal feeds a QAM demapper. After equalization the SINR for UE k anchored to BS j can be written as

$$\mathrm{SINR}^{(k)} = \frac{\dfrac{1}{\left|\mathcal{N}^{(k)}\right|} \left| \displaystyle\sum_{n \in \mathcal{N}^{(k)}} E_n^{(j)} H_n^{(j,k)} \right|^2}{\displaystyle\sum_{n \in \mathcal{N}^{(k)}} \left| E_n^{(j)} H_n^{(j,k)} \right|^2 - \frac{1}{\left|\mathcal{N}^{(k)}\right|} \left| \sum_{n \in \mathcal{N}^{(k)}} E_n^{(j)} H_n^{(j,k)} \right|^2 + \sum_{n \in \mathcal{N}^{(k)}} \gamma_n^{(j,k)} \left| E_n^{(j)} \right|^2} \,, \tag{7.5}$$

where at the denominator the first two terms take into account the inter-symbol interference (ISI), whereas the third term includes both noise and ICI. Note that we omitted index j from $\mathrm{SINR}^{(k)}$ as the UE index uniquely identifies its anchor BS j by the set $\mathcal{K}^{(j)}$. From (7.5) the achievable throughput turns out to be

$$R^{(k)} = \left| \mathcal{N}^{(k)} \right| B \log_2 \left(1 + \mathrm{SINR}^{(k)} \right) \,, \tag{7.6}$$

where B is the subcarrier bandwidth.

Two equalizers are typically used:

- zero forcing (ZF), which nulls ISI by imposing

$$E_n^{(j,\mathrm{ZF})} = 1 / H_n^{(j,k)} \,, \tag{7.7}$$

- minimum mean square error (MMSE), which takes into account noise, ISI and ICI by imposing

$$E_n^{(j,\mathrm{MMSE})} = H_n^{(j,k)*} / \left(\left| H_n^{(j,k)} \right|^2 + \gamma_n^{(j,k)} \right) \,. \tag{7.8}$$

With these two equalizers (7.6) can be simplified into (see also [86])

$$R^{(k,\mathrm{ZF})} = \left| \mathcal{N}^{(k)} \right| B \log_2 \left(1 + \frac{1}{\dfrac{1}{\left|\mathcal{N}^{(k)}\right|} \displaystyle\sum_{n \in \mathcal{N}^{(k)}} \dfrac{\gamma_n^{(j,k)}}{\left| H_n^{(j,k)} \right|^2}} \right) \,, \tag{7.9a}$$

$$R^{(k,\mathrm{MMSE})} = \left|\mathcal{N}^{(k)}\right| B \log_2 \left(\frac{1}{\frac{1}{\left|\mathcal{N}^{(k)}\right|} \sum_{n \in \mathcal{N}^{(k)}} \frac{1}{\frac{\left|H_n^{(j,k)}\right|^2}{\gamma_n^{(j,k)}} + 1}} \right) . \tag{7.9b}$$

7.1.2 Backhaul model and system architecture

We consider a star network topology, where a lossless and low-latency backhaul link connects each BS to the CU: therefore all communications among the BSs occur through the CU, and no direct transmission between two BSs is possible. Moreover, with the aim of reducing both complexity at the CU and the backhaul rate, we assume that signal detection is distributed and BS j detects all and only the messages sent by the UEs in $\mathcal{K}^{(j)}$.

At each BS, after reception of the signals sent by UEs, two phases follow: in the first phase, each BS may send received signals to the CU and in the second phase the CU forwards them to BSs. After these two phases, detection of signals coming from UEs is performed at the corresponding serving BS. We consider that each backhaul link has a maximum rate, or equivalently, as all signals are represented by a fixed number of bits, we assume that there is a maximum number of RB signals $S_{\max}$ that can be exchanged (sent in the first phase and received in the second phase) by each BS. For $s \in \mathcal{S}$, $j \in \mathcal{J}$, $i \in \mathcal{J}$, with $i \neq j$, we define the following binary optimization variable

$$x_s^{(j,i)} = \begin{cases} 1, & \text{BS } i \text{ sends to BS } j \text{ signals received on RB } s\,, \\ 0, & \text{otherwise}\,. \end{cases} \tag{7.10}$$

Note that when $x_s^{(j,i)} = 1$, in the first phase the CU receives from BS i samples $Y_n^{(i)}$, $n \in \mathcal{N}_s$, and these samples are then forwarded to BS j in the second phase.

Moreover, $x_s^{(j,j)} = 1$ indicates that the signals received by BS j on wireless links are also used for detection at the same BS, while $x_s^{(j,j)} = 0$ indicates that only the signals coming from the backhaul are used for detection.

The backhaul constraints on the two phases can be written, respectively, as

$$\sum_{s \in \mathcal{S}} \mathbb{1} \left(\sum_{i \in \mathcal{J} \setminus \{j\}} x_s^{(i,j)} \right) \leq S_{\max}\,,\ j \in \mathcal{J}\,, \tag{7.11a}$$

$$\sum_{s \in \mathcal{S}} \sum_{i \in \mathcal{J} \setminus \{j\}} x_s^{(j,i)} \leq S_{\max}\,,\ j \in \mathcal{J}\,, \tag{7.11b}$$

where step function $\mathbb{1}(x)$ has been defined in (5.8). Note that in the second phase (7.11b) we force the total number of RB signals sent by BSs toward BS j to be less than or equal

to $S_{\max}$. On the other hand, in the first phase (7.11a), if BS j needs to send signals of RB s toward more than one BS, BS j can save backhaul rate by simply sending these signals toward the CU once: this explains the step function $\mathbb{1}(x)$ in (7.11a).

Let us stress that the scheduling of RB signals exchanged on the backhaul is performed by the CU before transmission from the UEs, and will be explained in detail in Section 7.2. In fact, as mentioned before, we assume that before transmission, channel estimation is performed at the BSs thanks to either training sequences in TDD or feedback report in FDD. This information is, in turn, forwarded to the CU, which by a scheduler establishes which BSs cooperate on which RBs. Moreover, the CU allows BSs to have perfect CSI.

To reduce the scheduler complexity and by assuming that the coherence bandwidth of the channel is higher than the RB bandwidth, the scheduler *makes decisions* only based on the *RB (average) channel* rather than on subcarrier channel. Hence, we introduce the channel between UE k and BS j on RB s as

$$G_s^{(j,k)} = \frac{1}{M} \sum_{n \in \mathcal{N}_s} H_n^{(j,k)} \,. \tag{7.12}$$

The scheduler assumes that all subcarriers $n \in \mathcal{N}_s$ between UE k and BS j have the same channel (7.12).

7.2 CoMP for SC-CDMA systems

In this section we first describe how each BS can exploit the signals received by the other BSs in order to detect the messages sent by its UEs. Then we describe the criterion on which the scheduler makes decisions, i.e., the system sum rate maximization.

7.2.1 Cell signal combining

With cell signal combining (CSC) each BS j utilizes a linear combiner to exploit all the signals received from the CU. With reference to RB s, we denote with $\mathcal{J}_s^{(j)} = \left\{\mathcal{J}_s^{(j)}(1), \mathcal{J}_s^{(j)}(2), \ldots, \mathcal{J}_s^{(j)}\left(\left|\mathcal{J}_s^{(j)}\right|\right)\right\} = \left\{i \in \mathcal{J} : x_s^{(j,i)} = 1\right\}$ the ordered set of BSs (i.e., $\mathcal{J}_s^{(j)}(c_1) < \mathcal{J}_s^{(j)}(c_2)$, if $c_1 < c_2$) whose signals are used by BS j for combining. Note that for CSC we always have $x_s^{(j,j)} = 1$, since BS j always detects the data of UEs in $\mathcal{K}^{(j)}$ by utilizing also the signals received on its wireless links.

As the scheduler is concerned, by introducing the equivalent vector channel $\boldsymbol{G}_s^{(j,k)}$ between UE $k \in \mathcal{K}$ and BS j on RB s

$$\boldsymbol{G}_s^{(j,k)} = \left[G_s^{\left(\mathcal{J}_s^{(j)}(1),k\right)}, G_s^{\left(\mathcal{J}_s^{(j)}(2),k\right)}, \ldots, G_s^{\left(\mathcal{J}_s^{(j)}\left(\left|\mathcal{J}_s^{(j)}\right|\right),k\right)}\right]^T, \; k \in \mathcal{K} \,, \tag{7.13}$$

the column vector collected by BS j can be written as

$$\boldsymbol{Y}_n^{(j)} = \boldsymbol{G}_s^{(j,k)} X_n^{(k)} + \sum_{k' \in \mathcal{K}_s \setminus \{k\}} \boldsymbol{G}_s^{(j,k')} X_n^{(k')} + \boldsymbol{W}_n^{(j)} \,, \; n \in \mathcal{N}_s \,, \; s \in \mathcal{S}^{(k)} \,, \; k \in \mathcal{K}^{(j)} \,, \quad (7.14)$$

where $\boldsymbol{W}_n^{(j)} \sim \mathcal{CN}\left(\boldsymbol{0}_{\left|\mathcal{J}_s^{(j)}\right| \times 1}, \boldsymbol{I}_{\left|\mathcal{J}_s^{(j)}\right|}\right)$. In the frequency domain a suitable row combiner $\boldsymbol{F}_s^{(j)}$ of size $\left|\mathcal{J}_s^{(j)}\right|$ is applied to all vectors $\boldsymbol{Y}_n^{(j)}$ with $n \in \mathcal{N}_s$. Detection is then performed on signals $\boldsymbol{F}_s^{(j)} \boldsymbol{Y}_n^{(j)}$ to recover $X_n^{(k)}$, $k \in \mathcal{K}^{(j)}$, $s \in \mathcal{S}^{(k)}$, $n \in \mathcal{N}_s$. Let us define the 3-dimensional variable matrix $\boldsymbol{x} \in \{0,1\}^{S \times J \times J}$, with elements $[\boldsymbol{x}]_{s,j,i} = x_s^{(j,i)}$, $s \in \mathcal{S}$, $j \in \mathcal{J}$, $i \in \mathcal{J}$, fully identifying a backhaul scheduling. From (7.14), and extending the rate achieved by a conventional SC-FDMA system (7.6), the rate achieved by UE k anchored to BS j can be written as

$$\begin{aligned} R^{(k)}(\boldsymbol{x}) = \left|\mathcal{N}^{(k)}\right| B \log_2 \Bigg(& 1 + \frac{1}{\left|\mathcal{S}^{(k)}\right|} \left| \sum_{s \in \mathcal{S}^{(k)}} \boldsymbol{F}_s^{(j)} \boldsymbol{G}_s^{(j,k)} \right|^2 \times \\ & \times \Bigg(\sum_{s \in \mathcal{S}^{(k)}} \left| \boldsymbol{F}_s^{(j)} \boldsymbol{G}_s^{(j,k)} \right|^2 - \frac{1}{\left|\mathcal{S}^{(k)}\right|} \left| \sum_{s \in \mathcal{S}^{(k)}} \boldsymbol{F}_s^{(j)} \boldsymbol{G}_s^{(j,k)} \right|^2 + \\ & + \sum_{s \in \mathcal{S}^{(k)}} \left(\left\| \boldsymbol{F}_s^{(j)} \right\|^2 + \sum_{k' \in \mathcal{K}_s \setminus \{k\}} \left| \boldsymbol{F}_s^{(j)} \boldsymbol{G}_s^{(j,k')} \right|^2 \right) \Bigg)^{-1} \Bigg) \,. \end{aligned} \quad (7.15)$$

Note that the optimization variables $x_s^{(j,i)}$ affect both the content and the size of vectors $\boldsymbol{G}_s^{(j,k)}$ and $\boldsymbol{F}_s^{(j)}$ in (7.15) through set $\mathcal{J}_s^{(j)}$.

By denoting with $R(\boldsymbol{x})$ the system sum rate achieved by a backhaul scheduling $\boldsymbol{x}$, i.e.,

$$R(\boldsymbol{x}) = \sum_{k \in \mathcal{K}} R^{(k)}(\boldsymbol{x}) \,, \quad (7.16)$$

the sum rate maximization problem at the scheduler can be formulated as

$$\max_{\boldsymbol{x}} \; R(\boldsymbol{x}) \,, \quad (7.17a)$$

subject to

$$(7.11a), (7.11b),$$

$$x_s^{(j,i)} \in \{0,1\} \,, s \in \mathcal{S}, \; j \in \mathcal{J} \,, \; i \in \mathcal{J} \,. \quad (7.17b)$$

Problem (7.17) turns out to be a non-linear integer optimization problem and we

propose to solve it by the greedy algorithm described in Section 7.3.

Regarding the design of equalizer $\boldsymbol{F}_s^{(j)}$, in the following we extend the ZF and MMSE approaches introduced in Section 7.1.1.

With CSC the ZF combiner is designed with the aim of nulling ISI and by assuming that the ICI plus noise is uncorrelated and with the same power across the BSs in $\mathcal{J}_s^{(j)}$, it is

$$\boldsymbol{F}_s^{(j,\mathrm{ZF})} = \boldsymbol{G}_s^{(j,k)H} / \left\| \boldsymbol{G}_s^{(j,k)} \right\|^2 , \tag{7.18}$$

where k is the index of the UE anchored to BS j and transmitting on RB s. Even if this design criterion is suboptimal, it allows a simple implementation and requires no knowledge of either the noise or the interfering signal power.

The MMSE combiner instead is designed by minimizing the mean square error, thus becoming

$$\boldsymbol{F}_s^{(j,\mathrm{MMSE})} = \boldsymbol{G}_s^{(j,k)H} \left(\boldsymbol{G}_s^{(j,k)} \boldsymbol{G}_s^{(j,k)H} + \boldsymbol{I}_{\left|\mathcal{J}_s^{(j)}\right|} + \sum_{k' \in \mathcal{K}_s \setminus \{k\}} \boldsymbol{G}_s^{(j,k')} \boldsymbol{G}_s^{(j,k')H} \right)^{-1} . \tag{7.19}$$

7.2.2 Cell signal selection

The evaluation of the objective function (7.17a) for a feasible solution requires the computation of JS equalizers, one for each BS $j \in \mathcal{J}$ and RB $s \in \mathcal{S}$, and using the MMSE criterion each equalizer needs a matrix inversion. This results in an important computational complexity for any kind of heuristic algorithm that tries to solve (7.17). Therefore, in this section we propose cell signal selection (CSS) as an alternative solution: the main idea is that BS j detects the message sent by UE $k \in \mathcal{K}^{(j)}$ by simply selecting for each subcarrier the signal characterized by the highest SINR among the ones received on the wireless channel and through the CU. This is obtained by solving (7.17) with the additional constraints

$$\sum_{i \in \mathcal{J}} x_s^{(j,i)} = 1 \, , \; s \in \mathcal{S} \, , \; j \in \mathcal{J} \, , \tag{7.20}$$

which force BS j to use only one signal that can be either its own or one received by another BS. In this way the vector $\boldsymbol{F}_s^{(j)}$ becomes a scalar and the matrix inversion in (7.19) is not required anymore. Note that in this case we are implicitly imposing $\left|\mathcal{J}_s^{(j)}\right| = 1$, thus considerably shrinking the set of feasible solutions. Moreover, differently from CSC, where for equalization BS j is always using the signals received on the wireless links by imposing $x_s^{(j,j)} = 1$, $j \in \mathcal{J}$, with CSS this condition does not hold anymore.

7.2.3 Interference cancellation

Depending on the value of the backhaul matrix $\boldsymbol{x}$, it might happen that the message sent by a UE is detected by its anchor BS without the cooperation of other BSs. We

denote this set of UEs with $\tilde{\mathcal{K}}^{(\mathrm{I})}$, which from (7.10) can be written as

$$\tilde{\mathcal{K}}^{(\mathrm{I})} = \bigcup_{j\in\mathcal{J}} \left\{ k \in \mathcal{K}^{(j)} : \sum_{s\in\mathcal{S}^{(k)}} \sum_{i\in\mathcal{J}\setminus\{j\}} x_s^{(j,i)} = 0 \right\} . \tag{7.21}$$

In turn, we indicate with $\tilde{\mathcal{K}}^{(\mathrm{II})} = \mathcal{K} \setminus \tilde{\mathcal{K}}^{(\mathrm{I})}$ the set of UEs whose messages are detected by exploiting the cooperation, i.e., their anchor BS utilizes also signals from the CU.

In this section we exploit this implicit UE partitioning to improve the system performance by performing IC, which we now describe for BS i. First, BS i detects all messages sent by UEs that are both anchored to itself ($p \in \mathcal{K}^{(i)}$) and whose indices belong to $\tilde{\mathcal{K}}^{(\mathrm{I})}$. Then, it suitably combines with coefficient $\alpha_s^{(j,i)}$ the received signals on RB s with the detected signals and sends their combinations on the backhaul to BS j. In detail, by assuming perfect detection and if $x_s^{(j,i)} = 1$, the signal transmitted on the backhaul by BS i to BS j is

$$\tilde{Y}_n^{(i)} = \begin{cases} Y_n^{(i)} - \alpha_s^{(j,i)} X_n^{(p)} & , p \in \mathcal{K}^{(i)} \cap \tilde{\mathcal{K}}^{(\mathrm{I})} , \\ Y_n^{(i)} & , p \in \mathcal{K}^{(i)} \cap \tilde{\mathcal{K}}^{(\mathrm{II})} , \end{cases} \qquad n \in \mathcal{N}_s \, , \, s \in \mathcal{S}^{(p)} . \tag{7.22}$$

Parameter $\alpha_s^{(j,i)}$ is designed jointly with combiner $\boldsymbol{F}_s^{(j)}$ to null the interference due to UE $p \in \mathcal{K}^{(i)} \cap \tilde{\mathcal{K}}^{(\mathrm{I})}$ at BS j on RB s. By using (7.22), we can define a new equivalent channel $\tilde{\boldsymbol{G}}_s^{(j,p)}$ between UE p and BS j which is obtained by substituting $G_s^{(i,p)}$ with $G_s^{(i,p)} - \alpha_s^{(j,i)}$ in (7.13). Then, for any combiner $\boldsymbol{F}_s^{(j)}$ used by BS j on RB s, we select $\alpha_s^{(j,i)}$ by imposing

$$\boldsymbol{F}_s^{(j)} \tilde{\boldsymbol{G}}_s^{(j,p)} = 0 \, , \tag{7.23}$$

which is a linear equation in the only variable $\alpha_s^{(j,i)}$. By defining the set $\tilde{\mathcal{K}}_s^{(j,\mathrm{I})}$ that includes all UEs whose messages at BS j on RB s are canceled by (7.22) and (7.23), i.e.,

$$\tilde{\mathcal{K}}_s^{(j,\mathrm{I})} = \bigcup_{i\in\mathcal{J}_s^{(j)}\setminus\{j\}} \left\{ p \in \mathcal{K}^{(i)} \cap \mathcal{K}_s \cap \tilde{\mathcal{K}}^{(\mathrm{I})} \right\} , \tag{7.24}$$

the vector signal (7.14) collected by BS j on the RB s associated to UE k with $k \in \mathcal{K}^{(j)}$ can now be written by neglecting the contribution of UEs in $\tilde{\mathcal{K}}_s^{(j,\mathrm{I})}$, i.e.,

$$\tilde{\boldsymbol{Y}}_n^{(j)} = \boldsymbol{G}_s^{(j,k)} X_n^{(k)} + \sum_{k'\in\mathcal{K}_s\setminus\left(\{k\}\cup\tilde{\mathcal{K}}_s^{(j,\mathrm{I})}\right)} \boldsymbol{G}_s^{(j,k')} X_n^{(k')} + \boldsymbol{W}_n^{(j)} \, , \, n \in \mathcal{N}_s \, , \, s \in \mathcal{S}^{(k)} . \tag{7.25}$$

Therefore, by using the IC scheme described above, both the MMSE combiner and the corresponding achievable rate can be derived from (7.19) and (7.15), respectively, by neglecting the ICI due to UEs included in $\tilde{\mathcal{K}}_s^{(j,\mathrm{I})}$.

While the proposed approach reduces the level of ICI, from (7.23) we observe that BSs

which perform detection before backhaul transmission, may be required to send for the same RB a different signal toward other BSs. Therefore, by defining the set $\tilde{\mathcal{S}}^{(j,\mathrm{I})}$ that includes all RBs whose signals are used for detection by BS j before backhaul transmission, i.e.,

$$\tilde{\mathcal{S}}^{(j,\mathrm{I})} = \bigcup_{k \in \mathcal{K}^{(j)} \cap \tilde{\mathcal{K}}^{(\mathrm{I})}} \mathcal{S}^{(k)} , \tag{7.26}$$

the constraint on the first phase of the backhaul transmission (7.11a) is rewritten to take into account this drawback, i.e.,

$$\sum_{s \in \tilde{\mathcal{S}}^{(j,\mathrm{I})}} \sum_{i \in \mathcal{J} \setminus \{j\}} x_s^{(i,j)} + \sum_{s \in \mathcal{S} \setminus \tilde{\mathcal{S}}^{(j,\mathrm{I})}} \mathbb{1} \left(\sum_{i \in \mathcal{J} \setminus \{j\}} x_s^{(i,j)} \right) \leq S_{\max} , \; j \in \mathcal{J} . \tag{7.27}$$

Note that other methods can be considered to implement IC besides the proposed approach. For instance, after detecting message sent by UE p, in (7.22) BS i could select $\alpha_s^{(j,i)} = G_s^{(i,p)}$: this condition simply nulls the interference due to UE p on one component of vector $\tilde{\boldsymbol{Y}}_n^{(j)}$, however BS j still suffers interference from UE p. A further method could be that BS i sends to BS j symbol $X_n^{(p)}$, and, in turn, BS j cancels from its received signal the interference due to UE p. With this method $\tilde{\boldsymbol{Y}}_n^{(j)}$ does not suffer any ICI from UE p, but has a reduced size, i.e., there is a diversity loss with respect to our proposal.

7.3 Heuristic solution by a greedy algorithm

The sum rate maximization with CSS and CSC is a non-linear integer optimization problem where the number of optimization variables is SJ^2. In LTE the number S of RBs can be 100 when the signal bandwidth is 20 MHz [2] and, if we are managing a network with a huge number of interfering BSs, the exhaustive search is not a viable solution to solve the scheduling problem. Hence, we propose to solve (7.17) by considering a greedy algorithm, which is reported in Algorithm 3. The algorithm operates iteratively. We denote with $\mathcal{T}_t$ the set of feasible solutions explored at iteration t. Solution $\boldsymbol{x}_t$ at the same iteration is selected with the aim of maximizing the sum rate (7.16), i.e.,

$$\boldsymbol{x}_t = \underset{\boldsymbol{x} \in \mathcal{T}_t}{\operatorname{argmax}} \; R(\boldsymbol{x}) \; . \tag{7.28}$$

We start from the non-cooperative solution, i.e., $[\boldsymbol{x}_0]_{s,j,j} = 1$, $s \in \mathcal{S}$, $j \in \mathcal{J}$. At iteration t we modify the solution $\boldsymbol{x}_{t-1}$ selected at the previous iteration by changing one value, i.e., by adding or removing one signal from the cooperation.

Therefore, the set of solutions explored at iteration t with CSC is

$$\mathcal{T}_t^{(\mathrm{CSC})} = \left\{ \boldsymbol{x} : \sum_{s,j,i} |[\boldsymbol{x}]_{s,j,i} - [\boldsymbol{x}_{t-1}]_{s,j,i}| = 1, \text{ s.t. (7.11a) and (7.11b)} \right\} . \tag{7.29a}$$

Algorithm 3 Greedy RB Scheduling

$[\boldsymbol{x}_0]_{s,j,j} \leftarrow 1\,,\ s \in \mathcal{S}\,,\ j \in \mathcal{J}$
$[\boldsymbol{x}_0]_{s,j,i} \leftarrow 0\,,\ s \in \mathcal{S}\,,\ j \in \mathcal{J}\,,\ i \in \mathcal{J}\,, j \neq i$
compute $\mathcal{T}_1$ from (7.29)
for $t = 1$ **to** $\min\{S_{\max}J, SJ(J-1)\}$ **do**
    if $\mathcal{T}_t = \emptyset$ **then**
        break
    end if
    $\boldsymbol{x}_t \leftarrow \underset{\boldsymbol{x}\in\mathcal{T}_t}{\operatorname{argmax}}\ R(\boldsymbol{x})$
    if $R(\boldsymbol{x}_t) \leq R(\boldsymbol{x}_{t-1})$ **then**
        $\boldsymbol{x}^{(*)} \leftarrow \boldsymbol{x}_{t-1}$
        break
    else
        $\boldsymbol{x}^{(*)} \leftarrow \boldsymbol{x}_t$
        compute $\mathcal{T}_{t+1}$ from (7.29)
    end if
end for

Note that (7.29a) forces the set of solutions to differ by one value from $\boldsymbol{x}_{t-1}$.

For CSS, instead, at each iteration we switch the signal used for the detection of one UE on a certain RB. Therefore, in this case the set of feasible solutions explored at iteration t can be written as

$$\mathcal{T}_t^{(\mathrm{CSS})} = \left\{ \boldsymbol{x} : \sum_{s,j,i} |[\boldsymbol{x}]_{s,j,i} - [\boldsymbol{x}_{t-1}]_{s,j,i}| = 2,\ \text{s.t. (7.11a), (7.11b), and (7.20)} \right\}, \quad (7.29b)$$

where now the sum is forced to 2, since we remove the index of the signal previously used for detection and substitute it with a new signal.

The algorithm stops when either the backhaul is not able to support any further transmission or the sum rate is not increasing anymore. Lastly, $\boldsymbol{x}^{(*)}$ denotes the final solution.

With IC, the proposed algorithm needs only slight modifications. In detail, in (7.29) $\boldsymbol{x} \in \mathcal{T}_t$ needs to satisfy (7.27) instead of (7.11a), and the sum rate (7.16) is evaluated by considering that combiners and SINRs are based on (7.25) instead of (7.14).

Note that the sum rate in (7.16) is utilized by the CU for scheduling and it assumes that $G_s^{(j,k)}$ is the channel between UE k and BS j on all the M subcarriers in $\mathcal{N}_s$. However, as the BSs have perfect CSI, we consider that they utilize a different combiner for each subcarrier of a RB. These combiners and the effective sum rate achieved on the wireless channel for the considered solution $\boldsymbol{x}^{(*)}$ can be computed from (7.18), (7.19), and (7.16) by simply substituting $G_s^{(j,k)}$ with $H_n^{(j,k)}$, $n \in \mathcal{N}_s$.

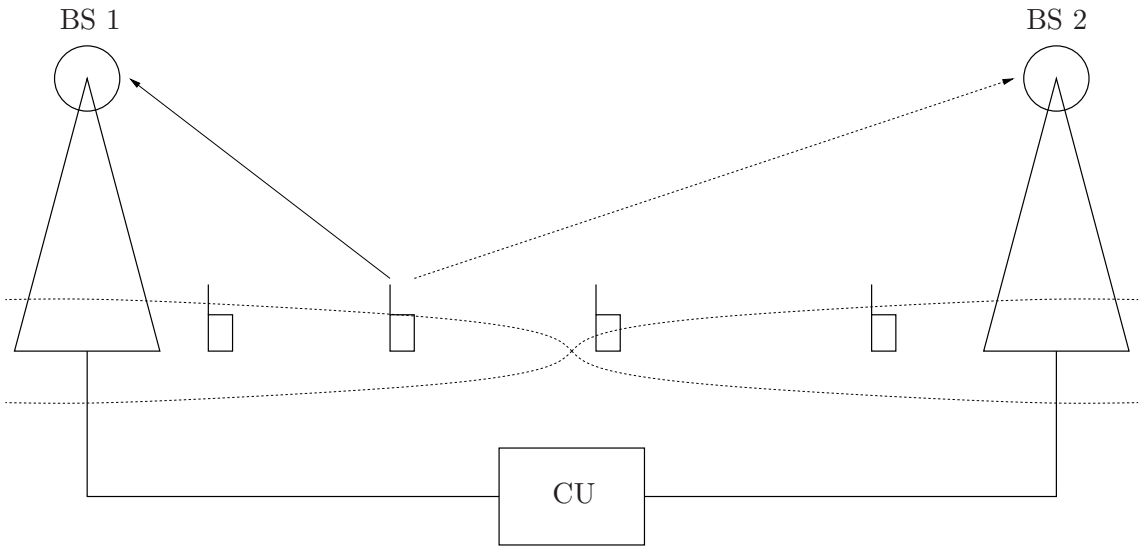

Figure 7.1: Linear array with $J = 2$ BSs serving $K = 4$ UEs.

7.4 Numerical results

We compare the performance of the proposed solutions by considering a simple scenario similar to the one of Fig. 7.1 with a linear array of $J = 2$ BSs, each one serving 3 UEs, i.e, $K = 6$ UEs overall. We consider an LTE simulation setup with a signal bandwidth of 3 MHz which is obtained by considering a DFT of size 256, with 180 active subcarriers organized in $S = 15$ RBs, each with $M = 12$ subcarriers of bandwidth $B = 15$ kHz [2]: each BS assigns 5 adjacent RBs to its scheduled UEs. We denote with $d_{\max}$ the distance between the two BSs, $d_{\min}$ the minimum distance between a UE and its anchor BS and $d_{j,k}$ the distance between UE k and BS j. We assume that each UE is randomly dropped in the coverage area of its anchor BS, i.e., $d_{j,k}$, $k \in \mathcal{K}^{(j)}$, is uniformly distributed between $d_{\min}$ and $d_{\max}/2$. We consider independent Rayleigh fading channels with a typical urban power delay profile with six taps [87]. Hence, we can write $H_n^{(j,k)} \sim \mathcal{CN}\left(0, \sigma_{j,k}^2\right)$ and assume that the average channel statistical power $\sigma_{j,k}^2$ depends only on the pathloss, i.e.,

$$\sigma_{j,k}^2 = \mathrm{SNR}^{(\mathrm{CE})} \left(\frac{d_{\max}/2}{d_{j,k}} \right)^{\eta}, \tag{7.30}$$

where $\eta = 3.5$ is the path-loss exponent and $\mathrm{SNR}^{(\mathrm{CE})}$ is the long-term SNR at the cell edge. We consider that $d_{\min}$ is selected from (7.30) by considering a maximum long-term SNR between a UE and its anchor BS of 30 dB.

In terms of the SC-FDMA system sum rate we compare the CSS and CSC schemes against a) single cell processing (SCP) where cooperation among the BSs is not allowed and b) full coordination (FC), where no constraint on the backhaul is considered. In detail, (7.6) is the rate achieved by UE k with SCP, whereas with FC both CSS and CSC

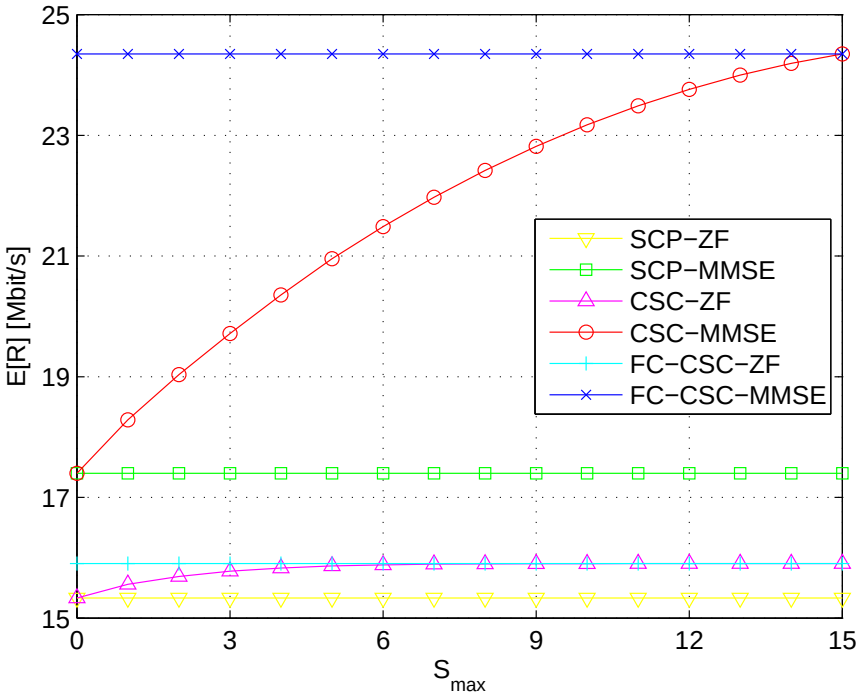

Figure 7.2: Average system sum rate with respect to $S_{\max}$ achieved by CSC with ZF and MMSE equalizers when $\text{SNR}^{(\text{CE})} = 10$ dB.

can be implemented, and each BS detects its UE messages by using the signals received by all other BSs in the network.

In Fig.s 7.2 and 7.3 we report the average system sum rate with respect to the backhaul constraint $S_{\max}$ when $\text{SNR}^{(\text{CE})} = 10$ dB achieved by CSC and CSS, respectively. Firstly, we observe that MMSE strongly outperforms ZF. Note that FC-CSC-ZF is outperformed by SCP-MMSE: even by removing the constraints on the backhaul, ZF simply nulls the ISI without taking into account the ICI, which indeed is the bottleneck in interference limited scenarios. As expected, the sum rate obtained by using both CSC and CSS increases with $S_{\max}$, approaching the performance limit of FC-CSC and FC-CSS, respectively. Overall, only CSC provides an important gain with respect to SCP: for instance, by using the MMSE equalizer and when $S_{\max} = 6$, i.e., when only 40% of all RBs can be exchanged, CSC outperforms SCP of about 24% by filling about 59% of the gap between SCP and FC-CSC. On the other hand, the gain achieved by CSS over SCP is less than 1%: in fact, by using CSS each BS simply selects the received signal with highest SINR, without reducing ICI.

Fig. 7.4 shows the average system sum rate with respect to $\text{SNR}^{(\text{CE})}$ by using the MMSE equalizer and when $S_{\max} = 6$. Note that different values of $\text{SNR}^{(\text{CE})}$ can be seen as different distances between BSs. Similarly to previous results, the gain achieved by CSS with respect to SCP is negligible. In a noise limited scenario, i.e., for lower values

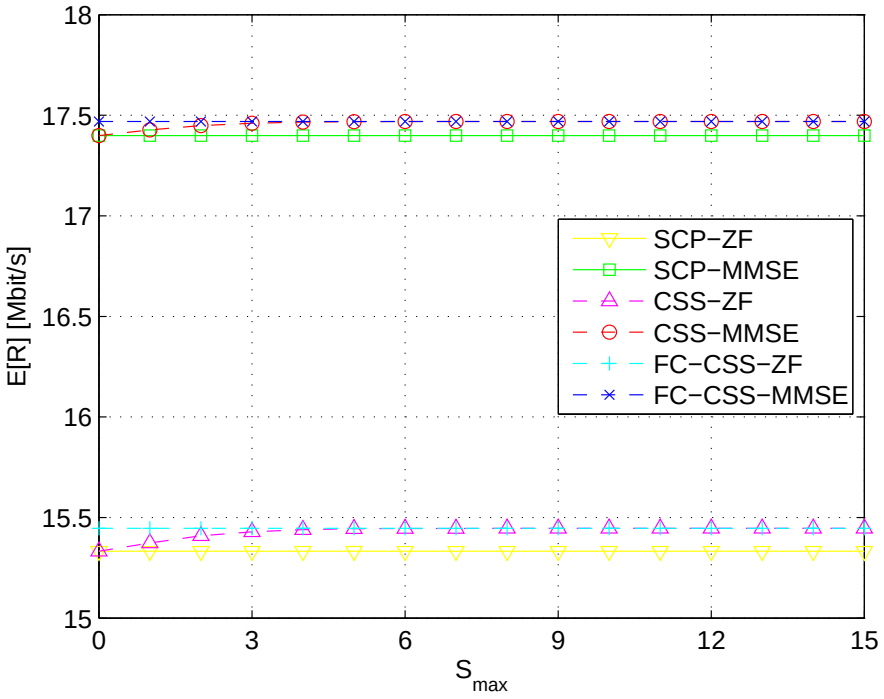

Figure 7.3: Average system sum rate with respect to $S_{\max}$ achieved by CSS with ZF and MMSE equalizers when $\mathrm{SNR}^{(\mathrm{CE})} = 10$ dB.

of $\mathrm{SNR}^{(\mathrm{CE})}$, the gain achieved by CSC over SCP is small, however it increases for higher values of $\mathrm{SNR}^{(\mathrm{CE})}$. We observe that all the schemes but FC-CSC, beyond a certain value of $\mathrm{SNR}^{(\mathrm{CE})}$, show a decrease in the achieved sum rate: in fact, beyond the useful signal power, also ICI power increases with $\mathrm{SNR}^{(\mathrm{CE})}$.

To evaluate the performance achieved with IC, in Fig. 7.5 we report the CDF of the sum rate when $\mathrm{SNR}^{(\mathrm{CE})} = 10$ dB, $S_{\max} = 6$ and the MMSE equalizer is used. First of all, we observe that the gain achieved by CSC over SCP is almost constant for different CDF values. Moreover, we also note that CSC-IC slightly outperforms CSC, with a higher gain for lower CDF values, i.e., when the UEs are close to the cell edge. In fact, in the considered scenario with two BSs and where the ICI is due to only one UE, when a BS exploits the cooperation of the other BS, the 2×1 vector signal (7.14) is, beyond the noise, the sum of the useful signal and only one interfering signal: therefore, the simple combiner (7.19) is able to properly deal with ICI. The slight gain achieved by IC for lower CDF values happens when the useful and interfering signals are almost parallel for some fading realizations: in such a case IC provides a gain with respect to the simple combiner.

To understand the performance of the proposed solutions in the worst case scenario where all the UEs are at the cell edge, in Fig. 7.6 we report the average system sum rate with respect to $S_{\max}$ when $\mathrm{SNR}^{(\mathrm{CE})} = 10$ dB, $d_{j,k} = d_{\max}/2$, $j \in \mathcal{J}$, $k \in \mathcal{K}$, and the MMSE equalizer is used. In this setup CSC-IC outperforms CSC with a gain in the sum rate of

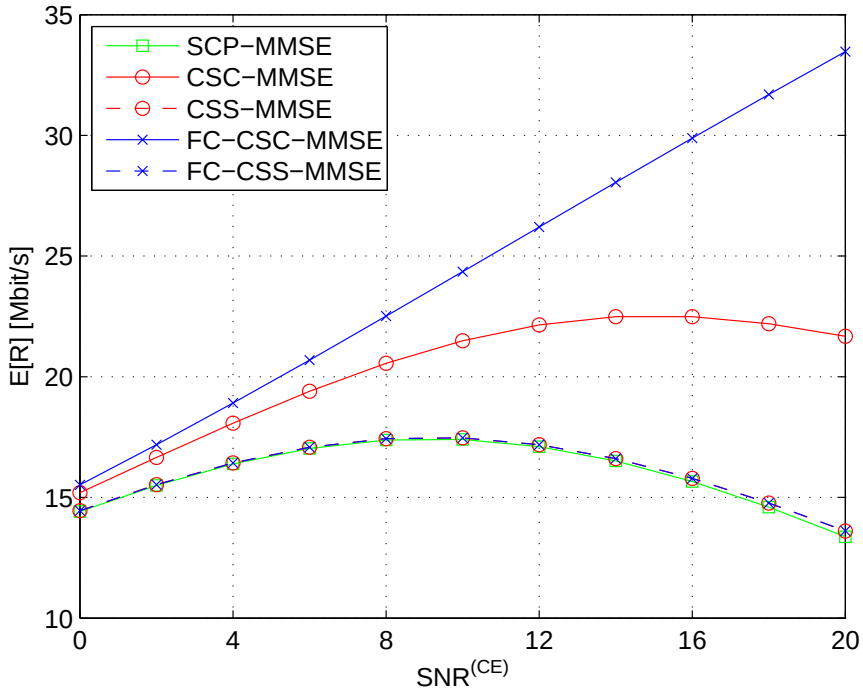

Figure 7.4: Average system sum rate with respect to $\mathrm{SNR}^{(\mathrm{CE})}$ achieved by CSC and CSS using the MMSE equalizer and $S_{\max} = 6$.

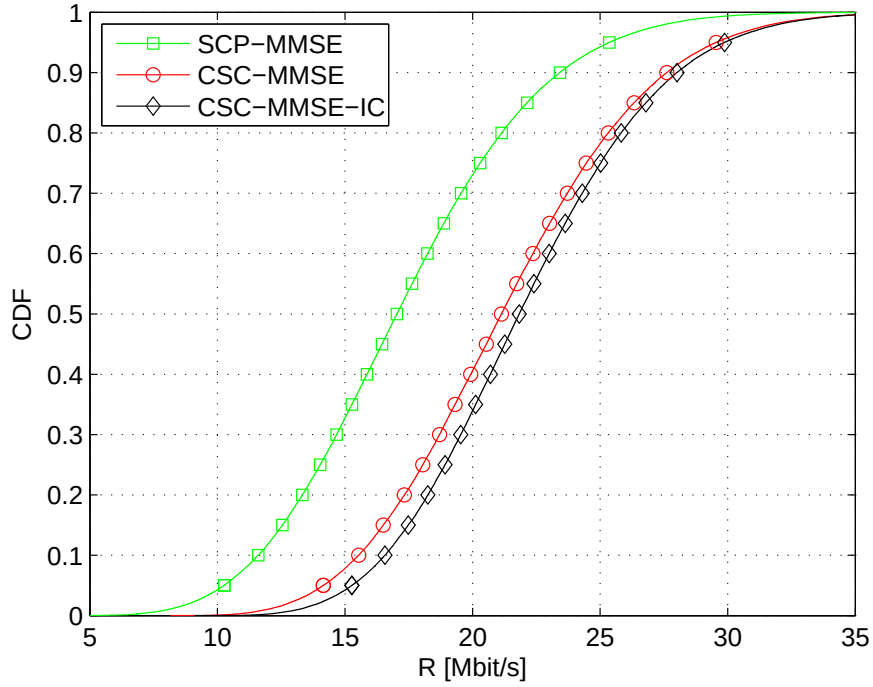

Figure 7.5: CDF of the system sum rate when $\mathrm{SNR}^{(\mathrm{CE})} = 10$ dB and $S_{\max} = 6$.

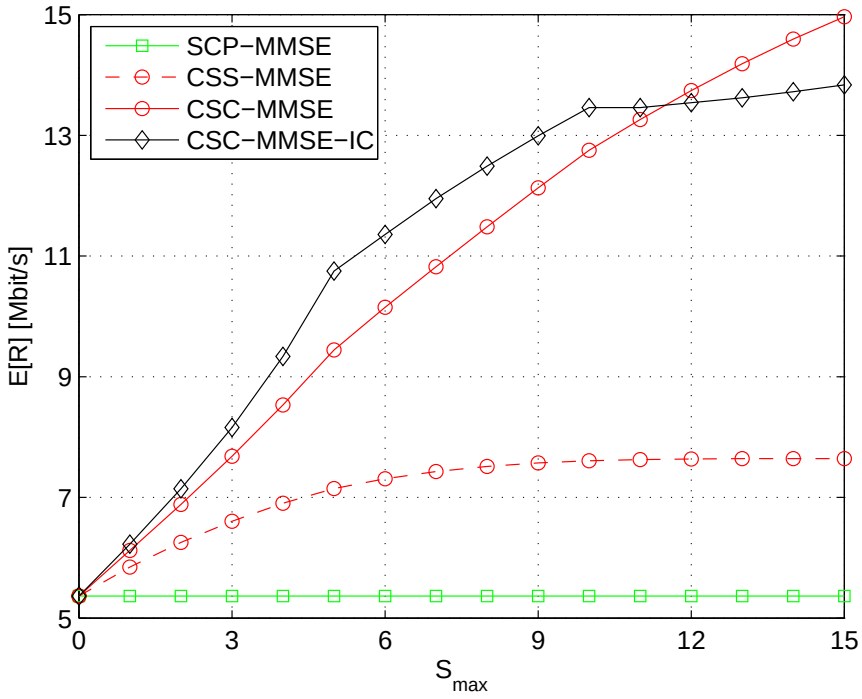

Figure 7.6: Average system sum rate with respect to $S_{\max}$ achieved by different configurations using MMSE equalizer, $\mathrm{SNR}^{(\mathrm{CE})} = 10$ dB and $d_{j,k} = d_{\max}/2$, $j \in \mathcal{J}$, $k \in \mathcal{K}$.

about 12% when $S_{\max} = 6$. Note that CSS, even if it is still strongly outperformed by CSC, achieves a considerable gain over SCP: for each RB the selection of the best BS turns out to be useful for the UEs at the cell edge. Finally, we note that the slope of CSC-IC changes when $S_{\max}$ increases from 5 to 6, and from 10 to 11. These two steps correspond to a change in the number of UEs included in the set $\tilde{\mathcal{K}}^{(\mathrm{II})}$. As we are considering 5 RBs assigned to each UE, when $S_{\max} \leq 5$, the proposed greedy algorithm tends to include only one UE per BS in the set $\tilde{\mathcal{K}}^{(\mathrm{II})}$ with the aim of exploiting IC. On the other hand, when $S_{\max}$ increases from 5 to 6, the algorithm starts to include in the set $\tilde{\mathcal{K}}^{(\mathrm{II})}$ also a second UE per BS. This provides a gain for the UE that switches from $\tilde{\mathcal{K}}^{(\mathrm{I})}$ into $\tilde{\mathcal{K}}^{(\mathrm{II})}$, as its anchor BS detects its message by exploiting signals received from the CU, but a loss for other UEs in set $\tilde{\mathcal{K}}^{(\mathrm{II})}$ whose anchor BS receives now from the CU signals with more interference. An analogous situation occurs when $S_{\max}$ increases from 10 to 11.

7.5 Conclusions

In this chapter we have considered the uplink of a cellular system where UEs transmit by using SC-FDMA toward BSs which cooperate in detecting the transmitted messages. By assuming a constraint on the number of signals that can be exchanged among the BSs through the backhaul links, we have proposed a scheme where only signals received on

a subset of subcarriers assigned to the same UE can be exchanged. Different equalizers are compared, including cell signal combining (CSC), where each BS combines the signal received on the wireless link with the signals received from the CU, and cell signal selection (CSS), where each BS simply selects the signal with the highest SINR. Moreover, interference cancellation (IC) has been considered to improve the system performance: with IC some UEs are detected by their anchor BS without cooperation and, in turn, this BS sends on the backhaul toward other BSs a linear combination of received and detected signals to allow a perfect cancellation of the interference caused by the detected messages at the cooperating BSs. A greedy algorithm is then developed as a viable solution to solve the system sum rate maximization problem. Numerical results presented for a typical LTE scenario show that CSC-MMSE strongly outperforms the solution without cooperation, and IC can be used to further improve the rates achieved by the cell-edge UEs.

Chapter 8

Conclusions

This thesis considers coordinated multi-point (CoMP) systems and investigates new transmission techniques and resource allocation algorithms to deal efficiently with inter-cell interference (ICI) under practical constraints.

We start our study in Chapter 2 by introducing several CoMP schemes and beamforming techniques that can be used in the downlink to serve the scheduled UEs by assuming perfect channel state information (CSI) at the BS. We show the huge performance improvement that can be achieved by the cooperation with respect to single cell processing (SCP). Moreover, we introduce clustering as a viable solution to limit the backhaul occupation and preserve the gain enabled by cooperation.

In Chapter 3 we consider a downlink scenario where a central unit (CU) coordinates a set of cooperative BSs and the link connecting each BS to the CU is constrained by a maximum available throughput. In this setting we develop a novel transmission scheme based on linear precoding and QAM where all the the cooperative BSs transmit a quantized version of the intended QAM symbol, while the serving BS also transmits a quantization error symbol. The two symbols combine through the channels at the UE yielding the intended QAM symbol, thus requiring no modification at the receiver side. Numerical results show that the proposed method achieves a network spectral efficiency close to that obtained by using the more complex Slepian-Wolf encoding.

In Chapter 4 we focus on joint clustering and scheduling optimization in downlink CoMP. We propose an algorithm to perform dynamic clustering, i.e., to organize in each time slot a set of non-overlapping clusters, and to schedule a set of UEs in each cluster by maximizing the system weighted sum rate. We compare several criteria to select a) the clusters and b) the UEs scheduled in each cluster. Numerical results in a LTE simulation setup show the gain achieved by the proposed approach with respect to both SCP and static clustering when the average cluster size is three. However, the spectral efficiency achieved by assuming full coordination and perfect CSI at the BSs is still very far, showing the impact of inter-cluster interference on system performance.

In Chapter 5 we deal with feedback design in FDD-CoMP. We consider a scheme de-

veloped in literature based on per-cell codebooks and we propose two practical algorithms that suit SU-CoMP to a) select for each UE a subset of preferred BSs and b) optimize the number of bits used to quantize each channel. As expected, the proposed methods allocate more feedback bits to quantize the strongest channels.

In Chapter 6 we consider that a set of relays is assisting the transmission of a BS toward a UE. We adapt the transmission scheme developed in Chapter 3 where now the links connecting the BS to the relays represent the backhaul infrastructure. In this framework and by assuming that relays are half-duplex, i.e., they can not transmit and receive simultaneously, we also develop a practical algorithm to perform power allocation and time-sharing optimization.

Finally, in Chapter 7 we focus on uplink CoMP with SC-FDMA, which is the modulation scheme employed in uplink LTE. We propose a new scheduler of the signals exchanged on the backhaul that allows each BS to share only a subset of the subcarriers of a SC-FDMA block. An important performance gain is achieved by using a MMSE combiner. Moreover, the spectral efficiency of cell-edge UEs can be further increased by implementing interference cancellation.

Bibliography

[1] H. Ekström, A. Furuskär, J. Karlsson, M. Meyer, S. Parkvall, J. Torsner, and M. Wahlqvist, "Technical solutions for the 3G long-term evolution," *IEEE Commun. Mag.*, vol. 44, no. 3, pp. 38–45, Mar. 2006.

[2] S. Sesia, I. Toufik, and M. Baker, *LTE: The UMTS Long Term Evolution.* John Wiley & Sons, 2009.

[3] F. Boccardi, B. Clerckx, A. Ghosh, E. Hardouin, G. Jöngren, K. Kusume, E. Onggosanusi, and Y. Tang, "Multiple-antenna techniques in LTE-advanced," *IEEE Commun. Mag.*, vol. 50, no. 3, pp. 114–121, Mar. 2012.

[4] J. G. Andrews, A. Ghosh, and R. Muhamed, *Fundamentals of WiMAX: understanding broadband wireless networking.* Prentice Hall, 2007.

[5] M. K. Karakayali, G. J. Foschini, and R. A. Valenzuela, "Network coordination for spectrally efficient communications in cellular systems," *IEEE Wireless Commun. Mag.*, vol. 13, no. 4, pp. 56–61, Aug. 2006.

[6] D. Gesbert, S. Hanly, H. Huang, S. Shamai, O. Simeone, and W. Yu, "Multi-cell MIMO cooperative networks: a new look at interference," *IEEE J. Sel. Areas Commun.*, vol. 28, no. 9, pp. 1380–1408, Dec. 2010.

[7] P. Marsch and G. Fettweis, *Coordinated multi-point in mobile communications.* Cambridge University Press, 2011.

[8] R. Irmer, H. Droste, P. Marsch, M. Grieger, G. Fettweis, S. Brueck, H.-P. Mayer, L. Thiele, and V. Jungnickel, "Coordinated multipoint: concepts, performance, and field trial results," *IEEE Commun. Mag.*, vol. 49, no. 2, pp. 102–111, Feb. 2011.

[9] D. Lee, H. Seo, B. Clerckx, E. Hardouin, D. Mazzarese, S. Nagata, and K. Sayana, "Coordinated multipoint transmission and reception in LTE-advanced: deployment scenarios and operational challenges," *IEEE Commun. Mag.*, vol. 50, no. 2, pp. 148–155, Feb. 2012.

[10] W. Yu and T. Lan, "Transmitter optimization for the multi-antenna downlink with per-antenna power constraints," *IEEE Trans. Signal Process.*, vol. 55, no. 6, pp. 2646–2660, Jun. 2007.

[11] P. Viswanath, D. Tse, and R. Laroia, "Opportunistic beamforming using dumb antennas," *IEEE Trans. Inf. Theory*, vol. 48, no. 6, pp. 1277–1294, Jun. 2002.

[12] D. Su, X. Hou, and C. Yang, "Quantization based on per-cell codebook in cooperative multi-cell systems," in *Proc. IEEE Wireless Communications and Networking Conference (WCNC)*, Cancun (Mexico), Mar. 2011.

[13] X. Hou and C. Yang, "Codebook design and selection for multi-cell cooperative transmission limited feedback systems," in *Proc. IEEE Vehicular Technology Conference (VTC Spring)*, Budapest (Hungary), May 2011.

[14] G. Caire and S. Shamai, "On the achievable throughput of a multiantenna Gaussian broadcast channel," *IEEE Trans. Inf. Theory*, vol. 49, no. 7, pp. 1691–1706, Jul. 2003.

[15] H. Weingarten, Y. Steinberg, and S. Shamai, "The capacity region of the Gaussian multiple-input multiple-output broadcast channel," *IEEE Trans. Inf. Theory*, vol. 52, no. 9, pp. 3936–3964, Sep. 2006.

[16] M. Costa, "Writing on dirty paper," *IEEE Trans. Inf. Theory*, vol. IT-29, no. 3, pp. 439–441, May 1983.

[17] T. Yoo and A. Goldsmith, "On the optimality of multiantenna broadcast scheduling using zero-forcing beamforming," *IEEE J. Sel. Areas Commun.*, vol. 24, no. 3, pp. 528–541, Mar. 2006.

[18] F. Boccardi, F. Tosato, and G. Caire, "Precoding schemes for the MIMO-GBC," in *Proc. IEEE International Zurich Seminar on Communications (IZS)*, Zurich (Switzerland), Sep. 2006.

[19] N. Hassanpour, J. E. Smee, J. Hou, and J. B. Soriaga, "Distributed beamforming based on signal-to-caused-interference ratio," in *Proc. International Symposium on Spread Spectrum Techniques and Applications (ISSSTA)*, Bologna (Italy), Aug. 2008.

[20] R. Zakhour and D. Gesbert, "Distributed multicell-MISO precoding using the layered virtual SINR framework," *IEEE Trans. Wireless Commun.*, vol. 9, no. 8, pp. 2444–2448, Aug. 2010.

[21] E. Björnson, R. Zakhour, D. Gesbert, and B. Ottersten, "Cooperative multicell precoding: rate region characterization and distributed strategies with instantaneous and statistical CSI," *IEEE Trans. Signal Process.*, vol. 58, no. 8, pp. 4298–4310, Aug. 2010.

[22] A. Papadogiannis, D. Gesbert, and E. Hardouin, "A dynamic clustering approach in wireless networks with multi-cell cooperative processing," in *Proc. IEEE International Conference on Communications (ICC)*, Beijing (China), May 2008.

[23] S. Boyd and L. Vandenberghe, *Convex optimization*. Cambridge University Press, 2004.

[24] M. Grant and S. Boyd. CVX: Matlab software for disciplined convex programming. [Online]. Available: http://www.stanford.edu/~boyd/cvx/

[25] General algebraic modeling system (GAMS). [Online]. Available: http://www.gams.com

[26] A. Goldsmith, *Wireless communications*. Cambridge University Press, 2005.

[27] F. Boccardi, H. Huang, and A. Alexiou, "Network MIMO with reduced backhaul requirements by MAC coordination," in *Proc. IEEE Conference on Signals, Systems and Computers (Asilomar)*, Pacific Grove (CA), Oct. 2008.

[28] R. Zhang and L. Hanzo, "Cooperative downlink multicell preprocessing relying on reduced-rate back-haul data exchange," *IEEE Trans. Veh. Technol.*, vol. 60, no. 2, pp. 539–545, Feb. 2011.

[29] P. Marsch and G. Fettweis, "A framework for optimizing the downlink performance of distributed antenna systems under a constrained backhaul," in *Proc. European Wireless Conference (EW)*, Paris (France), Apr. 2007.

[30] O. Simeone, O. Somekh, H. V. Poor, and S. Shamai, "Downlink multicell processing with limited-backhaul capacity," *EURASIP Journal on Advances in Signal Processing*, Jun. 2009.

[31] P. Marsch and G. Fettweis, "On base station cooperation schemes for downlink network MIMO under a constrained backhaul," in *Proc. IEEE Global Communications Conference (GLOBECOM)*, New Orleans (LA), Dec. 2008.

[32] R. Zakhour and D. Gesbert, "On the value of data sharing in constrained-backhaul network MIMO," in *Proc. IEEE International Zurich Seminar on Communications (IZS)*, Zurich (Switzerland), Mar. 2010.

[33] ——, "Optimized data sharing in multicell MIMO with finite backhaul capacity," *IEEE Trans. Signal Process.*, vol. 59, no. 12, pp. 6102–6111, Dec. 2011.

[34] D. Slepian and J. K. Wolf, "A coding theorem for multiple access channels with correlated sources," *Bell System Technical Journal*, vol. 52, no. 7, pp. 1037–1076, Sep. 1973.

[35] N. Benvenuto and G. Cherubini, *Algorithms for communications systems and their applications*. John Wiley & Sons, 2002.

[36] G. Ungerboeck, "Channel coding with multilevel/phase signals," *IEEE Trans. Inf. Theory*, vol. 28, no. 1, pp. 55–67, Jan. 1982.

[37] T. M. Cover and J. A. Thomas, *Elements of information theory*. John Wiley & Sons, 2006.

[38] C. Studholme and I. F. Blake, "Random matrices and codes for the erasure channel," *Algorithmica*, vol. 56, no. 4, pp. 605–620, Apr. 2010.

[39] J. Zhang, R. Chen, J. G. Andrews, A. Ghosh, and R. W. Heath, "Networked MIMO with clustered linear precoding," *IEEE Trans. Wireless Commun.*, vol. 8, no. 4, pp. 1910–1921, Apr. 2009.

[40] J.-M. Moon and D.-H. Cho, "Inter-cluster interference management based on cell-clustering in network MIMO systems," in *Proc. IEEE Vehicular Technology Conference (VTC Spring)*, Budapest (Hungary), May 2011.

[41] J. Liu and D. Wang, "An improved dynamic clustering algorithm for multi-user distributed antenna system," in *Proc. IEEE International Conference on Wireless Communications & Signal Processing (WCSP)*, Nanjing (China), Nov. 2009.

[42] S. Zhou, J. Gong, Z. Niu, Y. Jia, and P. Yang, "A decentralized framework for dynamic downlink base station cooperation," in *Proc. IEEE Global Communications Conference (GLOBECOM)*, Honolulu (HI), Dec. 2009.

[43] R. Weber, A. Garavaglia, M. Schulist, S. Brueck, and A. Dekorsy, "Self-organizing adaptive clustering for cooperative multipoint transmission," in *Proc. IEEE Vehicular Technology Conference (VTC Spring)*, Budapest (Hungary), May 2011.

[44] A. Papadogiannis, H. J. Bang, D. Gesbert, and E. Hardouin, "Efficient selective feedback design for multicell cooperative networks," *IEEE Trans. Veh. Technol.*, vol. 60, no. 1, pp. 196–205, Jan. 2011.

[45] J. Gong, S. Zhou, Z. Niu, L. Geng, and M. Zheng, "Joint scheduling and dynamic clustering in downlink cellular networks," in *Proc. IEEE Global Communications Conference (GLOBECOM)*, Houston (TX), Dec. 2011.

[46] A. Papadogiannis, H. J. Bang, D. Gesbert, and E. Hardouin, "Downlink overhead reduction for multi-cell cooperative processing enabled wireless networks," in *Proc. IEEE International Symposium on Personal, Indoor and Mobile Radio Communications (PIMRC)*, Cannes (France), Sep. 2008.

[47] V. Chvatal, "A greedy heuristic for the set-covering problem," *Mathematics of Operations Research*, vol. 4, no. 3, pp. 233–235, Aug. 1979.

[48] T. Hytönen, "Optimal wrap-around network simulation," Helsinki University of Technology, Report A432, 2001.

[49] F. Boccardi and H. Huang, "Limited downlink network coordination in cellular networks," in *Proc. IEEE International Symposium on Personal, Indoor and Mobile Radio Communications (PIMRC)*, Athens (Greece), Sep. 2007.

[50] M. Trivellato, F. Boccardi, and H. Huang, "On transceiver design and channel quantization for downlink multiuser MIMO systems with limited feedback," *IEEE J. Sel. Areas Commun.*, vol. 26, no. 8, pp. 1494–1504, Oct. 2008.

[51] R. Bhagavatula and R. W. Heath, "Adaptive limited feedback for sum-rate maximizing beamforming in cooperative multicell systems," *IEEE Trans. Signal Process.*, vol. 59, no. 2, pp. 800–811, Feb. 2011.

[52] ——, "Adaptive bit partitioning for multicell intercell interference nulling with delayed limited feedback," *IEEE Trans. Signal Process.*, vol. 59, no. 8, pp. 3824–3836, Aug. 2011.

[53] B. Özbek and D. Le Ruyet, "Adaptive limited feedback for intercell interference cancelation in cooperative downlink multicell networks," in *Proc. IEEE International Symposium on Wireless Communication Systems (ISWCS)*, York (United Kingdom), Sep. 2010.

[54] ——, "Adaptive bit partitioning strategy for cell-edge users in multi-antenna multicell networks," in *Proc. IEEE International Workshop on Signal Processing Advances in Wireless Communications (SPAWC)*, San Francisco (CA), Jun. 2011.

[55] R. Bhagavatula, R. W. Heath, and B. Rao, "Limited feedback with joint CSI quantization for multicell cooperative generalized eigenvector beamforming," in *Proc. IEEE International Conference on Acoustics, Speech and Signal Processing (ICASSP)*, Dallas (TX), Mar. 2010.

[56] S. Zhou, J. Gong, and Z. Niu, "Distributed adaptation of quantized feedback for downlink network MIMO systems," *IEEE Trans. Wireless Commun.*, vol. 10, no. 1, pp. 61–67, Jan. 2011.

[57] Y. Cheng, V. K. N. Lau, and Y. Long, "A scalable limited feedback design for network MIMO using per-cell product codebook," *IEEE Trans. Wireless Commun.*, vol. 9, no. 10, pp. 3093–3099, Oct. 2010.

[58] N. Jindal, "MIMO broadcast channels with finite-rate feedback," *IEEE Trans. Inf. Theory*, vol. 52, no. 11, pp. 5045–5060, Nov. 2006.

[59] M. Abramowitz and I. A. Stegun, *Handbook of mathematical functions with formulas, graphs, and mathematical tables*. Dover Publications, 1964.

[60] C. K. Au-Yeung and D. J. Love, "On the performance of random vector quantization limited feedback beamforming in a MISO system," *IEEE Trans. Wireless Commun.*, vol. 6, no. 2, pp. 458–462, Feb. 2007.

[61] J. Riordan, *Introduction to combinatorial analysis*. Dover Publications, 2002.

[62] T. M. Cover and A. El Gamal, "Capacity theorems for the relay channel," *IEEE Trans. Inf. Theory*, vol. 25, no. 5, pp. 572–584, Sep. 1979.

[63] A. Sendonaris, E. Erkip, and B. Aazhang, "User cooperation diversity–part I and part II," *IEEE Trans. Commun.*, vol. 51, no. 11, pp. 1927–1948, Nov. 2003.

[64] A. Høst-Madsen and J. Zhang, "Capacity bounds and power allocation for wireless relay channels," *IEEE Trans. Inf. Theory*, vol. 51, no. 6, pp. 2020–2040, Jun. 2005.

[65] B. Rankov and A. Wittneben, "Spectral efficient protocols for half-duplex fading relay channels," *IEEE J. Sel. Areas Commun.*, vol. 25, no. 2, pp. 379–389, Feb. 2007.

[66] Y. Yang, H. Hu, J. Xu, and G. Mao, "Relay technologies for WiMax and LTE-advanced mobile systems," *IEEE Commun. Mag.*, vol. 47, no. 10, pp. 100–105, Oct. 2009.

[67] C. Hoymann, W. Chen, J. Montojo, A. Golitschek, C. Koutsimanis, and X. Shen, "Relaying operation in 3GPP LTE: challenges and solutions," *IEEE Commun. Mag.*, vol. 50, no. 2, pp. 156–162, Feb. 2012.

[68] A. Reznik, S. R. Kulkarni, and S. Verdu, "Degraded Gaussian multirelay channel: capacity and optimal power allocation," *IEEE Trans. Inf. Theory*, vol. 50, no. 12, pp. 3037–3046, Dec. 2004.

[69] G. Kramer, M. Gastpar, and P. Gupta, "Cooperative strategies and capacity theorems for relay networks," *IEEE Trans. Inf. Theory*, vol. 51, no. 9, pp. 3037–3063, Sep. 2005.

[70] F. Xue and S. Sandhu, "Cooperation in a half-duplex Gaussian diamond relay channel," *IEEE Trans. Inf. Theory*, vol. 53, no. 10, pp. 3806–3814, Oct. 2007.

[71] M. A. Khojastepour, A. Sabharwal, and B. Aazhang, "Bounds on achievable rates for general multi-terminal networks with practical constraints," in *Proc. ACM International Conference on Information Processing in Sensor Networks (IPSN)*, Palo Alto (CA), Apr. 2003.

[72] P. Marsch and G. Fettweis, "Rate region of the multi-cell multiple access channel under backhaul and latency constraints," in *Proc. IEEE Wireless Communications and Networking Conference (WCNC)*, Las Vegas (NV), Apr. 2008.

[73] A. Sanderovich, O. Somekh, and S. Shamai, "Uplink macro diversity with limited backhaul capacity," in *Proc. IEEE International Symposium on Information Theory (ISIT)*, Nice (France), Jun. 2007.

[74] O. Somekh, O. Simeone, A. Sanderovich, B. M. Zaidel, and S. Shamai, "On the impact of limited-capacity backhaul and inter-user links in cooperative multicell networks," in *Proc. IEEE 42nd Annual Conference on Information Sciences and Systems (CISS)*, Princeton (NJ), Mar. 2008.

[75] P. Marsch and G. Fettweis, "Uplink CoMP under a constrained backhaul and imperfect channel knowledge," *IEEE Trans. Wireless Commun.*, vol. 10, no. 6, pp. 1730–1742, Jun. 2011.

[76] ——, "A framework for optimizing the uplink performance of distributed antenna systems under a constrained backhaul," in *Proc. IEEE International Conference on Communications (ICC)*, Glasgow (United), Jun. 2007.

[77] F. Diehm, P. Marsch, G. Fettweis, and B. Ramamurthi, "A low-complexity algorithm for uplink scheduling in cooperative cellular networks with a capacity-constrained backhaul infrastructure," in *Proc. IEEE Global Communications Conference (GLOBECOM)*, Honolulu (HI), Dec. 2009.

[78] D. Zennaro, S. Tomasin, and L. Vangelista, "Base station selection in uplink macro diversity cellular systems with hybrid ARQ," *IEEE J. Sel. Areas Commun.*, vol. 29, no. 6, pp. 1249–1259, Jun. 2011.

[79] M. Kamoun and L. Mazet, "Base-station selection in cooperative single frequency cellular network," in *Proc. IEEE International Workshop on Signal Processing Advances in Wireless Communications (SPAWC)*, Helsinki (Finland), Jun. 2007.

[80] O. Bulakci, A. B. Saleh, S. Redana, B. Raaf, and J. Hamalainen, "Flexible backhaul resource sharing and uplink power control optimization in LTE-advanced relay networks," in *Proc. IEEE Vehicular Technology Conference (VTC Fall)*, San Francisco (CA), Sep. 2011.

[81] H. G. Myung and D. J. Goodman, *Single carrier FDMA: a new air interface for Long Term Evolution.* John Wiley & Sons, 2008.

[82] N. Benvenuto, R. Dinis, D. Falconer, and S. Tomasin, "Single carrier modulation with nonlinear frequency domain equalization: an idea whose time has come–again," *Proc. IEEE*, vol. 98, no. 1, pp. 69–96, Jan. 2010.

[83] N. Benvenuto and S. Tomasin, "On the comparison between OFDM and single carrier modulation with a DFE using a frequency-domain feedforward filter," *IEEE Trans. Commun.*, vol. 50, no. 6, pp. 947–955, Jun. 2002.

[84] E. Yaacoub and Z. Dawy, "Joint uplink scheduling and interference mitigation in multicell LTE networks," in *Proc. IEEE International Conference on Communications (ICC)*, Kyoto (Japan), Jun. 2011.

[85] J. Ellenbeck, H. Al-Shatri, and C. Hartmann, "Performance of decentralized interference coordination in the LTE uplink," in *Proc. IEEE Vehicular Technology Conference (VTC Fall)*, Anchorage (AK), Sep. 2009.

[86] T. Shi, S. Zhou, and Y. Yao, "Capacity of single carrier systems with frequency-domain equalization," in *Proc. IEEE 6th Circuits and System Symposium on Emerging Technologies: Frontiers of Mobile and Wireless Commununications*, Shanghai (China), Jun. 2004.

[87] *3rd Generation Partnership Project; Technical Specification Group GSM/EDGE Radio Access Network; Radio transmission and reception (Release 1999)*, 3GPP TS 05.05 V8.20.0.

List of Publications

The work presented in this thesis has in part been published in the references listed below.

Journal Papers

[J1] P. Baracca, S. Tomasin, and N. Benvenuto, "Resource allocation with multicell processing, interference cancelation and backhaul rate constraint in single carrier FDMA systems," *Elsevier Physical Communication*, Oct. 2012 (invited).

[J2] P. Baracca, N. Laurenti, and S. Tomasin, "Physical layer authentication over MIMO fading wiretap channels," *IEEE Trans. Wireless Commun.*, vol. 11, no. 7, pp. 2564–2573, Jul. 2012.

[J3] P. Baracca, S. Tomasin, and N. Benvenuto, "A practical scheduling and power/ constellation allocation for three relay networks," *Eurasip journal on wireless communications and networking*, 2012:128, Mar. 2012.

[J4] P. Baracca, S. Tomasin, and N. Benvenuto, "Constellation quantization in constrained backhaul downlink network MIMO," *IEEE Trans. Commun.*, vol. 60, no. 3, pp. 830-839, Mar. 2012.

[J5] P. Baracca, S. Tomasin, L. Vangelista, N. Benvenuto, and A. Morello, "Per sub-block equalization of very long OFDM blocks in mobile communications," *IEEE Trans. Commun.*, vol. 59, no. 2, pp. 363-368, Feb. 2011.

Conference Papers

[C1] P. Baracca, F. Boccardi, V. Braun, and A. Tulino, "Base station selection and per-cell codebook optimization for CoMP with joint processing," in Proc. *IEEE International Symposium on Personal, Indoor and Mobile Radio Communications* (PIMRC), Sydney (Australia), Sep. 2012.

[C2] P. Baracca, F. Boccardi, and V. Braun, "A dynamic joint clustering scheduling algorithm for downlink CoMP systems with limited CSI," in Proc. *IEEE International*

Symposium on Wireless Communication Systems (ISWCS), Paris (France), Aug. 2012.

[C3] P. Baracca, S. Tomasin, and N. Benvenuto, "Power and time-sharing optimization for three half-duplex relay networks," in Proc. *IEEE Asian Himalayas International Conference on Internet* (AH-ICI), Kathmandu (Nepal), Nov. 2011.

[C4] P. Baracca, S. Tomasin, and N. Benvenuto, "Downlink multicell processing employing QAM quantization under a constrained backhaul," in Proc. *IEEE Signal Processing Advances in Wireless Communications* (SPAWC), San Francisco (CA), Jun. 2011.

[C5] P. Baracca, N. Benvenuto, and L. Vangelista, "A frequency-domain pre-equalizer for MIMO-OFDM mobile communication systems employing Alamouti coding," in Proc. *IEEE Signal Processing Advances in Wireless Communications* (SPAWC), San Francisco (CA), Jun. 2011.

[C6] P. Baracca, N. Laurenti, and S. Tomasin, "Physical layer authentication over an OFDM fading wiretap channel," in Proc. *ACM International Conference on Performance Evaluation Methodologies and Tools* (VALUETOOLS), Cachan (France), May 2011.

[C7] P. Baracca, S. Tomasin, and N. Benvenuto, "Optimization of base station coordination and power allocation in cellular network downlink," in Proc. *IEEE International Conference on Communication and Technology* (ICCT), Nanjing (China), Nov. 2010.

[C8] P. Baracca, S. Tomasin, and N. Benvenuto, "Equalization of OFDM over doubly very selective channels," in Proc. *IEEE International Conference on Communication and Technology* (ICCT), Nanjing (China), Nov. 2010.

[C9] P. Baracca, S. Tomasin, L. Vangelista, N. Benvenuto, and A. Morello, "Per sub-block equalization and channel estimation for next generation handheld DVB," in Proc. *IEEE International Conference on Ultra Modern Telecommunications* (ICUMT), St. Petersburg (Russia), Oct. 2009.

[C10] P. Baracca, S. Tomasin, L. Vangelista, N. Benvenuto, and A. Morello, "Per sub-block equalization of OFDM for mobile digital video transmission," in Proc. *International Broadcasting Convention* (IBC), Amsterdam (the Netherlands), Sep. 2009.